2008

Numerical modeling of galvanic corrosion

Long Jian Liu
University of Windsor

NOTE TO USERS

This reproduction is the best copy available.

UMI®

NUMERICAL MODELING

OF

GALVANIC CORROSION

by

Long Jian Liu

A Thesis

Submitted to the Faculty of Graduate Studies through the

Department of Physics in Partial Fulfillment of the

Requirements for the Degree of Master of

Science at the University of Windsor

Windsor, Ontario, Canada

2008

Canada

Author's Declaration of Originality

I hereby certify that I am the sole author of this thesis and that no part of this thesis has been published or submitted for publication.

I certify that, to the best of my knowledge, my thesis does not infringe upon anyone's copyright nor violate any proprietary rights and that any ideas, techniques, quotations, or any other material from the work of other people included in my thesis, published or otherwise, are fully acknowledged in accordance with the standard referencing practices. Furthermore, to the extent that I have included copyrighted material that surpasses the bounds of fair dealing within the meaning of the Canada Copyright Act, I certify that I have obtained a written permission from the copyright owner(s) to include such material(s) in my thesis and have included copies of such copyright clearances to my appendix.

I declare that this is a true copy of my thesis, including any final revisions, as approved by my thesis committee and the Graduate Studies office, and that this thesis has not been submitted for a higher degree to any other University or Institution.

ABSTRACT

Numerical modeling has become a trend in galvanic corrosion research. We summarize the forms of corrosion and focus on the galvanic corrosion, especially about the corrosion of magnesium and its alloys. We discuss the governing equations and the boundary conditions of galvanic corrosion. Based on the present status of galvanic corrosion research, we model the corrosion processes of magnesium alloy when the protective films (one situation is with high resistivity film and another is with zinc) are broken. We introduc the finite element method (FEM) and finite differential method (FDM) as tools for modeling and use FEM to solve an equation with different boundary conditions as a sample calculation and get some meaningful results.

ACKNOWLEDGEMENT

TABLE OF CONTENTS

1. Introduction

Corrosion is a universal problem as it creates substantial property losses every year. In the United States, the annual direct cost of corrosion to the industrial economy is about 3.1% of the country's gross national product (GNP), which is over \$276 B per year [1]. If we understand the corrosion processes, we can predict, detect and even slow it down. That will be of significant benefit. Most corrosion processes involve at least two electrochemical reactions (one anodic and one cathodic). In general, fundamentally, the driving force that causes metals to corrode is a natural consequence of their temporary existence in metallic form. To reach this metallic state from their occurrence in nature in the form of various chemical compounds (ores), it is necessary for them to absorb and store up chemical potential energy for later return via corrosion which is the energy required to release the metals from their original compounds.

Mass transport is a very important characteristic of corrosion, which is related to three main parameters of convection, migration and diffusion [2-5]. Corrosion processes are usually electrochemical in nature, having the essential features of a battery. A corroding surface can be thought of as a short-circuited battery. Galvanic corrosion naturally becomes the representative of corrosion. According to Faraday's law, the mass loss m of the material in the progress of galvanic corrosion is proportional to the galvanic current density i_g [6].

$$m = \frac{M i_g t A}{zF}$$ (1-1)

Where M is the molar mass of the material, t is the time, A is the area that the current density flows through, z is the valence and F is the Faraday's constant (96485.34C/mol). In the case of absence of an electrical field, the migration term is negligible while the convection force disappears in stagnant conditions. Thus mass transfer rate due to diffusion through a boundary layer in terms of current density is [7]

$$i_D = \frac{DzFc}{\delta}$$ (1-2)

Where D is the diffusion coefficient of the species, c is the concentration of reacting species in the bulk solution and δ is the thickness of the diffusion boundary layer. The galvanic corrosion rate is basically determined by the galvanic current I_g and its distribution. Theoretically [6, 8]

$$I_g = (\phi_c - \phi_a)/(R_a + R_c + R_s + R_m) \tag{1-3}$$

where I_g is the galvanic current between the anode and the cathode, ϕ_c and ϕ_a are the open circuit potentials of the cathode and anode, R_c and R_a are the cathode resistance and anode resistance respectively, R_s is resistance of the solution between the anode and cathode, and R_m is the metal resistance from the anode surface to the cathode surface through a metallic path. Normally R_m is negligible if the two electrode metals are in a direct electrical contact. Any factor that can affect these parameters will influence the galvanic corrosion rate. We can use a schematic to express the corrosion principle as a galvanic cell shown in Fig. 1-1.
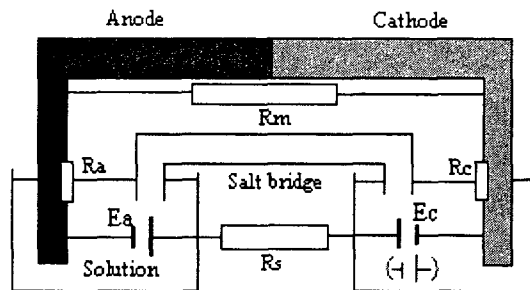
Fig. 1-1 Galvanic cell of corrosion process

However, equation (1-3) is just a theoretical or conceptual relationship (Ohm's law). In practice, there are complicated interactions among these factors. As a matter of fact, R_s depends on the geometric shape of the solution path between the anode and cathode. The distributions of current density and potential are always closely related to the geometric shape of the system. Therefore, the estimation of galvanic current or galvanic current density sometimes is very difficult for a practical system. Only for a galvanic corrosion specimen with a very simple geometry, can the analytical prediction of galvanic current density or distribution of galvanic current density be possible. Usually, numerical techniques and computer modelling have to be used for a complex geometric system and

2

the numerical approach has become a trend in galvanic corrosion research [2-5, 6, 8, 9-12]. Because of the complicated mathematical calculation, most of the models dealing with the propagation stage are based on numerical solution of the mass transport equations of chemical species at steady state across a one-dimensional crevice [4, 13-17] though some effort made to simplify the method [18]. The finite element method (FEM), the finite difference method (FDM) and the boundary element method (BEM) are efficient tools for modeling the process of corrosion. By using these numerical methods, one can simulate the distribution of the electrical potential and current on the surface of the material in the surrounding electrolytic solution. In this thesis we introduce and apply mainly the FEM and the FDM tools.

Because of the light weight and relative strength, the applications of magnesium alloys are increasing every year in the automotive and aircraft industries. However, the corrosion of magnesium and its alloys is a big problem [8, 19-25]. Because of the low standard electrode potential, magnesium is the most reactive metal. It will readily form galvanic corrosion system with another metal and even a micro-galvanic corrosion system with some secondary phases (such as α-phase and β-phase) and impurity grains [26-28] in an aqueous environment. It is very meaningful to discuss the possible galvanic corrosion current density and over-potential of micro-galvanic corrosion system. Especially, different from most of other metals such as Fe and Cu, magnesium and its alloys show the negative difference effect, which is a very important property in the process of magnesium corrosion. Finding the correct reason will give rise to compelling progress in magnesium corrosion research.

2. Corrosion

Generally speaking, corrosion is the degradation of 'materials' properties due to interactions with their environment, and corrosion of most metals (and many materials for that matter) are inevitable. It is the primary means by which metals deteriorate. Protection of structures and equipment from corrosion is both necessary and possible. The trends in corrosion research include the development of environmentally benign inhibitors, accurate prediction of structure service life and finding ways to make corrosion a good thing. For example, one can use dissolution to selectively remove one component from a material (known as dealloying), leaving a porous structure, which may be used to hold and slowly elute drugs when the structure is implanted. [1]

Most metals corrode on contact with water (include moisture in the air), acids, bases, salts, oils, aggressive metal polishes, and other solid and liquid chemicals. Metals will also corrode when exposed to gaseous materials like acid vapors, formaldehyde gas, ammonia gas, and sulfur containing gases. Corrosion thus refers to any process involving the deterioration or degradation of metal components. The best known case of corrosion is that of the rusting of iron or steel [29].

Just as Song and Atrens [30] indicated: no material can be highly corrosion resistant in all environments. The high corrosion resistance of a material always refers to some particular environment. A particular material could have a high corrosion resistance in a certain environment but a low corrosion resistance in another.

2.1. Form of Corrosion:

Traditionally, corrosion may be classified into eight categories based on the morphology of the attack, as well as the character of the environment that the material is exposed. Most corrosion processes can be explained based on the principle of electrochemistry, especially for the case of uniform corrosion [31-34], galvanic corrosion [5,8,10,11,19,20] and crevice and pitting corrosion [2,4,9,21,34-41]. In recent years, a considerable amount of research has been done on galvanic and pitting corrosions.

Galvanic Corrosion: Galvanic corrosion occurs when two different metals or alloys with different compositions are electrically coupled in the presence of an electrolyte. The more reactive metal will experience severe corrosion. Even in the same alloy, e.g. AZ91D magnesium alloy, when some secondary phases or impurity grains exist, the most reactive metal magnesium, forms galvanic cells even micro-galvanic cells with those secondary phase/impurity grains [30] that may cause serious corrosion in an aqueous environment. Two conditions must be satisfied for galvanic corrosion to occur: (1) dissimilar metal-to-metal contact and (2) bridging of the bimetal junction by a conductive solution (electrolyte). Perhaps the most infamous examples of this type of corrosion are combinations such as steel (Fe) and brass (Cu) or copper (Cu) and steel. Typically, steel will corrode over an area near the brass or copper in a water environment and particularly in a seawater environment. This phenomenon often happens between the aluminum alloys and steel fasteners. More seriously, when a steel (Fe) screw is used to connect the magnesium alloy vehicle body or aircraft body directly, because the difference of the electrode standard potential between Mg (-2.37V) and Fe (-0.44V) is much bigger than that between Fe and Cu (+0.34V), magnesium around steel screws may corrode through when in a conductive solution or moisture environment. In all probability, the most common way of avoiding galvanic corrosion is to electrically attach a third anodic metal to the other two. This is referred to as cathodic protection.

Though we are more interested in galvanic corrosion, considering the complete set of knowledge structure of corrosion, we quote the definition of seven categories of corrosion from website [31]: http://www.cheresources.com/corrosion.shtml.

Uniform Attack: Uniform attack is a form of electrochemical corrosion that occurs with equal intensity on the entire surface of the metal. Iron rusts when exposed to air and water, and silver tarnishes due to exposure to air. Potentially a key problem, this type of corrosion is very easy to predict and is usually associated with "common sense" when making material decisions. Uniform or general corrosion (such as rusting, tarnishing and patina) is the most prevalent type of this corrosion. Fortunately, uniform corrosion is predictable and can be controlled by various methods such as painting the surface or

applying a layer of a sacrificial metal like zinc to steel.

Crevice Corrosion: Another form of electrochemical corrosion is crevice corrosion. Crevice corrosion is a consequence of concentration differences of ions or dissolved gases in an electrolytic solution. The stagnant liquid in the crevice will eventually have a lowered dissolved oxygen concentration and crevice corrosion takes place. In the absence of oxygen, the metal and/or its passive layer begin to oxidize. To prevent crevice corrosion, one should use welds rather than rivets or bolted joints whenever possible. Also consider non-absorbing gaskets. Remove accumulated deposits frequently and design containment vessels to avoid stagnant areas as much as possible.

Pitting Corrosion: Pitting, just as it sounds, is used to describe the formation of small pits on the surface of a metal or alloy. Pitting is suspected to occur in much the same way crevice corrosion does, but on a flat surface. A small imperfection in the metal is thought to begin the process, and then a "snowball" effect takes place. Pitting can go on undetected for extended periods of time, until a failure occurs. Pitting would overrun the stainless steel in a matter of weeks due to its very poor resistance to chlorides, which are notorious for their ability to initiate pitting corrosion. Alloy blends with more than 2% Molybdenum show better resistance to pitting attack. Titanium is usually the material of choice if chlorides are the main corrosion concern. (Pd stabilized forms of Ti are also used for more extreme cases).

Inter-granular Corrosion: Occurring along grain boundaries for some alloys, inter-granular corrosion can be a real danger in the "right" environment. For example, the heating of some materials causes, for the purpose of tough and stainless, chromium carbide to form from the chromium and the carbon in the metals in which they are present. This leaves a chromium deficient boundary just shy of where the metal was heated for welding which may become a good galvanic corrosion system. To avoid this problem, the material can be subjected to high temperatures to re-dissolve the chromium carbide particles. Low carbon materials can also be used to minimize the formation of chromium carbide. Finally, the material can be alloyed with another material such as

Titanium which readily forms carbides so that the chromium remains in place.

Selective Leaching: When one element or constituent of a metal is selectively corroded out of a material it is referred to as selective leaching. The most common example is the dezincification of brass. After leaching has occurred, the mechanical properties of the metal are obviously impaired and some metal will begin to crack.

Erosion-Corrosion: Erosion-corrosion arises from a combination of chemical attack and the physical abrasion as a consequence of the fluid motion. Virtually all alloy or metals are susceptible to some type of erosion-corrosion as this type of corrosion is very dependent on the fluid. Materials that rely on a passive layer are especially sensitive to erosion-corrosion. Once the passive layer has been removed, the bare metal surface is exposed to the corrosive material. If the passive layer cannot be regenerated quickly enough, significant damage can be seen. Fluids that contain suspended solids are often times responsible for erosion-corrosion. The best way to limit erosion-corrosion is to design systems that will maintain a low fluid velocity and to minimize sudden line size changes and elbows. An imperfection on the surface of the material probably causes an eddy current which provides a perfect location for erosion-corrosion.

Stress Corrosion: Stress corrosion can result from the combination of an applied tensile stress and a corrosive environment. In fact, some materials only become susceptible to corrosion in a given environment once a tensile stress is applied. Once stress cracks begin, they easily propagate throughout the material, which in turn allows additional corrosion and cracking to take place. The tensile stress is usually the result of expansions and contractions facilitated by violent temperature changes or thermal cycles. The best defence against stress corrosion is to limit the magnitude and/or frequency of the tensile stress. In sour environments, such as containing chloride ions and hydrogen sulfide, it is very easy to cause sulfide stress cracking (SSC) and stress corrosion cracking (SCC) to low-alloy steels and corrosion resistant alloys, such as stainless steels and Ni-based alloys.

2.2. Corrosion Chemistry

As noted above, the ultimate force that causes metals to corrode is a natural consequence of their temporary existence in metallic form. To reach this metallic state from their occurrence in nature in the form of various chemical compounds (ores), it is necessary for them to absorb and store up chemical potential energy for later return via corrosion, which is the energy, required to release the metals from their original compounds.

Corrosion occurs not only in acids, but also in fresh water, seawater, salt solutions, and alkaline or basic media, as well as in some gas environments and organic compounds.

2.2.1. Corrosion in Acids

According to Roberge [35] as well as website: http://corrosion-doctors.org/Chemistry-of-Corrosion/Introduction.htm, low pH (acidic) aqueous environments accelerate corrosion by supplying hydrogen ions to the corrosion process. Even pure water contains some free hydrogen ions. Dissolved carbon dioxide in the water can increase the hydrogen ion concentration. The CO_2 may react with water to form carbonic acid as shown in Eq. (2-1).

$$CO_2 + H_2O \rightleftarrows HCO_3, \qquad (2\text{-}1)$$

Carbonic acid subsequently dissociates into bicarbonate and carbonate ions as expressed in the following equations:

$$H_2CO_3 \rightleftarrows HCO_3^- + H^+, \qquad (2\text{-}2)$$

$$H_2CO_3^- \rightleftarrows CO_3^{2-} + H^+, \qquad (2\text{-}3)$$

This process increases hydrogen ions in the water. Even more acidity is sometimes encountered in mine waters and in water contaminated by industrial wastes. Many salts added to an aqueous system also have a direct effect on the pH of that mixture through the following process of hydrolysis shown here for the addition of ferric ions to water:

$$Fe^{3+} + 3H_2O \rightleftarrows Fe(OH)_3 + 3H^+ \qquad (2\text{-}4)$$

This process also increases the hydrogen ions. In recent years, the study of corrosion of magnesium and its alloys is increasing. In fact, when we put magnesium into a dilute acid such as hydrochloric or sulfuric, there is a rapid reaction in which the magnesium is attacked or "dissolved" and hydrogen is evolved as a gas. These reactions are described in the following equations to:

$$Mg + 2HCl \rightarrow MgCl_2 + H_2\uparrow \tag{2-5}$$

$$Mg + 2H^+ + 2Cl^- \rightarrow Mg^{2+} + 2Cl^- + H_2\uparrow \tag{2-6}$$
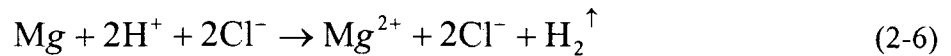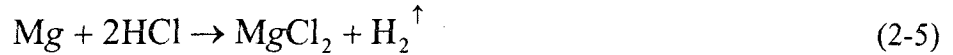
From these equations, we can see that the chloride ions do not participate directly in this reaction, although they could play an important role in real corrosion situations.

Similarly, magnesium combines with sulfuric acid to form magnesium sulfate (a soluble salt) and hydrogen gas as shown in the following equations:

$$Mg + H_2SO_4 \rightarrow MgSO_4 + H_2\uparrow \tag{2-7}$$

$$Mg + 2H^+ + SO_4^{2-} \rightarrow Mg^{2+} + SO_4^{2-} + H_2\uparrow \tag{2-8}$$
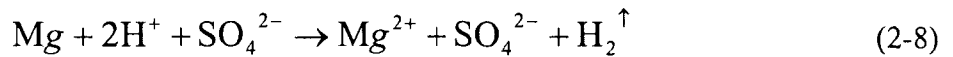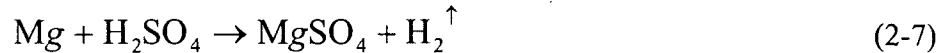
As in the preceding reaction, the sulfate ions that are an integral part of sulfuric acid do not participate directly in the corrosion attack and therefore one could write these equations in a simpler form:

$$Mg + 2H^+ \rightarrow Mg^{2+} + H_2\uparrow \tag{2-9}$$

Many other metals are also corroded by acids often yielding soluble salts and hydrogen gas as shown in Equations and for iron and zinc respectively:

$$2Fe + 6H^+ \rightarrow 2Fe^{3+} + 3H_2\uparrow \tag{2-10}$$

$$Zn + 2H^+ \rightarrow Zn^{2+} + H_2\uparrow \tag{2-11}$$
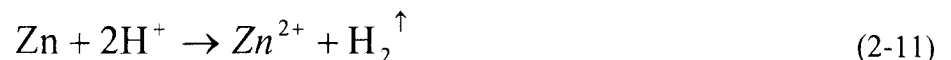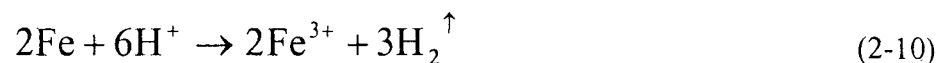
2.2.2. Corrosion in Neutral or Alkaline Environments

According to the expression on the website: http://www.corrosion-doctors.org/Chemistry-of-Corrosion/corrosion-in-neutral.htm, In the environment of fresh water, seawater, salt solutions, and alkaline or basic media, corrosion occurs mainly only if dissolved oxygen is also present. Water solutions rapidly dissolve oxygen from the air, and this is the source of the oxygen required in the corrosion process. The most familiar corrosion of this type is the rusting of iron when exposed to a moist atmosphere.

$$4Fe + 6H_2O + 3O_2 \rightarrow 4Fe(OH)_{3\downarrow} \qquad (2\text{-}12)$$
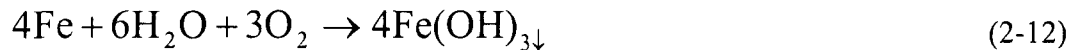
In this equation, iron combines with water and oxygen to produce an insoluble reddish-brown corrosion product that falls out of the solution. During rusting in the atmosphere, there is an opportunity for drying, and this ferric hydroxide dehydrates and forms the familiar red-brown ferric oxide (rust) or Fe_2O_3, as shown below:

$$2Fe(OH)_3 \rightarrow Fe_2O_3 + 3H_2O \qquad (2\text{-}13)$$
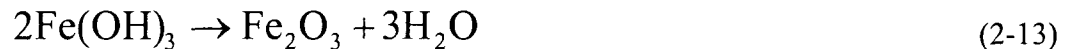
For magnesium and its alloys, when exposed to water or moist atmosphere, the similar reactions are:

$$2Mg + 2H_2O + O_2 \rightarrow 2Mg(OH)_{2\downarrow} \qquad (2\text{-}14)$$

$$Mg(OH)_2 \rightarrow MgO + H_2O \qquad (2\text{-}15)$$
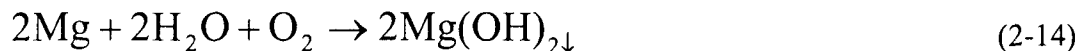
Similar reactions occur when zinc is exposed to water or moist air followed by natural drying.

$$2Zn + 2H_2O + O_2 \rightarrow 2Zn(OH)_{2\downarrow} \qquad (2\text{-}16)$$

$$Zn(OH)_2 \rightarrow ZnO + H_2O \qquad (2\text{-}17)$$
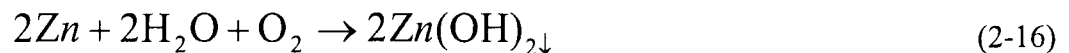
The resulting zinc oxide is the whitish deposit seen on galvanized pails, rain gutters, and imperfectly chrome-plated bathroom faucets. It is also familiarly called 'white rust', a

non-protective and destructive form of corrosion that attacks incompletely passivated galvanized steel material or galvanized components subjected to marine atmospheres.

Note that there is no oxidation or reduction (electron transfer) during either reaction. In both cases the valences of the elements on the left of each reaction remain the same as the right. The valences of iron, zinc, hydrogen, and oxygen elements remain unchanged throughout the course of these reactions, and it is consequently not possible to divide these reactions into individual oxidation and reduction reactions.

2.3. Standard Electrode Potentials

The standard electrode potential is a vital factor of galvanic corrosion system. In this system, an anode and a cathode form an electrochemical cell in electrolyte. Because of the redox on the two different electrodes, an electric potential is created between two dissimilar metals. This potential is a measure of the energy per unit charge which is available from the oxidation/reduction reactions to drive the reaction. We always visualize the cell reaction in terms of two half-reactions: an oxidation half-reaction and a reduction half-reaction [42].

Reduced species → oxidized species + ne⁻ | Oxidation at anode |

Oxidized species + ne⁻ → reduced species | Reduction at cathode |
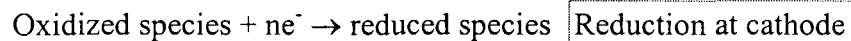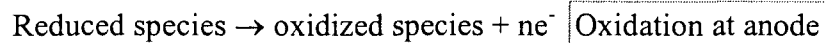
The potential on one electrode always refers relatively to the potential on another electrode. Although the overall potential of a cell can be measured, there is no practical way to accurately measure the electrode/electrolyte potentials in isolation directly. We can only directly measure the potential difference between two points. Hence, the need to have an electrode with zero potential by definition is used as a reference electrode. As a matter of fact, hydrogen has been defined the electrode with zero potential. In addition, the electric potential varies with temperature, concentration and pressure. Since the oxidation potential of a half-reaction is the negative of the reduction potential in a redox reaction, it is sufficient to determine either one of the potentials. Therefore, standard electrode potential is commonly written as standard reduction potential. Since the

electrode potentials are conventionally defined as reduction potentials, the sign of the potential for the metal electrode being oxidized must be reversed when calculating the overall cell potential. Note that the electrode potentials are independent of the number of electrons transferred -that is, they are set to one mole of electrons transferred- and so the two electrode potentials can be simply combined to give the overall potential even if different numbers of electrons are involved in the two electrode reactions [42].

The cell potential (often called the electromotive force or emf) has a contribution from the anode, which is a measure of its ability to lose electrons - it is called as "oxidation potential". The cathode has a contribution based on its ability to gain electrons; it is "reduction potential". The cell potential can then be written

$$E_{cell} = \text{reduction potential} - \text{oxidation potential} \qquad (2\text{-}18)$$

Note that:

1. The electrode potential cannot be determined in isolation, but in a reaction with some other electrode.
2. The electrode potential depends upon the concentrations of the substances, the temperature, and the pressure in the case of a gas electrode.

In practice, the first of these hurdles is overcome by measuring the potentials with respect to a standard hydrogen electrode. Tabulating all electrode potentials with respect to the same standard electrode provides a practical working framework for a wide range of calculations and predictions. The standard hydrogen electrode is assigned a potential of zero volts.

The second hurdle is overcome by choosing standard thermodynamic conditions for the measurement of the potentials. The standard electrode potentials are customarily determined at solute concentrations of 1 Molar, gas pressures of 1 atmosphere, and a standard temperature which is usually 25°C. The standard cell potential is denoted by a degree sign as a superscript.

$$E^\circ_{Cell}$$

1. Measured against standard hydrogen electrode.
2. Concentration 1 Molar
3. Pressure 1 atmosphere
4. Temperature 25°C

Now let us take Mg/H₂ pair as an example and show how to calculate the standard Mg-electrode potential ϕ^o_{Mg}.

$$\text{Anode reaction: } Mg \rightarrow Mg^{2+} + 2e^- \qquad (\phi^o_{Mg}) \qquad (2\text{-}19)$$

$$\text{Cathode reaction: } 2H^+ + 2e^- \rightarrow H_2\uparrow \qquad (0V) \qquad (2\text{-}20)$$

$$\text{Overall reaction: } Mg + 2H^+ \rightarrow Mg^{2+} + H_2\uparrow \qquad (E^\circ_{measure}=2.38V)$$
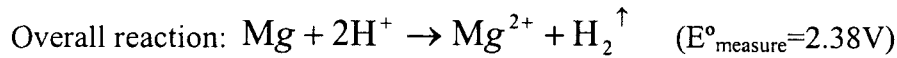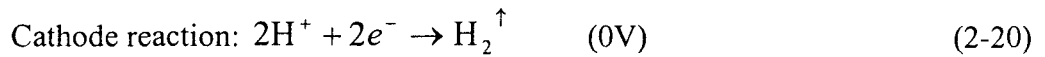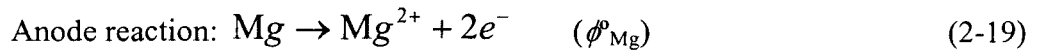
2.38=0-ϕ^o_{Mg} , ϕ^o_{Mg} =-2.38V.

Similarly, for Cu/H₂ pair, we can measure E°=0.34V

0.34V=ϕ^o_{Cu}-0, so, ϕ^o_{Cu}=0.34V

Now, for Mg/Cu cell, E°=ϕ^o_{Cu} - ϕ^o_{Mg} =0.34-(-2.38)=2.72V.

When it is not at standard condition, for A/B coupling pair (A is a metal, B may be a metal, may be not),

$$A + aB^{m+} = A^{z+} + bB_n \quad (a=bn, am=z) \qquad (2\text{-}21)$$
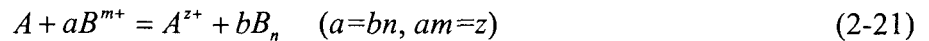
According to the Nernst equation, we have:

$$\phi_A = \phi^\circ_A - \frac{RT}{zF} \lg \frac{[A^{z+}]}{[A]} = \phi^\circ_A - \frac{RT}{zF} \lg[A^{z+}] \qquad (2\text{-}22)$$

$$\phi_B = \phi^\circ_B - \frac{RT}{zF} \lg \frac{[B^{m+}]^a}{[B_n]^b} \qquad (2\text{-}23)$$

$$E = E^\circ - \frac{RT}{zF} \lg \frac{[A^{z+}][B_n]^b}{[B^{m+}]^a} \qquad (2\text{-}24)$$

The smaller the electrode potential, the more reactive the metal is. The reaction of a redox always happens to the direction of $\Delta G=-zFE<0$. It requires E=ϕ_B -ϕ_A >0. Thus, oxidation occurs at anode where the electrode potential is lower and reduction occurs at cathode where the electrode potential is higher. That is why we put a more reactive metal (less electrode potential) on an expected-to-protect metal (noble metal) in cathode protection.

2.4. Factors Influencing Corrosion Reactions

The factors influencing corrosion reactions can be sorted into two parts according to reference [29] or website http://www.corrosion-doctors.org/Principles/Theory.htm.

One is the sort of factors associated mainly with the metal. They are:

(1) Effective electrode potential of a metal in a solution

(2) Overvoltage of hydrogen on the metal

(3) Chemical and physical homogeneity of the metal surface

(4) Inherent ability to form an insoluble protective film

Another is the sort of factors which vary mainly with the environment. They are:

(1) Hydrogen-ion concentration (pH) in the solution

(2) Influence of oxygen in solution adjacent to the metal

(3) Specific nature and concentration of other ions in solution

(4) Rate of flow of the solution in contact with the metal

(5) Ability of environment to form a protective deposit on the metal

(6) Temperature

(7) Cyclic stress (corrosion fatigue)

Here, we would like to further discuss influencing factors from the hydrogen-ion concentration (pH) in the solution.

As we discussed above, in the aqueous environment, the cathodic reaction is:

$$2H^+ + 2e \rightleftarrows H_2 \qquad \phi^\circ = 0$$

or: $$O_2 + 4H^+ + 4e \rightleftarrows 2H_2O \qquad \phi^\circ = 1.23V$$
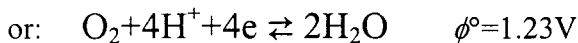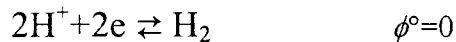
According to the Eernst equation,

$$\phi_{H^+/H_2} = \phi^\circ_{H^+/H_2} + \frac{RT}{2F} \lg \frac{[H^+]^2}{p_{H_2}}$$

$$\phi_{O_2/H_2O} = \phi^\circ_{O_2/H_2O} + \frac{RT}{4F} \lg(p_{O_2}[H^+]^4)$$

When at 25°C, $p_{H_2} = 1\,atm$ / $p_{O_2} = 1\,atm$, we have

$$\phi_{H^+/H_2} = 0.05917 \lg[H^+] = -0.05917 pH$$

$$\phi_{O_2/H_2O} = 1.23 + 0.05197 \lg[H^+] = 1.23 - 0.05917 pH$$

This means that changing the pH value of the solution will change the overvoltage of hydrogen on the metal.

From the governing equations of corrosion (convection-diffusion transport equation) and their boundary conditions (Butler—Volmer equation) that we will discuss later, we can understand the detail meaning of these factors.

2.5. Corrosion of Magnesium and its Alloys

In its pure form, magnesium is soft and mechanically weak. By careful selection of alloying elements, magnesium alloys can be produced for general purposes and special applications. In recent years, the use of magnesium alloys keeps rising greatly in the automotive and aircraft industries because it is light and strong. Correspondingly, a large number of studies about the corrosion of magnesium alloys were carried out [7, 18-24]. The electrochemical reactions on pure magnesium are of particular interest. They provide the base for understanding the corrosion properties of magnesium alloys. Magnesium alloys are mainly composed by elements Al, Mn, Si, Cu, Zn, Ni and Fe. The chemical composition of some mainly magnesium alloys are listed in following table [43]:

%	Al	Mn	Si	Cu	Zn	Ni	Fe	other	Mg
AM60A	5.5-6.5	≥0.13	≤0.50	≤0.35	≤0.22	≤0.03	/	/	Balance
AM60B	5.5-6.5	≥0.25	≤0.10	≤0.010	≤0.22	≤0.002	≤0.005	≤0.003tot	Balance
AZ91A	8.3-9.7	≥0.13	≤0.50	≤0.10	0.35-1.0	≤0.03	/	≤0.30	Balance
AZ91B	8.3-9.7	≥0.13	≤0.50	≤0.35	0.35-1.0	≤0.03	/	≤0.30	Balance
AZ91C	8.1-9.3	≥0.13	≤0.30	≤0.10	0.40-1.0	≤0.01	/	≤0.3tot	Balance
AZ91D	8.3-9.7	≥0.15	≤0.10	≤0.03	0.35-1.0	≤0.002	≤0.005	≤0.02ea.	Balance
AZ91E	8.1-9.3	0.17-0.35	≤0.20	≤0.015	0.4-1.0	≤0.0010	≤0.005	≤0.01ea. ≤0.30tot.	Balance

The standard electrode potential of some elements are:

Element	Mg	Al	Ti	Mn	Zn	Cr	Fe	Ni	Si	H	Cu
Potential (Volts)	-2.37	-1.67	-1.63	-1.18	-0.76	-0.74	-0.44	-0.24	-0.14	0.00	+0.34

Legend: (s)–solid; (l)–liquid; (g)–gas; (aq)–aqueous (default for all charged species); (Hg) – amalgam.

Half-reaction	$E°$ (V)	Half-reaction	$E°$ (V)
$Mg^{2+} + 2\ e^- \rightarrow Mg(s)$	-2.38	$Cr^{3+} + 3\ e^- \rightarrow Cr(s)$	-0.74
$Al(OH)_4^- + 3\ e^- \rightarrow Al(s) + 4OH^-$	-2.33	$Cr^{3+} + e^- \rightarrow Cr^{2+}$	-0.42
$Al(OH)_3(s) + 3\ e^- \rightarrow Al(s) + 3OH^-$	-2.31	$Fe^{2+} + 2\ e^- \rightarrow Fe(s)$	-0.44
$Al^{3+} + 3\ e^- \rightarrow Al(s)$	-1.66	$Fe_3O_4(s) + 8H^+ + 8e^- \rightarrow 3Fe(s) + 4H_2O$	+0.085
$Ti^{2+} + 2\ e^- \rightarrow Ti(s)$	-1.63	$[Fe(CN)_6]^{3-} + e^- \rightarrow [Fe(CN)_6]^{4-}$	+0.36
$TiO(s) + 2\ H^+ + 2\ e^- \rightarrow Ti(s) + H_2O$	-1.31	$Ni^{2+} + 2\ e^- \rightarrow Ni(s)$	-0.25
$Ti_2O_3(s) + 2\ H^+ + 2\ e^- \rightarrow 2\ TiO(s) + H_2O$	-1.23	$NiO_2(s) + 4H^+ + 2\ e^- \rightarrow Ni^{2+} + 2OH^-$	+1.59
$Ti^{3+} + 3\ e^- \rightarrow Ti(s)$	-1.21	$Si(s) + 4H^+ + 4e^- \rightarrow SiH_4(g)$	-0.14
$Mn^{2+} + 2\ e^- \rightarrow Mn(s)$	-1.18	**$2\ H^+ + 2\ e^- \rightarrow H_2(g)$**	0
$MnO_4^- + H^+ + e^- \rightarrow HMnO_4^-$	+0.90	$Cu^{2+} + 2\ e^- \rightarrow Cu(s)$	+0.34
$MnO_2(s) + 4H^+ + e^- \rightarrow Mn^{3+} + 2H_2O$	+0.95	$Cu(NH_3)_4^{2+} + e^- \rightarrow Cu(NH_3)_2^+ + 2NH_3$	+0.10
$MnO_2(s) + 4H^+ + 2e^- \rightarrow Mn^{2+} + 2H_2O$	+1.23	$Cu^{2+} + e^- \rightarrow Cu^+$	+0.16
$MnO_4^- + 8H^+ + 5e^- \rightarrow Mn^{2+} + 4H_2O$	+1.51	$Cu^+ + e^- \rightarrow Cu(s)$	+0.52
$MnO_4^- + 4\ H^+ + 3\ e^- \rightarrow MnO_2(s) + 2\ H_2O$	+1.70	$ZrO_2(s) + 4H^+ + 4e^- \rightarrow Zr(s) + 2H_2O$	-1.553
$HMnO_4^- + 3H^+ + 2e^- \rightarrow MnO_2(s) + 2H_2O$	+2.09	$Zr^{4+} + 4\ e^- \rightarrow Zr(s)$	-1.45
$Zn^{2+} + 2\ e^- \rightarrow Zn(s)$	-0.76		

Macro-galvanic corrosion occurs when magnesium is coupled with a metal such as steel because Mg is the most active engineering metal and consequently its corrosion potential is more negative than that of all the other engineering metals. Magnesium dissolution in aqueous environments proceeds by an electrochemical reaction with water to produce magnesium hydroxide and hydrogen gas. The overall reaction for the corrosion of Mg can be expressed simply as

$$Mg + 2H_2O \rightarrow Mg(OH)_{2\downarrow} + H_2^{\uparrow}$$
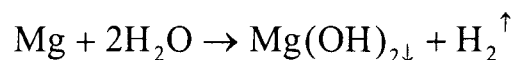
The poor corrosion resistance of magnesium alloys in aqueous solutions results from the high intrinsic dissolution tendency of magnesium, which is only weakly inhibited by

corrosion-product films. Magnesium has a standard electrode potential of -2.37V, assuming that bare metal is in contact with its divalent ion in solution. The actual corrosion potential of Mg is usually about -1.7V in aqueous solutions. This means that bare Mg metal is not in contact with the solution. Magnesium forms a magnesium hydroxide film, which can provide some protection over a wide pH range [30].

The existence of a partially protective film, and the way chance determines the progression of corrosion means that "general corrosion" is not an issue. The common form of corrosion is localized corrosion, which for magnesium is much different from that of steels and stainless steels. The lack of a surface film on the impurities together with the negative corrosion potentials allows impurities to be efficient cathodes for hydrogen discharge, thereby providing significant micro-galvanic acceleration of the corrosion rate. This is one of the possible forms of micro-galvanic corrosion [30].

Magnesium corrosion is relatively insensitive to the oxygen concentration, although the oxygen concentration is an important factor in atmospheric corrosion. The corrosion attack in aqueous environment often involves micro-galvanic coupling between cathodic and anodic areas [30]. Magnesium is the most reactive metal in its environment. The anode matrix has a corrosion potential lower than that of the second phases which is formed by the reaction of magnesium with a less reactive metal. This process leads a micro-galvanic corrosion.

Factors that affect the corrosion properties of magnesium are alloy composition, heavy-metal impurities, casting variables, metallographic structure, environment, surface condition, and contact with other materials. Thermodynamically, magnesium should react completely with oxygen and as well as with water. The fact that it reacts with neither of those is caused by passive behavior in many environments. In a corrosive environment, pitting or other forms of local corrosion occur as a result of film breakdown.

Magnesium alloys of suitable composition and purity are corrosion resistant. They are being used successfully in a variety of applications. Automotive parts made of

commercial high-purity die-cast AZ91D alloy located in the worst splash zone under a car, illustrate the excellent corrosion resistance of magnesium [44]. The following excerpt is from website: http://www.magnesium.com/w3/data-bank/index.php?mgw=166.

Composition

The corrosion of magnesium alloys is commonly measured in a sodium chloride solution, by using either immersion or salt spray tests. These tests relate to important practical uses of magnesium alloys in automotive, aircraft, and military applications.

Most of the elements present in, or added to, magnesium alloys have limited solid solubility in the alloy, and therefore occur as precipitated phases. In virtually all cases, these phases are more noble (i.e., have a higher redox potential) than the matrix. Their influence on saltwater corrosion depends heavily on their potential relative to the matrix, as well as their efficiency as cathodic sites, i.e., the ease with which they liberate hydrogen gas (overvoltage).

Elements generally present in commercial magnesium alloys, which influence saltwater corrosion can be classified as follows:

1) generally benign or beneficial: aluminum, beryllium, manganese, rare earths, silicon, zinc, and zirconium;

    Aluminum has the most favorable effect on magnesium of any of the alloying elements. It improves strength and hardness, widens the freezing range, and makes the alloy easier to cast. When exceeding 6 wt%, the alloy becomes heat treatable, but commercial alloys rarely exceed 10 wt% aluminum. An aluminum content of 6 wt% yields the optimum combination of strength and ductility.

2) Moderately deleterious: silver;

3) Severely deleterious: nickel (and cobalt), iron, and copper.

    Iron is one of the most harmful impurities in magnesium alloys due to considerable reduction of corrosion resistance even if present in small amounts. In ordinary commercial-grade alloys, the iron content can average as high as 0.01-0.03 wt%.

However, for maximum corrosion resistance, 0.005% is specified as the upper limit for iron content.

Nickel, just like iron, is another harmful impurity in magnesium alloys because it also reduces the corrosion resistance if present, even in small amounts. In ordinary commercial-grade alloys, the nickel content can average as high as 0.01-0.03 wt%, but for maximum resistance to corrosion, 0.005% is specified as the upper limit for nickel content.

The commercially important Mg-Al-Zn alloys used for die-casting and sand casting have received intensive study, resulting in the development of alloys with outstanding saltwater corrosion resistance. These alloys have a very low critical impurity content (Ni, Fe, Cu), and a controlled manganese content.

Structure

The size and distribution of the cathodic phases play an important role in corrosion and are influenced by process parameters and heat treatment. Homogenized and artificially aged specimens of AZ91E (T6) show considerably lower corrosion than cast (F) and homogenized (T4) specimens. Heat treatment influences mainly the distribution of the inter-metallic Beta-phase ($Mg_{17}Al_{12}$) in the alloy. Aging to T6 temper causes precipitation of this phase as an almost continuous network of secondary particles along the grain boundaries. In the T4 condition, the Beta-phase is fully dissolved. By air cooling from T4, only traces of Beta-phases can have the same effect as a full T6 treatment. Tolerance limits in cast AZ91 for the most important impurity elements (iron, copper, and nickel) are influenced by the cooling plate. In the early stages of corrosion, filiform attack an initiating pit adjacent to inter-metallic particles and the role of $Mg_{17}Al_{12}$ concentrated in grain boundaries can be clearly illustrated. Cold working of magnesium alloys (e.g., by stretching or bending) has no appreciable effect on corrosion rate. As references [26] and [27] indicate: there are α-phase (Mg-Al-Zn solid solution) and β-phase ($Mg_{17}Al_{12}$) as a primary microstructure in AZ-series magnesium alloys. The two-phase microstructure leads to localized micro-galvanic corrosion. This corrosion is strongly dependent on metallic impurities. Some typical contamination elements like Cu, Ni, Mn and Si in

magnesium alloys may strongly alter their microstructure. As a consequence the corrosion rate can vary by nearly two orders of magnitude in comparison to the high purity AZ-magnesium alloys.

Surface Contamination

Producers of magnesium have demonstrated the importance of high-purity alloys for structural applications. However, surface contamination from handling and mechanical treatment can greatly degrade the corrosion resistance of high-purity alloys. This helps explain why ceramic blasting media containing iron oxide can be just as harmful to the corrosion properties of magnesium as steel grit.

Atmosphere

A magnesium alloy surface exposed to a salt-free atmosphere develops a gray film consisting mainly of magnesium hydroxide that protects the metal from corrosion. Chlorides, sulfates, or other hydrophilic substances promote corrosion by destroying this film. Structural magnesium alloys are resistant to rural atmospheres and moderately resistant to industrial or mild marine atmospheres. The corrosion rate in marine atmospheres is significantly lower for the high-purity Mg-Al-Zn alloys.

The surface film that usually forms on magnesium alloys, exposed to the atmosphere, gives limited protection from further attack. Unprotected magnesium and magnesium-alloy parts are resistant to rural atmospheres and moderately resistant to industrial and mild marine atmospheres, provided that they do not contain joints or recesses that entrap water in association with an active galvanic couple.

Corrosion of magnesium alloys increases with relative humidity. At 9.5% humidity, neither pure magnesium nor any of its alloys exhibit evidence of surface corrosion after 18 months. At 30% humidity, only minor corrosion may occur. At 80% humidity, the surface may exhibit considerable corrosion. In marine atmospheres heavily loaded with salt spray, magnesium alloys require protection for prolonged survival.

Water

When magnesium is immersed in distilled water without the possibility of carbon dioxide absorption, the initial corrosion rate decreases rapidly to a very low value. A protective film of magnesium hydroxide forms on the surface. The solubility product of magnesium hydroxide in the solution is quickly reached, dissolution of the hydroxide is inhibited, and corrosion essentially stops. If the water is replenished, corrosion continues and increases on absorption of carbon dioxide due to dissolution of the protective film. Raising the temperature of distilled or natural water also increases the corrosion rate of magnesium alloys. Aluminum is beneficial as an alloying ingredient because it promotes the formation of protective hydrotalcite [$Mg_6Al_2 (OH)_{16}CO_3 \cdot 4H_2O$] films.

Acids

Magnesium is attacked by all acids except hydrofluoric or chromic acid. Passive films are formed in most concentrations of these acids, accounting for their use in many conversion-coating processes.

Hydrofluoric acid does not attack magnesium to an appreciable extent, because it forms an insoluble, protective magnesium fluoride film on the surface; however, pitting develops at low acid concentrations. With increasing temperature, the rate of attack increases at the liquid line, but to a negligible extent elsewhere.

Pure H_2CrO_4 attacks magnesium and its alloys at a very low rate. However, traces of chloride ion in the acid will markedly increase this rate. A bolting solution of 20% H_2CrO_4 in water is widely used to remove corrosion products from magnesium alloys without attacking the base metal. Magnesium resists dilute alkalis, and 10% caustic solution is commonly used for cleaning at temperatures up to the boiling point.

Salt Solutions

Neutral solutions of salts of heavy metals such as nickel, iron, and copper are corrosive to magnesium alloys. Such corrosion occurs when the heavy metal plates out to form active cathodes on the anodic magnesium surface.

Chloride solutions are corrosive because chlorides, even in small amounts, usually break down the protective film on magnesium. Fluorides form insoluble magnesium fluoride and consequently tend to passivate. Oxidizing salts, especially those containing chlorine or sulfur atoms, are more corrosive than non-oxidizing salts, but chromates, vanadates, phosphates, and others are film forming, and thus retard corrosion, except at elevated temperatures.

Gases

Iodine, bromine, fluorine, and dry chlorine cause little or no corrosion of magnesium at room or slightly elevated temperature. Even when it contains 0.02% H_2O, dry bromine causes no more attack at its boiling temperature (58 °C/136 °F) than at room temperature. The presence of a small amount of water causes pronounced attack by chlorine, some attack by iodine and bromine, and negligible attack by fluorine. Wet chlorine, iodine, or bromine below the dew point of any aqueous phase causes severe attack on magnesium. Dry, gaseous sulfur dioxide causes no attack at ordinary temperatures. If water vapor is present, some corrosion may occur.

Organic compounds

Aliphatic and aromatic hydrocarbons, ketones, and ethers are not corrosive to magnesium and its alloys. Ethanol and higher alcohols are not corrosive at ordinary temperatures, but they may react destructively at high temperature (150 °C/300 °F). Anhydrous methanol attacks magnesium alloys catastrophically at room temperature; however, the rate of attack is reduced by the presence of water. Gasoline-methanol fuel blends, in which the water content equals or exceeds about 0.25 wt% of the methanol content, do not attack magnesium.

Pure halogenated organic compounds do not attack magnesium at ambient temperatures. At elevated temperatures, or if water is present, such compounds can cause serious corrosion, particularly those compounds having acidic hydrolysis products.

Dry fluorinated hydrocarbons, such as the freon refrigerants, do not attack magnesium

alloys at room temperature, but when water is present they may stimulate significant attack. At elevated temperatures, fluorinated hydrocarbons may react violently with magnesium alloys.

Acidic foodstuffs, such as fruit juices and carbonated beverages, attack magnesium seriously. Milk causes attack, particularly when souring. At room temperatures ethylene-glycol solutions cause minor corrosion of magnesium that is used alone or galvanically connected to steel; at elevated temperatures such as 115 °C (240 °F), the rate increases and the corrosion is serious enough to preclude the use of solutions of ethylene glycol and water in liquid-cooled magnesium engines. Anhydrous propylene glycol coolant is reported to be successfully used in prototype magnesium-alloy engines having modified cooling systems.

2.6. The present status of corrosion study

Recently, Song et al. [8, 19, 20] Verbrugge [10], Lee [11] and Warkus [6] studied the galvanic corrosion aspect. By studying the microstructure of galvanic corrosion, Song's group studied the galvanic corrosion of magnesium and its alloy (AZ91D) in 5% NaCl solution. They gave details of the model of galvanic corrosion and designed an elaborate test panel to measure the distribution of the galvanic corrosion current density. They also used boundary element method to simulate the distribution of the corrosion and compared the results with the experiment results. Verbrugge studied the galvanic corrosion of two dissimilar semi-infinite conductive materials. They arrange two contacting metals in a plane and model the galvanic corrosion in an ionic conduction liquid system. Lee studied the galvanic corrosion of Ni/Fe interface (zinc was coated on steels) under a thin layer of electrolyte. By studying the microstructure of AZ-series magnesium [19, 26, 27, 30,], Apachitei [26], Shkurankov [27], Jia [19] and Song [19, 30] et al. reveal the micro-galvanic corrosion of magnesium alloys. Based on the technology of micro-electrochemistry such as microcell, scanning vibrating electrode and scanning Kelvin probe force microscopy, it is possible to investigate the local electrochemistry of structural features such as grain boundaries, second phase particles and solid solutions in different environments. This is particularly important for new magnesium alloys

development and application. The SKPFM techniques are used to study the magnesium alloys [19, 26, 45-48,]. The findings suggest that the Volta potential differences between the inter-metallics and the matrix, as well as the size, area fraction and distribution of micro-galvanic cells, may influence the local matrix corrosion rates and the general corrosion behaviour of the alloys.

S. M. Sharland et al. [2] gave us a good example in study of the pitting and crevice corrosion of iron in NaCl solution. They used FEM to model the propagation of corrosion crevices and pits. Based on this model, J. Warkus et al. [6] studied the corrosion of iron in the concrete environment. V. Botte et al. [3] studied the corrosion of iron in the acidic aqueous solution. F. D. A. Aarão Reis et al. [49] used the electrochemical basis of the model and the statistical model to simulate the corrosion of metal in an acidic or neutral medium.

2.6.1 The principle of corrosion

In summary, from an electrochemical approach, all corrosion reactions can be classified into anodic and cathodic processes [30]. The electrochemical process, which normally occurs at the galvanic couple of metals, is:

$$\text{Anode: M (metal)} \rightarrow M^{n+} + ne^-,$$
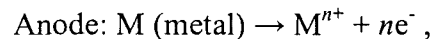
Where n is the valence of the metal.

$$\text{For magnesium: Mg} \rightarrow Mg^{2+} + 2e^-$$

$$\text{For iron: Fe} \rightarrow Fe^{2+} + 2e^-$$

$$\text{For zinc: Zn} \rightarrow Zn^{2+} + 2e^-$$

$$\text{Cathode: } 2H^+ + 2e^- \rightarrow H_2 \qquad \text{(dilute acidic solution)}$$

$$\text{Cathode: } 2H_2O + 2e^- \rightarrow H_2 + 2(OH)^- \qquad \text{(neutral or alkaline solution)}$$
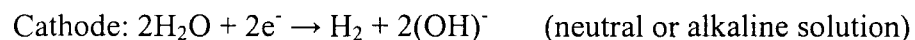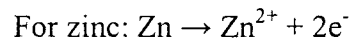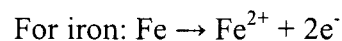
For magnesium and it alloys, in salt environments, the high solubility and acidic nature of the magnesium chloride formed at the anode can result in rapid penetration of magnesium alloys. Proper protection against galvanic corrosion begins with good design. This includes good drainage to prevent entrapment of electrolyte, selection of the most compatible metals, sealing of faying surfaces, small ratios of cathode to anode area, and use of alkali-resistant barrier coatings.

The closest approach to compatibility with magnesium is provided by aluminum alloys of the 5000-6000 series. Tin, cadmium, and zinc plating on steel fasteners reduces galvanic action on magnesium in salt spray by 60%-70%, which is sufficient for many practical applications. Supplementary polymer coatings on the plating can reduce galvanic corrosion further.

Additional resistance in the metallic or electrolytic portions of the galvanic cell circuit can reduce or eliminate galvanic current flow. Such resistance can be supplied by insulating materials such as non-metallic bolts, insulating washers or tapes, or organic coatings.

The combination of a small magnesium anode and a large cathode area can lead to intense corrosion penetration of the magnesium. In painting a galvanic couple, the cathode or the entire couple must be coated. In no case should the magnesium alone be coated. Small areas of magnesium exposed to paint defects or scratches could be subjected to intense corrosion penetration.

As a matter of fact, magnesium has a negative free-corrosion potential, E_{corr}, with a slightly more negative pitting potential, E_p, in solutions of practical importance such as 3% or 5% NaCl.

Pitting is an insidious and destructive form of corrosion: (1) it is difficult to detect. Pits may be small on the surface, but extensive below the surface from undercutting. They may be covered with deposit. (2) this can cause equipment to fail (by perforation) with very little weight loss. (3) It is difficult to measure as pit depth and distribution vary widely under (nominally) identical conditions. (4) The incubation period may be months or years. Pits usually occur on upward-facing horizontal surfaces, less frequently on vertical surfaces, rarely on downward-facing surfaces.

At the pitting potential the surface film begins to break down, and both hydrogen evolution and magnesium dissolution become much easier on the film free area. With

increasing potential, the film-free area increases, so there is more hydrogen evolution.

2.6.2. Governing equation of corrosion

Though the process of corrosion is determined by many variables such as the properties of the material itself, the environment characteristics and others [3, 50-53], the mass transport is a centrally important aspect. Convection, migration and diffusion are the main three factors involved. Based on the Planck-Nernst law [3, 10, 54], the mass flux $\vec{N}_k$ of species k in a specific medium (usually diluted acid or salt solution, even water) can be expressed as [2, 3, 5]

$$\vec{N}_k = -D_k \nabla c_k - \frac{z_k F D_k}{RT} c_k \nabla \phi \qquad (2\text{-}25)$$

where c_k represents the concentration of species k, D_k is the effective diffusion coefficient, z_k is the charge number, F is the Faraday's constant, ϕ is the electrostatic potential, R is the universal gas constant and T is the absolute temperature. For a flowing solution, Eq. (2-25) may be modified to [10]

$$\vec{N}_k = -D_k \nabla c_k - \frac{z_k F D_k}{RT} c_k \nabla \phi + c_k \vec{v} \qquad (2\text{-}26)$$

Where $\vec{v}$ represents the flowing velocity of the solution, usually, the solution is static or flows very slow. Thus the last term in Eq. (2-26) is negligible. The mass transport process can be expressed by a transport equation [2, 3, 5, 10], the mole balance of species k is

$$\frac{\partial c_k}{\partial t} = -\nabla \cdot \vec{N}_k + S_k \qquad (2\text{-}27)$$

Where S_k is the term of source (or sink) which represents the production (or depletion) of ions of species k. by putting Eqs. (2-25) and (2-27) together, we get a governing equation for expressing the corrosion process.

$$\frac{\partial c_k}{\partial t} = \nabla \cdot (D_k \nabla c_k) + \frac{z_k F}{RT} \nabla \cdot (D_k c_k \nabla \phi) + S_k \qquad (2\text{-}28)$$

It is the convection-diffusion transport equation. The transport velocity is proportional to $\nabla \phi$. In dilute aqueous solutions the diffusion coefficients of most ions are similar and have values that at room temperature are in the range of 0.6×10^{-9} to 2×10^{-9} m^2/s [55]. Eq. (2-28) becomes

$$\frac{\partial c_k}{\partial t} = D\nabla^2 c_k + \frac{z_k FD}{RT}\nabla \cdot (c_k \nabla \phi) + S_k \qquad (2\text{-}29)$$

Because corrosion usually happens on the surface of metal which is the interface between the medium (electrolyte) and metal, it can be taken as the boundary condition. Anyway, there is no source in the medium, $S_k=0$, in this case, Eq. (2-29) becomes

$$\frac{\partial c_k}{\partial t} = D\nabla^2 c_k + \frac{z_k FD}{RT}\nabla \cdot (c_k \nabla \phi) \qquad (2\text{-}30)$$

If the ions of the species distribute spatially uniform in the medium, Eq. (2-30) reduces to

$$\frac{dc_k}{c_k dt} = \frac{z_k FD}{RT}\nabla^2 \phi \qquad (2\text{-}31)$$

The solution composition must be electrically neutral, so

$$\sum_k z_k c_k = 0 \qquad (2\text{-}32)$$

In the steady state, Eq. (2-30) becomes,

$$D\nabla^2 c_k + \frac{z_k FD}{RT}\nabla \cdot (c_k \nabla \phi) = 0 \qquad (2\text{-}33)$$

If the ions of the species distribute uniformly in the medium, then Eq. (2-32) reduces to the Laplace equation.

$$\nabla^2 \phi = 0 \qquad (2\text{-}34)$$

For different kinds of corrosion, the related factors are different, so the form of differential equation may be different especially the boundary conditions are absolutely different. We can use different numerical methods to solve the different problems.

2.6.3. Boundary conditions

Numerical modeling starts from boundary conditions. As we have discussed, the potential in the space can be expressed as $\phi(x, y, z)$ and it is determined by a governing equation. Correspondingly, the localized current density in the space can be expressed as:

$$i(x, y, z) = -\sigma \nabla \phi(x, y, z) \qquad (2\text{-}35)$$

Where σ is the conductivity of the medium of corrosion environment (usually a kind of electrolyte). So, the boundary condition can be:

$$\phi(x_k, y_k, z_k) = U_0 \qquad (2\text{-}36)$$

If we know the potential U_0 at a certain point $\phi(x_k, y_k, z_k)$. Or,

$$-\sigma \frac{\partial \phi}{\partial n} = i \qquad (2\text{-}37)$$

If we know the current density i at a certain point, the **n** is the normal direction at the certain point. On an insulator surface, (e.g. the surface of a metal is covered by a layer of insulator film) there is no current in the normal direction, so the boundary condition is

$$-\frac{\partial \phi}{\partial n} = 0 \qquad (2\text{-}38)$$

On the exposed surface of an anode and cathode,

$$i = -\sigma \frac{\partial \phi}{\partial n} = i_0 f(\phi - \phi_0) \qquad (2\text{-}39)$$

In fact, the polarization in galvanic corrosion, the relationship between the current density i and the overvoltage $\phi - \phi_0$, is a complicated function. It depends on the types of metals and electrolytes as well as the temperatures. Additionally, the exact position of the electrodes in the corrosion process on the exposed metal surface depends on many factors and it is extremely difficult to be predicted [3]. This makes the corrosion process of metal be complicated. Usually, we can use Butler-Volmer equation or Tafel equation to express [55, 56]:

(1) According to the Tafel equation [55, 56], when an anode reaction occurs on the anode,

$$i_{anodic} = -\sigma \frac{\partial \phi}{\partial n} = i_0 \exp[\frac{\gamma z F}{RT}(\phi - \phi_0)] \qquad (2\text{-}40)$$

When a cathode reaction occurs on the cathode,

$$i_{cathodic} = -\sigma \frac{\partial \phi}{\partial n} = i_0 \exp[-\frac{(1-\gamma)zF}{RT}(\phi - \phi_0)] \qquad (2\text{-}41)$$

Where γ is a symmetry factor which can be determined by experiment (a good estimation is ½), i_0 is the exchange current density, z is the valence number. Both i_0 and ϕ_0 depend on factors such as the ion concentration in the electrolyte and the type of reference electrode used for potential measurements.

Let $\alpha = \dfrac{RT}{\gamma z F}$ and $\beta = \dfrac{RT}{(1-\gamma)zF}$, then

$$\frac{1}{\alpha} + \frac{1}{\beta} = \frac{zF}{RT} \qquad (2\text{-}42)$$

(2) When both the anode reaction and the cathode reaction occur on the same electrode, the electrode reaction is controlled by electrical charge transfer at the electrode:

$$i = -\sigma \frac{\partial \phi}{\partial n} = i_0[e^{\alpha(\phi-\phi_0)} - e^{-\beta(\phi-\phi_0)}] \qquad (2\text{-}43)$$

This is called Butler-Volmer equation. Usually, i_0 is also called corrosion current density and written as i_{corr}. Correspondingly, ϕ_0 is also called free corrosion potential and written as ϕ_{corr}. Equation (2-43) can also be written as:

$$i = i_{corr}[\exp(\frac{\phi-\phi_{corr}}{b_a}\ln 10) - \exp(-\frac{\phi-\phi_{corr}}{b_c}\ln 10)] \qquad (2\text{-}44)$$

The polarization curve is shown in the following Fig. 2-1 [5].

Fig. 2-1 polarization curve of Butler-Volmer equation [5]
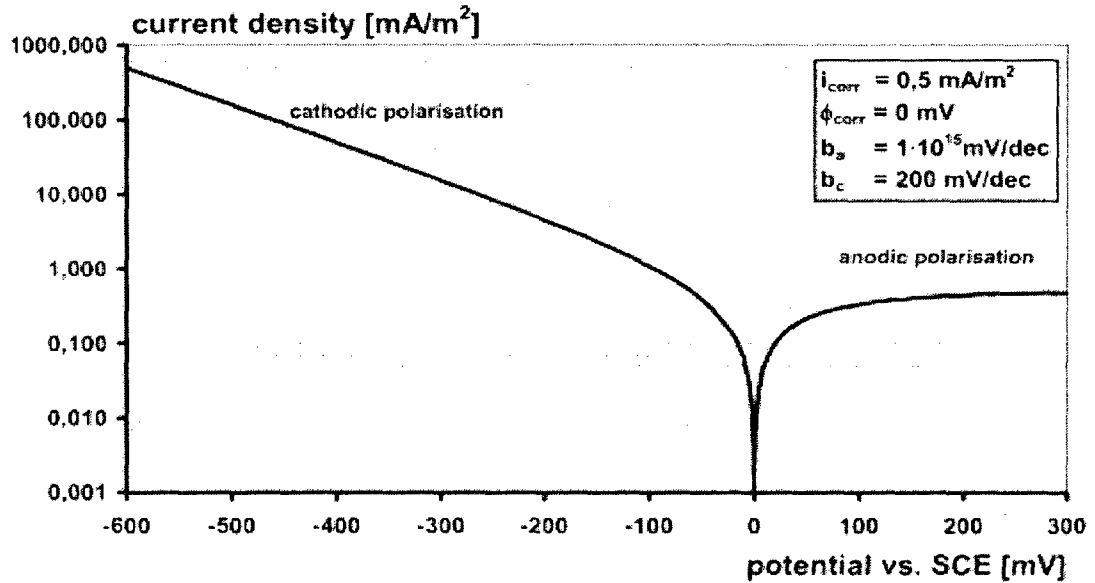
In the low over potential region, $\phi - \phi_0$ is small, Eq. (2-43) reduces to linear situation [9]:

$$i = -\sigma \frac{\partial \phi}{\partial n} = i_0 \frac{zF}{RT}(\phi - \phi_0) \qquad (2\text{-}45)$$

In the high over potential region, $\phi - \phi_0$ is large, Eq. (2-43) reduces to Tafel equation:

$$i \approx i_0 e^{\alpha(\phi-\phi_0)} \qquad (2\text{-}46)$$

29

2.6.4. Practical examples

Example 1: The crevice and pitting corrosion of magnesium

In reference [2], S. M. Sharland et al. gives us a good example for dealing with the problem of pitting or crevice corrosion.

The steady-state transport equation for species i is given

$$D_i(\frac{\partial^2 c_i}{\partial x^2} + \frac{\partial^2 c_i}{\partial y^2} + \frac{\partial^2 c_i}{\partial z^2}) + \frac{z_i D_i F}{RT}[\frac{\partial}{\partial x}(c_i\frac{\partial \phi}{\partial x}) + \frac{\partial}{\partial y}(c_i\frac{\partial \phi}{\partial y}) + \frac{\partial}{\partial z}(c_i\frac{\partial \phi}{\partial z})] + R_i = 0 \qquad (2\text{-}47)$$

If c_i does not change spatially, eq. (2-47) reduces to Poisson's equation:

$$\nabla^2\phi = \rho / \varepsilon \qquad (2\text{-}48)$$

If the crevice is a very long rectangular geometry, eq. (2-47) reduces to a 1-D problem. On the much larger scale of pits and crevices, the solution composition must be electrically neutral [2].

$$\sum_i z_i c_i = 0$$

The boundary condition on reactive surface is

$$\frac{i_d}{z_i F} = \vec{N_1} \cdot \vec{n} . \qquad (2\text{-}49)$$

Here, **n** is the outward unit normal vector at the surface, i_d is the reaction current density. For the anodic reaction, Turnbull and Gardiner [57] found that between pH3 and pH8.5, the dissolution current is satisfied the following expression [2]:

$$i = i_0 e^{\alpha FE/RT} \qquad (2\text{-}50)$$

And $E = \phi_M - \phi$, is the potential driving the corrosion reaction.

Where, ϕ_M is defined as the electrical potential of the corroding metal relative to some standard electrode in the bulk solution and ϕ as the potential drop in the solution in the crevice.

At first, let us consider the situation of pure magnesium. Suppose the magnesium is covered with a passive film and there is sufficient generation of cathodic charge on the outer surface to drive the localized corrosion. If there is a crevice and the covered surface film is broken there, some solution can get into the crevice resulting in corrosion. Suppose the solution is dilute NaCl. There are Mg^{2+}, $MgOH^+$, Na^+, Cl^-, H^+ and OH^-. The electrochemical reaction of corrosion is:

30

$$Mg \rightleftharpoons Mg^{2+} + 2e^-$$

$$Mg^{2+} + H_2O \rightleftharpoons Mg(OH)^+ + H^+ \tag{2-51}$$

$$Mg(OH)^+ + H_2O \rightleftharpoons Mg(OH)_2 + H^+ \tag{2-52}$$

$$H^+ + OH^- \rightleftharpoons H_2O \tag{2-53}$$

$$Mg^{2+} + Cl^- \rightleftharpoons MgCl^+ \tag{2-54}$$

$$MgCl^+ + Cl^- \rightleftharpoons MgCl_2 \tag{2-55}$$
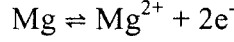
For a very long rectangular crevice, the steady-state transport equation for species i become:

$$D_i \frac{d^2 c_i}{dx^2} + \frac{z_i D_i F}{RT} \frac{d}{dx}(c_i \frac{d\phi}{dx}) + R_i = 0 \tag{2-56}$$

$c_1 = [Mg^{2+}]$, $c_2 = [MgOH^+]$, $c_3 = [Cl^-]$, $c_4 = [Na^+]$, $c_5 = [H^+]$, $c_6 = [OH^-]$.

The concentrations of the species are fixed at the crevice mouth and are equal to the values in the bulk solution outside the corrosion site. Suppose the forward and backward rate constant of the reactions in equations (22-49) to (2-51) are respectively k_{1F}, k_{1B}, k_{2F}, k_{2B}, k_{3F} and k_{3B}. The governing equations for every single ion/cluster are:

$$D_1[\frac{d^2 c_1}{dx^2} + \frac{2F}{RT} \frac{d}{dx}(c_1 \frac{d\phi}{dx})] - k_{1F}c_1 + k_{1B}c_2 c_5 = 0 \tag{2-57}$$

$$D_2[\frac{d^2 c_2}{dx^2} + \frac{F}{RT} \frac{d}{dx}(c_2 \frac{d\phi}{dx})] + k_{1F}c_1 - k_{1B}c_2 c_5 - k_{2F}c_3 + k_{2B}c_5 = 0 \tag{2-58}$$

$$D_3[\frac{d^2 c_3}{dx^2} - \frac{F}{RT} \frac{d}{dx}(c_3 \frac{d\phi}{dx})] = 0 \tag{2-59}$$

$$D_4[\frac{d^2 c_4}{dx^2} + \frac{F}{RT} \frac{d}{dx}(c_4 \frac{d\phi}{dx})] = 0 \tag{2-60}$$

$$D_5[\frac{d^2 c_5}{dx^2} + \frac{F}{RT} \frac{d}{dx}(c_5 \frac{d\phi}{dx})] + k_{1F}c_1 - k_{1B}c_2 c_5 + k_{2F}c_3 - k_{2B}c_5 + (k_{3F} - k_{3B})c_5 c_6 = 0 \tag{2-61}$$

$$D_6[\frac{d^2 c_6}{dx^2} - \frac{F}{RT} \frac{d}{dx}(c_6 \frac{d\phi}{dx})] + (k_{3F} - k_{3B})c_5 c_6 = 0 \tag{2-62}$$

$$2c_1 + c_2 - c_3 + c_4 + c_5 - c_6 = 0 \tag{2-63}$$

The boundary condition: the flux of species involved in the electrode processes (Mg^{2+}) is proportional to the corresponding current at the crevice tip. The flux of the other species at the crevice tip is zero.

$$D_1[\frac{dc_1}{dx} + \frac{2F}{RT}(c_1\frac{d\phi}{dx})]|_{x=0} = \frac{i_1}{2F}\exp[\alpha_1 F(\phi_M - \phi)/RT] \tag{2-64}$$

$$D_2[\frac{dc_2}{dx} + \frac{F}{RT}(c_2\frac{d\phi}{dx})]|_{x=0} = 0 \tag{2-65}$$

$$D_3[\frac{dc_3}{dx} - \frac{F}{RT}(c_3\frac{d\phi}{dx})]|_{x=0} = 0 \tag{2-66}$$

$$D_4[\frac{dc_4}{dx} + \frac{F}{RT}(c_4\frac{d\phi}{dx})]|_{x=0} = 0 \tag{2-67}$$

$$D_5[\frac{dc_5}{dx} + \frac{F}{RT}(c_5\frac{d\phi}{dx})]|_{x=0} = 0 \tag{2-68}$$

$$D_6[\frac{dc_6}{dx} - \frac{F}{RT}(c_6\frac{d\phi}{dx})]|_{x=0} = 0 \tag{2-69}$$

Example 2: Galvanic corrosion of magnesium covered with zinc

The corrosion protection of magnesium is very important; it has practical meaning. More detail study about the galvanic corrosion even micro-galvanic corrosion is expected though some excellent research works have been done [8, 30, 58-

Fig. 2-2 the geometry of the contaier

65]. Because of the effective corrosion protection and low cost, zinc is a popular material used for steel surface coating [66]. Today, we use profuse amounts of magnesium alloys in the automotive and aircraft industries. We also use zinc as a surface protective material and coat it on the surface of magnesium alloys. Under many environmental conditions, zinc may corrode by a factor of 5–100 times slower than iron [67, 68], even much slower than magnesium. The α-phase and the secondary β-phase of microstructure and some impurity grains in AZ-type alloys lead micro-galvanic corrosion [8, 19, 30, 69-75]. Therefore, it is very useful and practical to do some experimental and numerical modeling studies relative to the corrosion of magnesium alloys if the protection cover is broken in some area. Here, we only consider the galvanic corrosion. Suppose there is a magnesium

rectangular container ($2a \times 2b \times c$) that contains some alkaline or neutral liquid (height is h). Every wall of the container is covered by an insulator protective film. On the bottom, it is covered by a zinc protective film. There is an area where the protective film is broken. Then the corrosion happens there. Because the container is large and the corrosion process is relatively slow, we suppose the concentration of any particle is uniformly spaced. Because there is no source in the liquid, the distribution of the potential in the liquid meets:

$$\frac{\partial^2 \phi}{\partial x^2} + \frac{\partial^2 \phi}{\partial y^2} + \frac{\partial^2 \phi}{\partial z^2} = 0 \tag{2-70}$$

Where $-a \le x \le a$, $-b \le y \le b$, $0 \le z \le c$

There are three reactions in the corrosion process. They are:

Anode reaction on Mg: $Mg \rightarrow Mg^{2+} + 2e^-$

Cathode reaction: $O_2 + 4H^+ + 4e^- \rightarrow 2H_2O$

Anode reaction on Zn: $Zn \rightarrow Zn^{2+} + 2e^-$

We define the potential of the metals is V=0. The boundary conditions are:

(1) On the surface of each wall as well as the interface of air/electrolyte,

$$\frac{\partial \phi}{\partial n} = 0 \tag{2-71}$$

Where $\mathbf{n}$ is the outward direction of the normal of every surface.

(2) On the surface of Mg, z=0, $|x| < l$, $|y| < w$, both the mass-transfer limited reduction of oxygen and magnesium oxidation occurs:

$$\frac{\partial \phi}{\partial z}\Big|_{z=0} = -\frac{zFC_{O_2,sat}D_{O_2}}{\sigma h} - \frac{i_{0Mg}}{\sigma}\{\exp[\frac{\gamma_{Mg}zF}{RT}(\phi - \phi_{MgCorr})] - \exp[-\frac{(1-\gamma_{Mg})zF}{RT}(\phi - \phi_{MgCorr})]\} \tag{2-72}$$

In the linear polarization region, we have

$$\frac{\partial \phi}{\partial z}\Big|_{z=0} = -\frac{zFC_{O_2,sat}D_{O_2}}{\sigma h} - \kappa_{Mg}(\phi - \phi_{0Mg})] \tag{2-73}$$

Where $\kappa_{Mg} = \dfrac{i_{0Mg}zF}{\sigma RT}$

(3) On the surface of Zn, z=0, $l < |x| < a$, $w < |y| < b$,

$$\frac{\partial \phi}{\partial z}\Big|_{z=0} = -\frac{i_{0Zn}}{\sigma}\{\exp[\frac{\gamma_{Zn}zF}{RT}(\phi - \phi_{ZnCorr})] - \exp[-\frac{(1-\gamma_{Zn})zF}{RT}(\phi - \phi_{ZnCorr})]\} \tag{2-74}$$

In the linear polarization region, we have

$$\frac{\partial \phi}{\partial z}\bigg|_{z=0} = -\kappa_{Zn}(\phi - \phi_{0Zn})]$$ (2-75)

Where $\kappa_{Zn} = \dfrac{i_{0Zn}zF}{\sigma RT}$

Let us use FEM to solve this problem. The approximate function can be expressed as:

$$\phi = \sum \phi_n N_n$$ (2-76)

The weak formulation of equation (2-70) is

$$\iiint\limits_{\Omega} dV \left(\frac{\partial \phi}{\partial x}\frac{\partial \delta\phi}{\partial x} + \frac{\partial \phi}{\partial y}\frac{\partial \delta\phi}{\partial y} + \frac{\partial \phi}{\partial z}\frac{\partial \delta\phi}{\partial z} \right) = \iint\limits_{S} dS \frac{\partial \phi}{\partial n}\delta\phi$$ (2-77)

Because we cannot predict the locations of the electrode reaction and the polarization is complicated, a success modeling of the corrosion should be combined with experiments. From these examples of corrosion, we know that, the corrosion problem is the differential equation plus boundary condition, mostly, they are non-linear conditions. It is difficult to get a complete analytic solution. Numerical methods such as BEM, FEM and FDM become useful tools for these kinds of problems. In next section, we introduce the FEM and the FDM and then take example 2 as a sample calculation.

2.7. Consideration of the composition of magnesium alloy

Though we can find many references about the research of magnesium corrosion, some performed detailed research experimentally to evaluate the microstructure effect (such as α-phase and β-phase) on the corrosion behavior of Mg-alloys [28, 76], no one performed a numerical modeling or theoretical modeling to express the micro-process of the micro-galvanic corrosion theoretically and connect them to the composition of alloy elements. We know that the composition of alloy elements influences the corrosion properties seriously [77-82]; small ratio of Fe/Ni/Cu may heavily decrease the corrosion resistance. If we can set up a model to express the micro-process theoretically, that is really practical and meaningful. As we mentioned above, magnesium alloys are mainly composed by elements Al, Mn, Si, Cu, Zn, Ni and Fe. The chemical composition is about: Al: 6-10%, Mn: 0.1-0.3%, Si: 0.1-0.5%, Cu: 0.01-0.35%, Zn: 0.2-1%. The rate of Ni and Fe is very small. Though they can be mixed atomically uniform, every kind of alloy elements can still form a galvanic cell in the magnesium environment. We also call it micro-galvanic

cell. There may be some α-phase (Mg-Al-Zn solid solution), β-phase (Mg$_{17}$Al$_{12}$), Al-grains and impurities. Because the size of them is small, we collectively call them micro-grains. Because magnesium is chemically about 90%, the ratio of other elements is very small. Thus the possibility of forming galvanic cells between any other two alloy elements is very small. Then all the micro-galvanic cell is formed between one kind of the alloy elements/micro-grains and magnesium. The number of micro-galvanic cells should be proportional to the composition rate. Here we only take elements Al and Zn as an example. Assume the composition chemically Al 9% and Zn 1%, we can estimate the number of Al and Zn in a unit area. The number of galvanic cells should be proportional to the number of Al and Zn in a unit area. The number of Mg-Al micro-galvanic cells is about 10 times the number of Mg-Zn micro-galvanic cells. We may get the statistical number by experiment. Because $\phi^{\circ}{}_{Mg}$=-2.37V, $\phi^{\circ}{}_{Al}$=-1.67V, $\phi^{\circ}{}_{Zn}$=-0.76V. Mg is always an anode. In every micro-galvanic cell, Al and Zn are small grains of metal. Because the size of Mg or Zn grains is very small, we can take the potential on the surface of Al grains or Zn grains as a constant $\phi(\mathbf{r})$. The situation is show in Fig. 2-3.
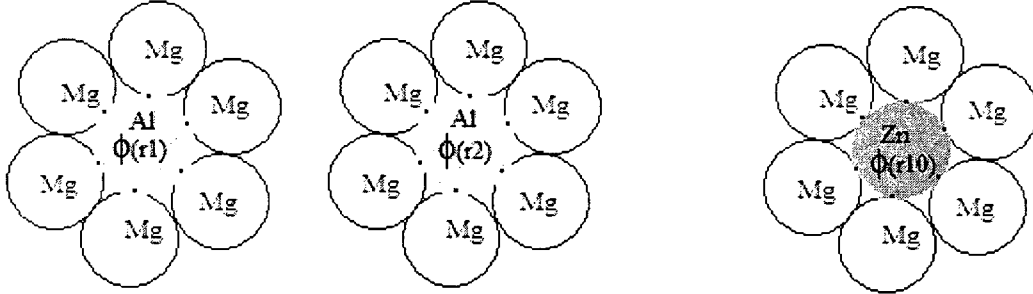
Fig. 2-3 Schematics of microgalvanic cells

At every connect point of Al-Mg, the potential should be the same as on the surface of Al grain. The overpotential on the Al grain is $E_{Al} = \phi - \phi_{0Al}$. According to the polarization relationship Eq. (2-39), for Al grain, the current density on the surface of Al grain can be expressed as:

$$i_{Al} = i_{0Al} f_c (\phi - \phi_{0Al}) \qquad (2\text{-}78)$$

Where, f_c is the polarization function of cathode. From Eq. (2-85), we can get:

$$\phi - \phi_{0Al} = f_c^{-1}(i_{Al}/i_{0Al}) . \qquad (2\text{-}79)$$

Similarly, for magnesium (anode), the overpotential at the connect point is $\phi - \phi_{0Mg}$, so

$$i_{Mg} = i_{0Mg} f_a (\phi - \phi_{0Mg})$$ (2-80)

Where, f_a is the polarization function of anode. From Eq. (2-87), we can get:

$$\phi - \phi_{0Mg} = f_a^{-1} (i_{Mg} / i_{0Mg})$$ (2-81)

As we know, electron currents always flow out from anode and flow in to cathode. The direction of the current density on the anode and that on the cathode is reverse, so the current density at the connect point is zero. Then

$$i_{Al} + i_{Mg} = i_{0Al} f_c (\phi - \phi_{0Al}) + i_{0Mg} f_a (\phi - \phi_{0Mg}) = 0$$ (2-82)

We can get the potential and the current density at the connect point. As an example, we suppose a linear polarization on both anode and cathode:

$$i_{Mg} = i_{0Mg} \frac{zF}{RT} (\phi - \phi_{0Mg}) = \kappa_a (\phi - \phi_{0Mg})$$ (2-83)

$$i_{Al} = i_{0Al} \frac{zF}{RT} (\phi - \phi_{0Al}) = \kappa_c (\phi - \phi_{0Al})$$ (2-84)

$$\phi = \frac{\kappa_a \phi_{0Mg} + \kappa_c \phi_{0Al}}{\kappa_a + \kappa_c}$$ (2-85)

$$i_{Mg} = -i_{Al} = \frac{\kappa_a \kappa_c (\phi_{0Al} - \phi_{0Mg})}{\kappa_a + \kappa_c}$$ (2-86)

Though all the alloy elements such as Al, Zn, Fe, Ni and Cu are small grains encircled by Mg, in an aqueous or moisture environment, they may cause the Mg around them to corrode in a small area, especially, the magnesium around Cu grains. Gradually, the proper structure is damaged.

It is creditable to research further the corrosion of alloy elements.

2.8. Negative difference effect of magnesium and discussion

In a normal situation, when we use the Butler-Volmer equation to express the corrosion system, the polarization is:

$$i_{net} = i_0 \{ \exp[\frac{\gamma_{Mg} 2F}{RT} (\phi - \phi_{MgCorr})] - \exp[-\frac{(1 - \gamma_{Mg}) 2F}{RT} (\phi - \phi_{MgCorr})] \}$$ (2-87)

Assume $i_0 = 1.0 \times 10^{-2} A/m^2$, $\phi_{MgCorr} = -1.7V$, then

$$i_{net} = 1.0 \times 10^{-2} \{ \exp[\frac{\gamma_{Mg} 2F}{RT} (\phi + 1.7)] - \exp[-\frac{(1 - \gamma_{Mg}) 2F}{RT} (\phi + 1.7)] \}$$ (2-88)

By using Mat lab, we show the current-potential polarization of magnesium based on the Butler-Volmer equation (2-88) in Fig. 2-4.
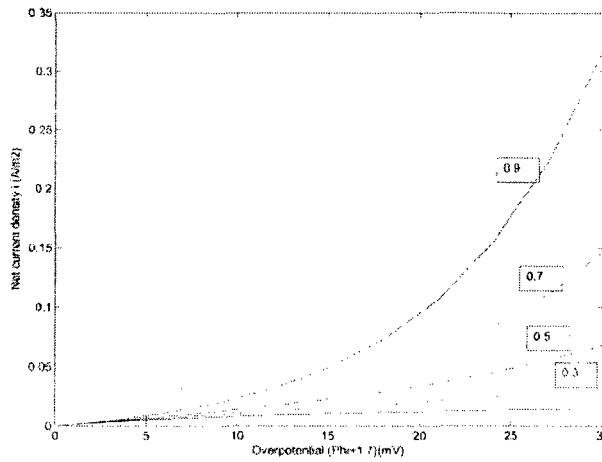
Fig2-4 Net current – potential curves of magnesium electrode for different γ

We can separate it into anodic reaction part and cathodic reaction part:

$$i_a = 1.0 \times 10^{-2} \exp[\frac{2\gamma_{Mg}F}{RT}(\phi + 1.7)] \qquad (2-89)$$

$$i_c = 1.0 \times 10^{-2} \exp[-\frac{2(1-\gamma_{Mg})F}{RT}(\phi + 1.7)] \qquad (2-90)$$

The polarizations for both anodic reaction and cathodic reaction are shown in Fig. 2-5 and Fig. 2-6.
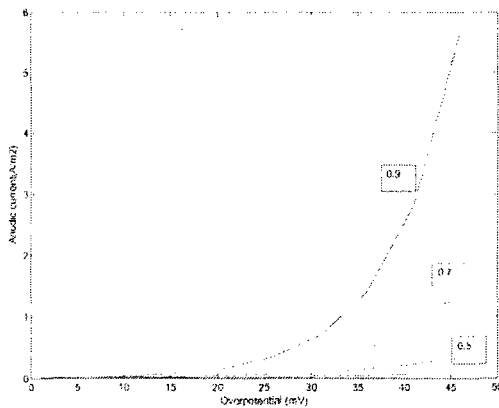
Fig2-5 the current—potential curves of anodic reaction for different γ
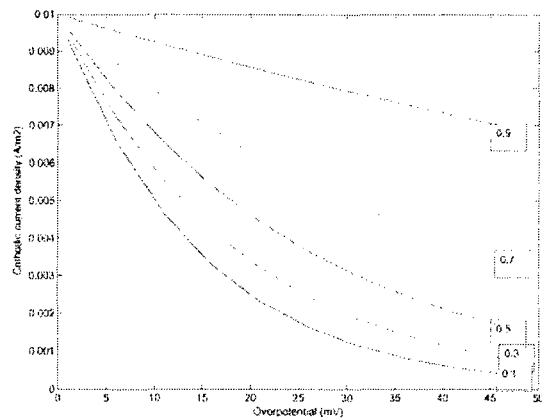
Fig2-6 the current—potential curves of cathodic reaction for different γ
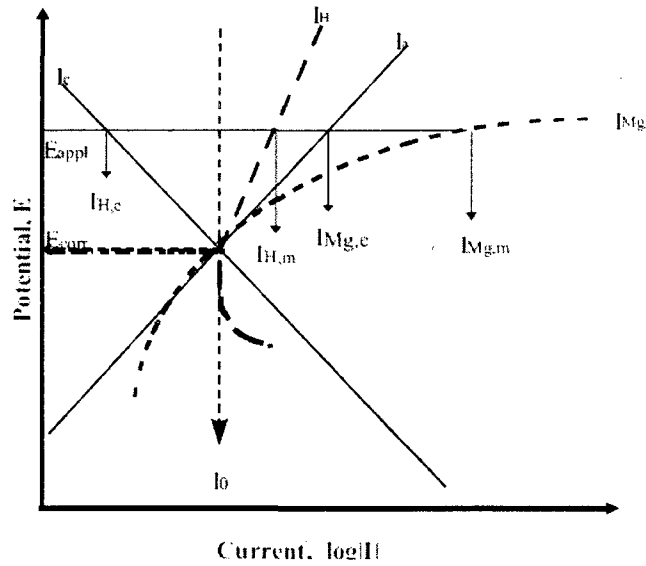
Fig.2-7 Schematic of the negative difference effect [30]

Experimentally, Song [30] and Atrens [83] et al. found that the magnesium and its alloys show the negative difference effect, which is shown in Fig. 2-7. Normally, for most metals such as Fe and Cu, when the potential, E_{appl}, is higher than the corrosion potential E_{corr} (corresponding current is I_0), the current on the cathode (along I_c), $I_{H,e}$, should be less than I_0 and that on the anode (along I_a), $I_{Mg,e}$, should be greater than I_0. However, for magnesium, the situation is totally different. Experiment results show that, instead of decreasing to $I_{H,e}$, the hydrogen evolution reaction rate increases to $I_{H,m}$ along the dash line I_H. Simultaneously, the dissolution current of the anodic magnesium increases faster (along the dash curve I_{Mg} to $I_{Mg,m}$) than expected (along the real line I_a to $I_{Mg,e}$). In summary, there are two aspects for the negative difference effect:

(1) The difference Δ between the spontaneous rate of the hydrogen evolution reaction (HER) on the Mg surface at the free corrosion potential and corresponds to the measured HER rate for the applied galvanostatic current $I_{applied}$ is negative, namely, $\Delta = I_0 - I_H < 0$, which is different from most metals such as Fe and Zn [83].

(2) The dissolution current I_{Mg} of the anodic magnesium increases faster than expected.

Song and Atrens [30] explained this anomalous behavior by proposing that the area free of surface film increases with the increase of the applied potential E_{appl}. These film-free areas are crucial to the NDE behavior. In the film-free areas, magnesium corrosion occurs

with the production of univalent magnesium ions (Mg$^+$) and the subsequent generation of hydrogen.

Now let us approach the NDE behavior numerically from Butler-Volmer/Tafel equation. 50 years ago, Petty et al. [84] found that when electrolysis of an aqueous solution of any one of several salts is carried out between magnesium electrodes in a divided cell, the metal dissolves anodically with an initial mean valence number appreciably lower than two. Also, they found that the measured hydrogen evolution volume was always slightly greater than that calculated when sodium sulfate solution is used as the electrolyte. The results, it is believed, point strongly toward the conclusion that the primary reactions at a magnesium anode consist of the oxidation of the metal to both the unipositive (Mg$^+$) and the dipositive (Mg^{2+}) state. They indicated that the low initial valence numbers obtained by the oxidation of a magnesium anode might be due to some sort of anodic activation. However, what is "the some sort of anodic activation"? This is the most important question. Is there any possible answer for it?

We adopt the proposal and suppose there are two kinds of anodic reactions for magnesium loss: one produces univalent magnesium ions (Mg$^+$) and another produces bivalent magnesium ions (Mg^{2+}). Assume the number of Mg$^+$ is N_1 per molar and the number of Mg^{2+} is N_2 per molar. Then the effective/average valence of anode reaction is

$$\bar{z} = \frac{N_1 + 2N_2}{N_1 + N_2} \qquad (2\text{-}91)$$

Where, $1 \leq \bar{z} \leq 2$. The polarization of the anode is expressed:

$$i_{Mg} = i_0 \exp[\frac{\gamma \bar{z} F}{RT}(E_{appl} - E_{corr})] \qquad (2\text{-}92)$$

(1) When the over potential $E_{appl}-E_{corr}$ is low, mostly the anodic reaction for magnesium loss is as:

$2Mg \rightarrow 2Mg^+ + 2e$ (anodic partial reaction),
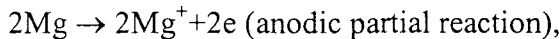
And then, $2Mg^+ + 2H_2O \rightarrow 2Mg^{2+} + 2OH^- + H_2$, is just a chemical reaction [30].

The cathodic partial reaction is: $2H^+ + 2e \rightarrow H_2$

There are mostly univalent magnesium ions (Mg$^+$) for magnesium dissolution reaction and $\bar{z} \approx 1$. Therefore,

$$i_{Mg} \approx i_0 \exp[\frac{\gamma F}{RT}(E_{appl} - E_{corr})] \qquad (2\text{-}93)$$

However, in the low overpotential region, the dissolution rate of magnesium is low, so the total number of Mg^+ is not big.

(2) When the over potential $E_{appl}-E_{corr}$ is high, mostly the anodic reaction for magnesium loss is as:

$Mg \rightarrow Mg^{2+}+2e$ (anodic partial reaction)
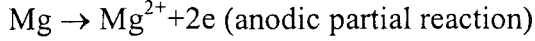
Still, the cathodic partial reaction is: $2H^+ + 2e \rightarrow H_2$

There are mostly bivalent magnesium ions (Mg^{2+}) for magnesium dissolution reaction and $\bar{z} \approx 2$. Therefore,

$$i_{Mg} \approx i_0 \exp[\frac{2\gamma F}{RT}(E_{appl} - E_{corr})] \qquad (2\text{-}94)$$

In the high overpotential region, the dissolution rate of magnesium is high, so the total number of both Mg^+ and Mg^{2+} is big even though $N_2 >> N_1$.

(3) In the middle region, both anodic partial reactions exist. (In fact, even for high over potential situation, there still exist some low over potential areas.)

$2Mg \rightarrow 2Mg^+ + 2e$ (N_1 Mg^+ produced from this anodic partial reaction)

$2H^+ + 2e \rightarrow H_2$ (I_{H1} produced from this cathodic partial reaction) $\qquad$ (2-95)

$2Mg^+ + 2H_2O \rightarrow 2Mg^{2+} + 2OH^- + H_2$

(I_{Hc}--$N_1/2$ H_2 produced from this chemical reaction) $\qquad$ (2-96)
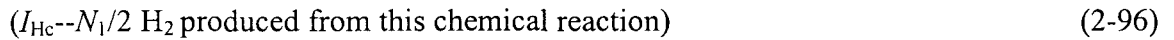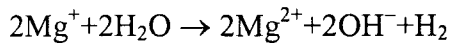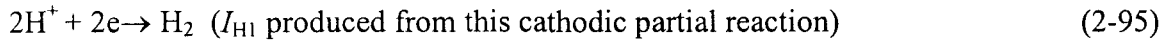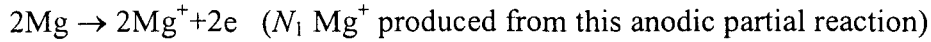
This reaction may occur slowly and Mg^+ can exist a sufficient long time for some minutes in aqueous solution [83] when the overpotential is very low. With the increase of the overpotential, this reaction may occur faster.

$Mg \rightarrow Mg^{2+}+2e$ (N_2 Mg^{2+} produced from this anodic partial reaction)

$2H^+ + 2e \rightarrow H_2$ (I_{H2} produced from this cathodic partial reaction) $\qquad$ (2-97)
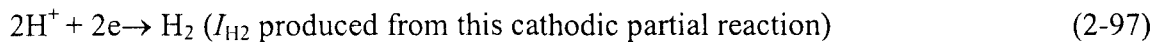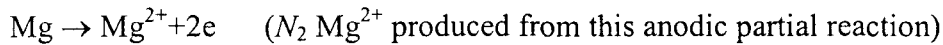
$\bar{z} = \dfrac{N_1 + 2N_2}{N_1 + N_2}$, the current density is expressed by equation (2-92)

In fact, as we have already known that the local potential between the electrode and the electrolyte distributes spatially different along the electrode surface. This makes the over potential distributes different along the electrode surface. Theoretically, if we know the critical value of over potential for producing univalent magnesium ions (Mg^+) and

bivalent magnesium ions (Mg^{2+}), we can calculate the rate of N_1/N_2 and then we know the value of $\bar{z}$. Here, we only give a qualitative discussion. The number N_2 of bivalent magnesium ions (Mg^{2+}) increases with the increase of the over potential $E_{appl}-E_{corr}$, so the anodic current density increases faster than expected because of the increase of $\bar{z}$ with the over potential going up. Eq. (2-92) may qualitatively explain the experiment result. The situation is shown in Fig. 2-8. We can try the curve fitting to get $\bar{z}$ by adjusting the symmetry factor γ and comparing with equation (2-91).
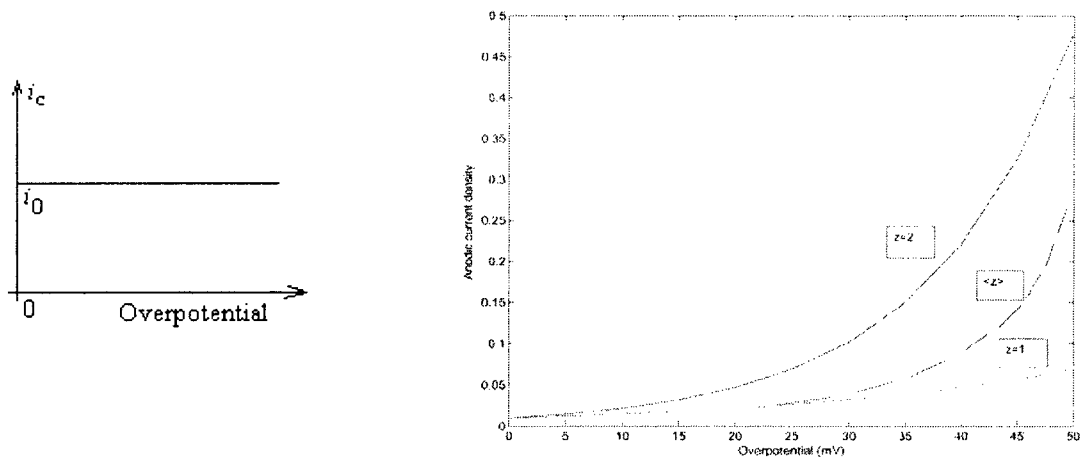
Fig2-8 the variation of current density on anode and cathode with NDE situation (γ=1)

On the other hand, the symmetry factor or the transfer coefficient is a very important parameter of the polarization for electrode reactions. It is related to the gradients of the potential energy-distance profile for the representative points of reactant and products [85]. If the slope of the relation near the intersection points is α for the product and β for the reactant [86, 87], then the symmetry factor can be expressed as:

$$\gamma = \frac{\tan\alpha}{\tan\alpha + \tan\beta} \qquad (2\text{-}98)$$

According to Bockris and Matthews [88], the symmetry factor γ is a coefficient controlling the transfer of electrical to chemical energy, it is also called transfer coefficient. Even today, only some very rudimentary attempts to calculate values of γ have been made. In practice, the symmetry factor γ is a coefficient determined by experiment. Based on the Tafel equation (2-89) for anode, we have:

$$\gamma = \frac{RT}{zF} \frac{d \ln i}{d\phi} \qquad (2\text{-}99)$$

Where $d\ln i/d\phi$ is the slope of curve $\ln i$ -- ϕ. Bauer [89] studied the history and basic concept of the symmetry factor and indicated that anodic symmetry factor/transfer coefficient plus the cathodic symmetry factor/transfer coefficient is not necessary to be "unity" 1. Also, there is no adequate justification for *a priori* introduction of the transfer coefficient γ as an implicitly potential-independent parameter. Savéant and Tessier [90] found that the electrochemical transfer coefficient is variation with potential for organic molecules.

$$\gamma = 0.5 + \frac{F}{4\lambda_0}(E - E^\circ - \phi) \qquad (2\text{-}100)$$

Where, λ_0 is the reorganization factor. Eq. (2-100) shows that the coefficient γ decreases with the increase of over potential. Thus this effect may not apply to the NDE behavior.

If we accept that the fast increasing of anodic current is just because of the increase of the effect valence $\bar{z}$, then for the hydrogen evolution reaction rate, the dash line I_H implies that the cathodic current density,

$$i_H = i_0 \exp[-\frac{(1-\gamma)\bar{z}F}{RT}(E_{appl} - E_{corr})], \qquad (2\text{-}101)$$

should decrease faster than expected, which conflicts with the experiment results. However, we always measure the amount of hydrogen evolution which reflects the cathodic current density. As we discussed above, the hydrogen evolution is composed of three parts

$$I_H = I_{H1} + I_{H2} + I_{Hc} \qquad (2\text{-}102)$$

From equation (2-101), we can see that the change of $\bar{z}$ is not the unique main contribution to the NDE behavior. It implies that the symmetry factor γ is also a parameter to influence the NDE behavior. There are three possible cases:

(1) If there are no Mg+ produced in the process of magnesium dissolution, $\bar{z} = 2$, and $I_{Hc}=0$, $I_{H1}=0$, only when $\gamma \rightarrow 1$, $1-\gamma \approx 0$, the I_{H2} will not change much, namely, $I_{H2} \rightarrow I_0$. Therefore, in this case, the hydrogen evolution cannot increase. This also indicates that Mg^+-ions must exist in the process of magnesium dissolution.

(2) When there are no Mg^{++} produced in the process of magnesium dissolution, $\bar{z}=1$, and $I_{H2}=0$. The maximum hydrogen evolution on the cathode will be the same as the hydrogen evolution on the anode which is produced by chemical reaction of Eq. (2-96). Therefore, even $\gamma \rightarrow 0$, $1-\gamma \approx 1$, the third part I_{Hc}, which comes from the reaction of Eq. (2-96), can make sure the hydrogen evolution increase.

(3) When there are partially Mg^+ and Mg^{++}, only when the value of symmetry factor γ is greater than a specific value γ_0, can the hydrogen evolution be made sure to increase. For example, assuming $N_1=N_2=N$ at overpotential $E_{appl}-E_{corr}$, then $\bar{z}=1.5$. The maximum hydrogen evolution on the cathode is $N_1/2+N_2=3N/2$. Correspondingly, the variation of the charge of electrons is $3N$. The hydrogen evolution on the anode is $N_1/2=N/2$, which is 1/3 of that on the cathode. Correspondingly, the variation of the charge of electrons is N, which is 1/3 of that on the cathode. It means that if the hydrogen evolution on the cathode decreases less then 1/3, the total hydrogen evolution still increases. Therefore,

$$i_H = i_0 \exp[-\frac{1.5(1-\gamma_0)F}{RT}(E_{appl}-E_{corr})] > \frac{2}{3}i_0$$

or: $$\gamma_0 > 1 - \frac{0.405RT}{1.5F(E_{appl}-E_{corr})}$$

Above inequation makes sure the total hydrogen evolution increase.

Note: it is important to understand that the dissolution rate of magnesium increases with increasing of overpotential, both N_1 and N_2 increase even though N_2 increases faster than N_1. This means that I_{Hc} in equation (2-102) increases because of the number of Mg^+ increase when the overpotential increases.

In this way, we may explain the NDE behavior consistently. But how to determine the rate of N_1/N_2 is still a problem. Anyway, as we mentioned above, we should combine with the results of experiments to check the numerical approach.

3. The FEM and the FDM

The Finite Element Method (FEM) and the Finite Difference method (FDM) are two widely used methods in modeling or more precisely in solving the partial differential equation. Sometimes, they are hybrid methods to find a good solution efficiently. The differences between FEM and FDM are:[91]

(1) The finite difference method is an approximation to the differential equation; the finite element method is an approximation to its solution.

(2) The most attractive feature of the FEM is its ability to handle complex geometries (and boundaries) with relative ease. While FDM in its basic form is restricted to handle rectangular shapes and simple alterations thereof, the handling of geometries in FEM is theoretically straightforward. The most attractive feature of the FDM is that it can be very easy to implement.

(3) There are several ways one could consider the FDM a special case of the FEM approach. One might choose basis functions as either piecewise constant functions or Dirac delta functions. In both approaches, the approximations are defined on the entire domain, but need not be continuous. Alternatively, one might define the function on a discrete domain, with the result that the continuous differential operator no longer makes sense, however this approach is not FEM.

(4) There are reasons to consider the mathematical foundation of the finite element approximation more sound, for instance, because the quality of the approximation between grid points is poor in FDM. The quality of a FEM approximation is often higher than in the corresponding FDM approach, but this is extremely problem dependent.

Generally, FEM is the method of choice in all types of analysis in structural mechanics (i.e. solving for deformation and stresses in solid bodies or dynamics of structures) while computational fluid dynamics (CFD) tends to use FDM or other methods (e.g., finite volume method). CFD problems usually require discretization of the problem into a large number of cells/gridpoints (millions and more), therefore cost of the solution favors simpler, lower order approximation within each cell. This is especially

true for 'external flow' problems, like air flow around the car or airplane, or weather simulation in a large area.

3.1 The Finite Element Method

In Fig. 3-1, the real line is the shape of an object. How to reproduce it from some dispersed points?
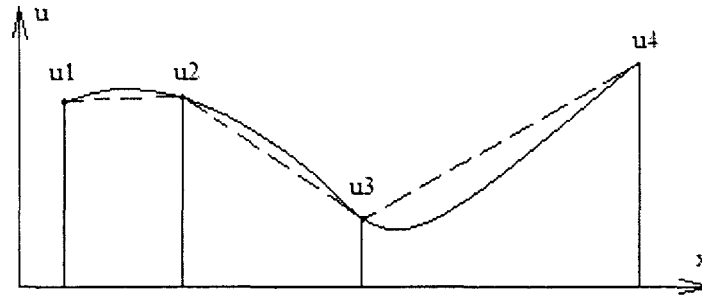
Fig. 3-1 Finite element approximation

How to get a solution from a differential equation with complicated boundary conditions?

The essence of the finite element method is to take a complex problem whose solution may be difficult if not impossible to obtain, and decompose it into pieces upon each of which a simple approximation of the solution may be constructed, and then put the local approximate solutions together to obtain a global approximate solution.[92]

When we model a practical situation or when we solve an equation to get a solution U, we mostly use an approximation solution u to compare with U. If $\Delta=u-U=0$, u=U. If Δ is smaller than an acceptable value, u is a good approximation.

In practical situation, we can only get some dispersed value like U_1, U_2, U_3 etc. of U. How can we get a good model or a good approximation u from these dispersed values U_1, U_2, U_3 ...? According to the properties or characteristics of the question and conditions, we can subdivide a given domain V into sub-domains V^e or elements. Choose a different nodal approximation on each sub-domain $u^e(\mathbf{r})$. The finite element approximation is a special case of nodal approximation by sub-domain. Its main features are: [93]

(1) The approximation over a sub-domain V^e depends only on the nodal values of that sub-domain or element

(2) The approximation $u^e(x)$ is required to guarantee a certain minimum degree of continuity over each element and its inter-element boundaries.

We can express $u(\mathbf{r})$ as: $u(\vec{r}) = \sum_{i=1}^{n} N_i(\vec{r})U_i$. We choose the interpolation $N_i(\mathbf{r})$ to make sure it meets $N_i(\mathbf{r}_j) = \delta_{ij}$ at the node points. So, $u_i(\mathbf{r}_i) = U_i$. We will use u_i instead of U_i. Between any two nodes, $N(\mathbf{r})$ is successive function. Practically, FEM is an approximate method that the value of u at the sample points (nodes) is guaranteed to be the exact value. But we will try to find an approximate function between two sample points (nodes) to make u a good approximation to U. The finite element solution converges to the true solution as the number of elements is increased.

Therefore, how to find a proper $N(\mathbf{r})$ is a key question. In fact, $N(\mathbf{r})$ can be any function that meets the conditions we discussed above. But only some of them make sense or are efficient. $N(\mathbf{r})$ can be linear, quadratic (parabola), cubic... $N(\mathbf{r})$ can be any function that meets the above condition, but only some of them make sense. We choose $N(\mathbf{r})$ to make $u(\mathbf{r})$ get closer to U (or the goal) more efficiently. The U(r), or $u(\mathbf{r})$, can be 1D, 2D or 3D. We can cut the domain of U into n elements, and every element has 2, 3, 4 ... nodes. Generally, we need to make a transformation to map every element in the real space $\mathbf{r}(x,y,z)$ to a single area in the reference space $\tau(\xi, \eta, \zeta)$. The advantage to do so is that we can integrate in the same area (or same integration limit) for different elements.

Usually, we can expand a function u to polynomial.

1D: $u(x) = \sum_{n} a_n x^n$ (n=0, 1, 2...)

2D: $u(x) = \sum_{n,m} a_n x^n + b_n y^n + c_{mn} x^m y^{n-m}$ (m=1, 2, ...n-1)

....

If n is finite, there is a finite complete basis for u. If n is infinite, e.g. $e^x = \sum_{n} a_n x^n$, the finite complete basis for it does not exist. There is no more than one complete basis for any function. Any other basis is incomplete basis. Thus we can choose linear, quadratic, cubic... approach. Today, with the help of a computer, we are more likely to choose linear elements. E.g. if we divide a domain into infinite element, we still can get an exact solution for $u(x)$. Certainly we cannot divide it into infinite elements, but we can choose enough finite elements to make the error small enough.

If we use the polynomial basis of the approximation <P> to express the u, we have [93]

$u=a_1P_1+a_2P_2+a_3P_3+\ldots+a_nP_n = P_1a_1+P_2a_2+P_3a_3+\ldots+P_na_n$

$$\therefore u = <P_1 \ \ P_2 \ \ P_3 \ldots\ldots P_n> \begin{Bmatrix} a_1 \\ a_2 \\ \ldots \\ a_n \end{Bmatrix} = \langle P \rangle \{a\}$$

Where, a_i is coefficient, $i=1, 2, 3\ldots n$

The value of every point $\tau_1, \ \tau_2, \tau_n$ should also be $u_1, u_2,\ldots u_n$, then

$$\begin{Bmatrix} u_1 \\ u_2 \\ \ldots \\ u_n \end{Bmatrix} = \begin{bmatrix} P_1(\vec{\tau}_1) & P_2(\vec{\tau}_1) & \cdots & P_n(\vec{\tau}_1) \\ P_1(\vec{\tau}_2) & P_2(\vec{\tau}_2) & \cdots & P_n(\vec{\tau}_2) \\ \vdots & \vdots & \cdots & \vdots \\ P_1(\vec{\tau}_n) & P_2(\vec{\tau}_n) & \cdots & P_n(\vec{\tau}_n) \end{bmatrix} \begin{Bmatrix} a_1 \\ a_2 \\ \ldots \\ a_n \end{Bmatrix} \rightarrow \{u_n\}=[P_n]\{a\}$$

Where, $\vec{\tau}_i = \vec{\tau}(\xi_i, \eta_i, \varsigma_i)$

For 1D: $P_1=1$, $P_2=\xi$, $P_3=\xi^2$, $P_4=\xi^3$, ...

For 2D: $P_1=1$, $P_2=\xi$, $P_3=\eta$, $P_4=\xi^2$, $P_5=\eta^2$, $P_6=\xi\eta$,....

For 3D: $P_1=1$, $P_2=\xi$, $P_3=\eta$, $P_4=\varsigma$, $P_5=\xi^2$, $P_6=\eta^2$, $P_7=\varsigma^2$, $P_9=\xi\eta$, $P_{10}=\eta\varsigma$, $P_{11}=\varsigma\xi$,...

Then, $\quad u=<N>\{u_n\}=<P>\{a\} \quad \{u_n\}=[P_n]\{a\} \rightarrow \{a\}=[P_n]^{-1}\{u_n\}$

$\therefore u=<N>\{u_n\}=<P>[P_n]^{-1}\{u_n\} \rightarrow <N(\tau)>=<P(\tau)>[P_n]^{-1} =<N_1(\tau) \ \ N_2(\tau) \ldots>$

Where, $<P>=<P_1 \ \ P_2 \ \ P_3 \ldots> \quad <N>=<N_1 \ \ N_2 \ \ N_3 \ldots> \rightarrow <N(\mathbf{r})>=<N_1(\mathbf{r}) \ N_2(\mathbf{r}) \ldots>$ and $<N(\tau)>=<N_1(\tau) \ N_2(\tau) \ldots>$

$$\{u_n\}=\begin{Bmatrix} u_1 \\ u_2 \\ \ldots \\ u_n \end{Bmatrix} \quad \{a\}=\begin{Bmatrix} a_1 \\ a_2 \\ \ldots \\ a_n \end{Bmatrix} \text{ and } [P_n]=\begin{bmatrix} P_1(\vec{\tau}_1) & P_2(\vec{\tau}_1) & \cdots & P_n(\vec{\tau}_1) \\ P_1(\vec{\tau}_2) & P_2(\vec{\tau}_2) & \cdots & P_n(\vec{\tau}_2) \\ \vdots & \vdots & \cdots & \vdots \\ P_1(\vec{\tau}_n) & P_2(\vec{\tau}_n) & \cdots & P_n(\vec{\tau}_n) \end{bmatrix},$$

$<x \ y \ z>=<N(\vec{\tau})>[\{x_n\} \ \{y_n\} \ \{z_n\}]$,

$$\frac{\partial}{\partial \xi} = \frac{\partial}{\partial x}\cdot\frac{\partial x}{\partial \xi} + \frac{\partial}{\partial y}\cdot\frac{\partial y}{\partial \xi} + \frac{\partial}{\partial z}\cdot\frac{\partial z}{\partial \xi},$$

$$\frac{\partial}{\partial \eta} = \frac{\partial}{\partial x}\cdot\frac{\partial x}{\partial \eta} + \frac{\partial}{\partial y}\cdot\frac{\partial y}{\partial \eta} + \frac{\partial}{\partial z}\cdot\frac{\partial z}{\partial \eta},$$

$$\frac{\partial}{\partial \varsigma} = \frac{\partial}{\partial x}\cdot\frac{\partial x}{\partial \varsigma} + \frac{\partial}{\partial y}\cdot\frac{\partial y}{\partial \varsigma} + \frac{\partial}{\partial z}\cdot\frac{\partial z}{\partial \varsigma}.$$

It can be expressed as:

$$\left\{\begin{array}{c}\partial/\partial\xi\\\partial/\partial\eta\\\partial/\partial\zeta\end{array}\right\}=\left[\begin{array}{ccc}\partial x/\partial\xi & \partial y/\partial\xi & \partial z/\partial\xi\\\partial x/\partial\eta & \partial y/\partial\eta & \partial z/\partial\eta\\\partial x/\partial\zeta & \partial y/\partial\zeta & \partial z/\partial\zeta\end{array}\right]\left\{\begin{array}{c}\partial/\partial x\\\partial/\partial y\\\partial/\partial z\end{array}\right\}=[J]\left\{\begin{array}{c}\partial/\partial x\\\partial/\partial y\\\partial/\partial z\end{array}\right\}\rightarrow\left\{\begin{array}{c}\partial/\partial x\\\partial/\partial y\\\partial/\partial z\end{array}\right\}=[j]\left\{\begin{array}{c}\partial/\partial\xi\\\partial/\partial\eta\\\partial/\partial\zeta\end{array}\right\}$$

Where, $[j]=[J]^{-1}$

$$[J]=\left[\begin{array}{c}\partial/\partial\xi\\\partial/\partial\eta\\\partial/\partial\zeta\end{array}\right]\langle x \quad y \quad z\rangle=\left[\begin{array}{c}<N_{,\xi}>\\<N_{,\eta}>\\<N_{,\zeta}>\end{array}\right][\{x_n\} \quad \{y_n\} \quad \{z_n\}], \qquad <N_{,\xi}>=<\frac{\partial N_1}{\partial\xi},\frac{\partial N_2}{\partial\xi},\cdots>$$

Assemble global equation

To assemble a global equation, each element stiffness matrix must be assembled into a global stiffness matrix.

Suppose we divide a domain into four elements. There are four nodes in every element. Let's take element four as an example. There are 4 global nodes 5, 6, 8 and 9 in this element and four local nodes in every element are ①, ②, ③ and ④ as shown in Fig. 3-1. The relation between the elements in the element stiffness matrix and that in the global stiffness matrix is as follows:

$E_{ij}^{(4)}$ -- element of local matrix, G_{mn} -- element of global matrix

$E_{11}^{(4)}\rightarrow G_{55}$ $E_{12}^{(4)}\rightarrow G_{56}$ $E_{13}^{(4)}\rightarrow G_{59}$ $E_{14}^{(4)}\rightarrow G_{58}$

$E_{21}^{(4)}\rightarrow G_{65}$ $E_{22}^{(4)}\rightarrow G_{66}$ $E_{23}^{(4)}\rightarrow G_{69}$ $E_{24}^{(4)}\rightarrow G_{68}$

$E_{31}^{(4)}\rightarrow G_{95}$ $E_{32}^{(4)}\rightarrow G_{96}$ $E_{33}^{(4)}\rightarrow G_{99}$ $E_{34}^{(4)}\rightarrow G_{98}$

$E_{41}^{(4)}\rightarrow G_{85}$ $E_{42}^{(4)}\rightarrow G_{86}$ $E_{43}^{(4)}\rightarrow G_{89}$ $E_{44}^{(4)}\rightarrow G_{88}$
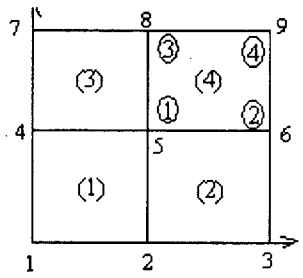
Fig. 3-2 global nodes and local nodes

Similarly, $E_{33}^{(1)}\rightarrow G_{55}$ $E_{44}^{(2)}\rightarrow G_{55}$ $E_{22}^{(3)}\rightarrow G_{55}$,

Finally, $G_{55}=E_{11}^{(4)}+E_{22}^{(3)}+E_{33}^{(1)}+E_{44}^{(2)}$

......

3.1.1 For1D

(1) Linear (2 nodes in every element)

In the real space, the positions of the two nodes are: $x=x_1$ and $x=x_2$, $(x_1\leq x\leq x_2)$. Correspondingly, in the reference space, the positions of the two nodes are:

Node 1: $\xi=-1$, and

Node 2: $\xi=1$ ($-1\le \xi \le 1$). They are shown in Fig. 3-2.

$<P>=<1 \quad \xi>$

$$[P_n]=\begin{bmatrix} 1 & -1 \\ 1 & 1 \end{bmatrix} \rightarrow [P_n]^{-1}=\frac{1}{2}\begin{bmatrix} 1 & 1 \\ -1 & 1 \end{bmatrix}$$

$$\langle N \rangle = \langle P \rangle [P_n]^{-1} = \frac{1}{2}\langle 1 \quad \xi \rangle \begin{bmatrix} 1 & 1 \\ -1 & 1 \end{bmatrix} = \frac{1}{2}\langle 1-\xi \quad 1+\xi \rangle$$

$N_1=(1-\xi)/2 \qquad N_2=(1+\xi)/2$

$$[J]=\frac{1}{2}\langle -1 \quad 1 \rangle \begin{Bmatrix} x_1 \\ x_2 \end{Bmatrix} = \frac{x_2-x_1}{2}$$

$$<x>=<N(\xi)>\{x_n\}=\frac{1}{2}\langle 1-\xi \quad 1+\xi \rangle \begin{Bmatrix} x_1 \\ x_2 \end{Bmatrix}$$

$$\therefore x = \frac{x_1+x_2}{2}+\frac{x_2-x_1}{2}\xi \rightarrow [J]=\frac{\partial x}{\partial \xi}=\frac{x_2-x_1}{2} \rightarrow [j]=[J]^{-1}=\frac{2}{x_2-x_1}$$
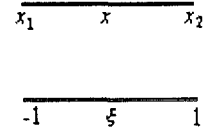
Fig.3-2 real space and reference space

(2) Quadratic / parabola (3 nodes in every element)

$<P>=<1 \quad \xi \quad \xi^2 > \qquad x_1\le x\le x_3 \rightarrow -1\le \xi \le 1$ node 1: $\xi=-1$ node 2: $\xi=0$, node 3: $\xi=1$

$x_2=(x_1+x_3)/2$

$$[P_n]=\begin{bmatrix} 1 & -1 & 1 \\ 1 & 0 & 0 \\ 1 & 1 & 1 \end{bmatrix} \qquad [P_n]^{-1}=\frac{1}{2}\begin{bmatrix} 0 & 2 & 0 \\ -1 & 0 & 1 \\ 1 & -2 & 1 \end{bmatrix}$$

$$\langle N \rangle = \langle P \rangle [P_n]^{-1}=\frac{1}{2}\langle 1 \quad \xi \quad \xi^2 \rangle \begin{bmatrix} 0 & 2 & 0 \\ -1 & 0 & 1 \\ 1 & -2 & 1 \end{bmatrix} = \frac{1}{2}\langle -\xi(1-\xi) \quad 2(1-\xi^2) \quad \xi(1+\xi) \rangle$$

$N_1=-\xi(1-\xi)/2 \qquad N_2=(1-\xi^2) \qquad N_3=\xi(1+\xi)/2$

$$x = \frac{1}{2}\langle -\xi(1-\xi) \quad 2(1-\xi^2) \quad \xi(1+\xi) \rangle \begin{Bmatrix} x_1 \\ (x_1+x_3)/2 \\ x_3 \end{Bmatrix} = \frac{x_1+x_3}{2}+\frac{x_3-x_1}{2}\xi \rightarrow$$

$$[J] = \frac{\partial x}{\partial \xi} = \frac{x_3 - x_1}{2} \qquad \text{or:} \quad [J] = \frac{1}{2}\langle 2\xi-1 \quad -4\xi \quad 2\xi+1 \rangle \begin{Bmatrix} x_1 \\ (x_1+x_3)/2 \\ x_3 \end{Bmatrix} = \frac{x_3-x_1}{2} \rightarrow$$

$$[j] = [J]^{-1} = \frac{2}{x_3 - x_1}$$

(3) Cubic (4nodes in every elements)

$x_1 \le x \le x_4 \rightarrow -1 \le \xi \le 1$ node 1: $\xi=-1$ (x_1),   node 2: $\xi=-1/3$ [$x_1+(x_4-x_1)/3$], node 3:

$\xi=1/3$ [$x_1+2(x_4-x_1)/3$], node 4: $\xi=1$ (x_4)

$<P>=<1 \quad \xi \quad \xi^2 \quad \xi^3 >$

$$[P] = \begin{bmatrix} 1 & -1 & 1 & -1 \\ 1 & -1/3 & 1/9 & -1/27 \\ 1 & 1/3 & 1/9 & 1/27 \\ 1 & 1 & 1 & 1 \end{bmatrix} \qquad [P]^{-1} = \frac{1}{16}\begin{bmatrix} -1 & 9 & 9 & -1 \\ 1 & -27 & 27 & -1 \\ 9 & -9 & -9 & 9 \\ -9 & 27 & -27 & 9 \end{bmatrix}$$

$$\langle N \rangle = \langle P \rangle [P_n]^{-1} = \frac{1}{16}\langle -(1-\xi)(1-9\xi^2) \quad 9(1-\xi^2)(1-3\xi) \quad 9(1-\xi^2)(1+3\xi) \quad -(1+\xi)(1-9\xi^2) \rangle$$

$$x = \frac{x_1 + x_4}{2} + \frac{x_4 - x_1}{2}\xi \rightarrow \qquad [J] = \frac{\partial x}{\partial \xi} = \frac{x_4 - x_1}{2}$$

3.1.2. For 2D

(1) Linear element (triangle, three nodes in every element)

$<P>=<1 \quad \xi \quad \eta >$ $(x_1, y_1), (x_2, y_2), (x_3, y_3) \rightarrow (\xi, \eta): (0, 0), (1, 0), (0, 1)$

$$[P_n] = \begin{bmatrix} 1 & 0 & 0 \\ 1 & 1 & 0 \\ 1 & 0 & 1 \end{bmatrix} \qquad [P_n]^{-1} = \begin{bmatrix} 1 & 0 & 0 \\ -1 & 1 & 0 \\ -1 & 0 & 1 \end{bmatrix}$$

$$\langle N \rangle = \langle P \rangle [P_n]^{-1} = \langle 1 \quad \xi \quad \eta \rangle \begin{bmatrix} 1 & 0 & 0 \\ -1 & 1 & 0 \\ -1 & 0 & 1 \end{bmatrix} = \langle 1-\xi-\eta \quad \xi \quad \eta \rangle$$

$N_1=1-\xi-\eta$ $N_2=\xi$ $N_3=\eta$ $<x \quad y>=<N>[\{x_n\} \quad \{y_n\}]$

$$\langle x \quad y \rangle = \langle 1 - \xi - \eta \quad \xi \quad \eta \rangle \begin{bmatrix} x_1^{(e)} & y_1^{(e)} \\ x_2^{(e)} & y_2^{(e)} \\ x_3^{(e)} & y_3^{(e)} \end{bmatrix}$$

$$[J] = \begin{bmatrix} -1 & 1 & 0 \\ -1 & 0 & 1 \end{bmatrix} \begin{pmatrix} x_1 & y_1 \\ x_2 & y_2 \\ x_3 & y_3 \end{pmatrix} = \begin{bmatrix} x_2 - x_1 & y_2 - y_1 \\ x_3 - x_1 & y_3 - y_1 \end{bmatrix}$$

(2) Bilinear Element (quadrilateral, four nodes)

$(x_1, y_1), (x_2, y_2), (x_3, y_3), (x_4, y_4) \rightarrow (\xi, \eta): (-1, -1), (1, -1), (1, 1), (-1, 1)$

<P>=<1 ξ η $\xi\eta$>

$$[P_n] = \begin{bmatrix} 1 & -1 & -1 & 1 \\ 1 & 1 & -1 & -1 \\ 1 & 1 & 1 & 1 \\ 1 & -1 & 1 & -1 \end{bmatrix} \qquad [P_n]^{-1} = \frac{1}{4} \begin{bmatrix} 1 & 1 & 1 & 1 \\ -1 & 1 & 1 & -1 \\ -1 & -1 & 1 & 1 \\ 1 & -1 & 1 & -1 \end{bmatrix}$$

$$\langle N \rangle = \langle P \rangle [P_n]^{-1} = \frac{1}{4} \langle 1 \quad \xi \quad \eta \quad \xi\eta \rangle \begin{bmatrix} 1 & 1 & 1 & 1 \\ -1 & 1 & 1 & -1 \\ -1 & 1 & 1 & -1 \\ 1 & -1 & 1 & -1 \end{bmatrix} = \frac{1}{4} \langle (1-\xi)(1-\eta) \quad (1+\xi)(1-\eta) \quad (1+\xi)(1+\eta) \quad (1-\xi)(1+\eta) \rangle$$

$$\langle x \quad y \rangle = \langle N \rangle [\{x_n\} \quad \{y_n\}] = \frac{1}{4} \langle (1-\xi)(1-\eta) \quad (1+\xi)(1-\eta) \quad (1+\xi)(1+\eta) \quad (1-\xi)(1+\eta) \rangle \begin{pmatrix} x_1 & y_1 \\ x_2 & y_2 \\ x_3 & y_3 \\ x_4 & y_4 \end{pmatrix}$$

$$[J] = \frac{1}{4} \begin{bmatrix} \eta-1 & 1-\eta & 1+\eta & -1-\eta \\ \xi-1 & -1-\xi & 1+\xi & 1-\xi \end{bmatrix} \begin{pmatrix} x_1 & y_1 \\ x_2 & y_2 \\ x_3 & y_3 \\ x_4 & y_4 \end{pmatrix}$$

$$= \frac{1}{4} \begin{bmatrix} -x_1 + x_2 + x_3 - x_4 + \eta(x_1 - x_2 + x_3 - x_4) & -y_1 + y_2 + y_3 - y_4 + \eta(y_1 - y_2 + y_3 - y_4) \\ -x_1 - x_2 + x_3 - x_4 + \xi(x_1 - x_2 + x_3 - x_4) & -y_1 - y_2 + y_3 + y_4 + \xi(y_1 - y_2 + y_3 - y_4) \end{bmatrix}$$

$\det(J) = A_0 + A_1 \xi + A_2 \eta$

$$A_0 = [(y_4 - y_2)(x_3 - x_1) - (y_3 - y_1)(x_4 - x_2)]/8$$

$$A_1 = [(y_3 - y_4)(x_2 - x_1) - (y_2 - y_1)(x_3 - x_4)]/8$$

$$A_2 = [(y_4 - y_1)(x_3 - x_2) - (y_3 - y_2)(x_4 - x_1)]/8$$

If the element is rectangular, the length is a and the width is b, as shown in Fig. 3-3, we get

$$x = \frac{x_1 + x_2}{2} + \frac{a}{2}\xi \qquad y = \frac{y_1 + y_4}{2} + \frac{b}{2}\eta$$

$A_0 = ab/4$, $A_1 = 0$, $A_2 = 0$

$\det(J) = A_0 = ab/4 \quad dxdy = (ab/4)d\xi d\eta$

$$\frac{\partial N_i}{\partial x} = \frac{\partial N_i}{\partial \xi} \cdot \frac{\partial \xi}{\partial x} + \frac{\partial N_i}{\partial \eta} \cdot \frac{\partial \eta}{\partial x} = \frac{2}{a}\frac{\partial N_i}{\partial \xi},$$

$$\frac{\partial N_i}{\partial y} = \frac{\partial N_i}{\partial \xi} \cdot \frac{\partial \xi}{\partial y} + \frac{\partial N_i}{\partial \eta} \cdot \frac{\partial \eta}{\partial y} = \frac{2}{b}\frac{\partial N_i}{\partial \eta}$$
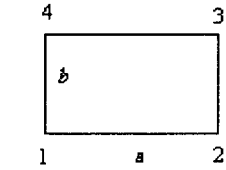
Fig. 3-3 rectangular element

(3) Quadratic Element (triangle, six nodes)

$P = <1 \quad \xi \quad \eta \quad \xi^2 \quad \xi\eta \quad \eta^2>$

$<x_i> = <x_1\ y_1;\ x_2\ y_2;\ x_3\ y_3;\ x_4\ y_4;\ x_5\ y_5;\ x_6\ y_6>$

$x_2 = (x_1 + x_3)/2 \quad x_4 = (x_3 + x_5)/2 \quad x_6 = (x_5 + x_1)/2$

$<\xi_i> = <0\ 0;\ 1/2\ 0;\ 1\ 0;\ 1/2\ 1/2;\ 0\ 1;\ 0\ 1/2>$

$$[P_n]^{-1} = \begin{bmatrix} 1 & 0 & 0 & 0 & 0 & 0 \\ -3 & 4 & -1 & 0 & 0 & 0 \\ -3 & 4 & -1 & 0 & 0 & 0 \\ 2 & -4 & 2 & 0 & 0 & 0 \\ 4 & -4 & 0 & 4 & 0 & -4 \\ 2 & 0 & 0 & 0 & 2 & -4 \end{bmatrix}$$

$\langle N \rangle = \langle P \rangle [P_n]^{-1} = \langle -\lambda(1-2\lambda) \quad 4\xi\lambda \quad -\xi(1-2\xi) \quad 4\xi\eta \quad -\eta(1-2\eta) \quad 4\eta\lambda \rangle \qquad (\lambda = 1-\xi-\eta)$

3.1.3. For 3D

(1) Linear Element (tetrahedron, four nodes)

$P = <1 \quad \xi \quad \eta \quad \zeta>$

$<x_i> = <x_1\ y_1\ z_1;\ x_2\ y_2\ z_2;\ x_3\ y_3\ z_3;\ x_4\ y_4\ z_4>$

$<\xi_i> = <0\ 0\ 0;\ 1\ 0\ 0;\ 0\ 1\ 0;\ 0\ 0\ 1>$

$$[P_n]=\begin{bmatrix}1 & 0 & 0 & 0\\1 & 1 & 0 & 0\\1 & 0 & 1 & 0\\1 & 0 & 0 & 1\end{bmatrix}\qquad [P_n]^{-1}=\begin{bmatrix}1 & 0 & 0 & 0\\-1 & 1 & 0 & 0\\-1 & 0 & 1 & 0\\-1 & 0 & 0 & 1\end{bmatrix}$$

$$\langle N\rangle=\langle P\rangle[P_n]^{-1}=\langle 1\ \ \xi\ \ \eta\ \ \zeta\rangle\begin{bmatrix}1 & 0 & 0 & 0\\-1 & 1 & 0 & 0\\-1 & 0 & 1 & 0\\-1 & 0 & 0 & 1\end{bmatrix}=\langle 1-\xi-\eta-\zeta\ \ \xi\ \ \eta\ \ \zeta\rangle$$

$$[J]=\begin{bmatrix}-1 & 1 & 0 & 0\\-1 & 0 & 1 & 0\\-1 & 0 & 0 & 1\end{bmatrix}\begin{pmatrix}x_1 & y_1 & z_1\\x_2 & y_2 & z_2\\x_3 & y_3 & z_3\\x_4 & y_4 & z_4\end{pmatrix}=\begin{bmatrix}x_2-x_1 & y_2-y_1 & z_2-z_1\\x_3-x_1 & y_3-y_1 & z_3-z_1\\x_4-x_1 & y_4-y_1 & z_4-z_1\end{bmatrix}$$

(2) Trilinear Element (hexahedron, eight nodes)

$P=\langle 1\ \ \xi\ \ \eta\ \ \zeta\ \ \xi\eta\ \ \eta\zeta\ \ \zeta\xi\ \ \xi\eta\zeta\rangle$

$\langle x_i\rangle=\langle x_1;\ x_2;\ x_3;\ x_4;\ x_5;\ x_6;\ x_7;\ x_8\rangle$

$\langle \xi_i\rangle=\langle$-1 -1 -1; 1 -1 -1; 1 1 -1; -1 1 -1; -1 -1 1; 1 -1 1; 1 1 1; -1 1 1$\rangle$

$\langle N\rangle=(1/8)\langle a_2b_2c_2\ \ a_1b_2c_2\ \ a_1b_1c_2\ \ a_2b_1c_2\ \ a_2b_2c_1\ \ a_1b_2c_1\ \ a_1b_1c_1\ \ a_2b_1c_1\rangle$

$a_1=1+\xi\ \ a_2=1-\xi\ \ b_1=1+\eta\ \ b_2=1-\eta\ \ c_1=1+\zeta\ \ c_2=1-\zeta$

(3) Complete Quadratic (tetrahedron, ten nodes)

$P=\langle 1\ \ \xi\ \ \eta\ \ \zeta\ \ \xi^2\ \ \xi\eta\ \ \eta^2\ \ \eta\zeta\ \ \zeta^2\ \ \zeta\xi\rangle$

$\langle x_i\rangle=\langle x_1;\ x_2;\ x_3;\ x_4;\ x_5;\ x_6;\ x_7;\ x_8;\ x_9;\ x_{10}\rangle$

$\langle \xi_i\rangle=\langle$0 0 0; ½ 0 0; 1 0 0; ½ ½ 0; 0 1 0; 0 ½ 0; 0 0 ½; ½ ½ 0; 0 ½ ½; 0 0 1$\rangle$

$\langle N\rangle=\langle-\lambda(1-2\lambda)\ \ 4\xi\lambda\ \ -\xi(1-2\xi)\ \ 4\xi\eta\ \ -\eta(1-2\eta)\ \ 4\eta\lambda\ \ 4\zeta\lambda\ \ 4\xi\zeta\ \ 4\eta\zeta\ \ -\zeta(1-2\zeta)\rangle$

Where $\lambda=1-\xi-\eta-\zeta$

3.2. The Finite Difference Method

In the steady state boundary value problems or the only spatial problems (not time concerned), the FEM has been the greater ease with which complex boundary shapes can be modeled or solved. But in the time-dependent problems the solution proceeds from an initial solution at $t = 0$, it is almost always convenient to calculate each new solution constant time interval (Δt) throughout the entire domain. In this case, for the time derivative problem, the FDM is usually preferred. Certainly, as a method of solving problem, it can be used for both time-dependent and time-independent problems.

3.2.1 Propagation or Initial value problems

(1) For a discrete system

$$[M]\frac{d^2}{dt^2}\{U\}+[C]\frac{d}{dt}\{U\}+[K]\{U\} = \{F(t)\} \qquad \text{for } t > t_0$$

with initial conditions $\{U\}=\{U_0\}$ $d\{U\}/dt=\{\dot{U}_0\}$ for $t=t_0$

Any function can be expanded to Taylor series,

$$U(t) = \sum_{n=0}^{\infty}\frac{(t-t_i)^n}{n!}(\frac{d^n u}{dt^n})_i$$

$$(\frac{dU}{dt})_i \approx \frac{U_{i+1}-U_{i-1}}{2\Delta t} \qquad \text{(Central difference)}$$

$$(\frac{d^2U}{dt^2})_i \approx \frac{U_{i+1}-2U_i+U_{i-1}}{(\Delta t)^2}$$

From equation (1), we get

$$\frac{d^2U_0}{dt^2} = \ddot{U}_0 = F(t_0)-kU_0-c\dot{U}_0$$

From equation (3), we get

$$U_{-1} = U_0 - \Delta t\dot{U}_0 + \frac{\Delta t^2}{2}\ddot{U}_0 = U_0 - \Delta t\dot{U}_0 + \frac{\Delta t^2}{2}[F(t_0)-kU_0-c\dot{U}_0]$$

From equation (2), we get

$$U_1 = U_{-1} + 2\Delta t\dot{U}_0 = U_0 + \Delta t\dot{U}_0 + \frac{\Delta t^2}{2}[F(t_0)-kU_0-c\dot{U}_0]$$

Let $i=1$, from equation (2), we get

$$\dot{U}_1 = \frac{U_2 - U_0}{2\Delta t}$$

$$\ddot{U}_1 \approx \frac{U_2 - 2U_1 + U_0}{(\Delta t)^2}$$

Put (5) and (6) into (1), we get

$$m\frac{U_2 - 2U_1 + U_0}{\Delta t^2} + c\frac{U_2 - U_0}{2\Delta t} + kU_1 = F_1$$

Combine Eqs.(4), (6) and (7), we get U_2 and $\dot{U}_1$. Then we can repeat the cycle and get all values of other nodes.

Newmark's Method

Based on the results of central difference method, let's introduce two adjustive empiric coefficients β and γ.

$$\dot{U}_{n+1} = \dot{U}_n + \Delta t[(1-\gamma)\ddot{U}_n + \gamma\ddot{U}_{n+1}]$$

$$U_{n+1} = U_n + \Delta t\dot{U} + \Delta t^2[(1/2 - \beta)\ddot{U}_n + \beta\ddot{U}_{n+1}]$$

$$(k + \frac{m}{\beta\Delta t^2})U_{n+1} = f_{n+1} + \frac{m}{\beta\Delta t^2}[U_n + \Delta t\dot{U}_n + \Delta t^2(1/2 - \beta)\ddot{U}_n]$$

$\gamma=1/2$ and $1/6 \leq \beta \leq 1/4$. $\gamma=1/2$, $\beta=1/4$ is called the average acceleration method. $\gamma=1/2$, $\beta=1/6$ corresponds to the linear acceleration method. Consider the initial condition,

$$\ddot{U}_0 = (f_0 - kU_0)/m$$

$$(k + \frac{m}{\beta\Delta t^2})U_1 = f_1 + \frac{m}{\beta\Delta t^2}[U_0 + \Delta t\dot{U}_0 + \Delta t^2(1/2 - \beta)\ddot{U}_0]$$

$$\ddot{U}_1 = \frac{1}{\beta\Delta t^2}[U_1 - U_0 - \Delta t\dot{U}_0 - \Delta t^2(1/2 - \beta)\ddot{U}_0]$$

......

In this way, we can get the values of all other points numerically one by one.

(2) For a continuous system

$$m\frac{\partial^2 \psi}{\partial t^2} + c\frac{\partial \psi}{\partial t} + \nabla^2 \psi + f_V = 0$$ on V, with boundary condition $\psi = f_S$ on S and initial

condition $\psi = \psi_0$ and $\partial \psi / \partial t = \dot{\psi}_0$ for $t=t_0$

where $\nabla^2 = \frac{\partial^2}{\partial x^2} + \frac{\partial^2}{\partial y^2} + \frac{\partial^2}{\partial z^2}$, $\psi = \psi(x, y, z, t)$

If we can use separation of variables, it becomes a time-dependent discrete system and a spatial-dependent problem.

We have discussed the time-dependent problem above. Now, let's discuss the spatial-dependent problem.

(a) in 1D

$$a\frac{d^2 u}{dx^2} + b\frac{du}{dx} + cu + g = 0$$

Any function can be expanded to Taylor series,

$$u(x) = \sum_{n=0}^{\infty} \frac{(x - x_i)^n}{n!} (\frac{d^n u}{dx^n})_i$$

Based on the definition of derivative and the Taylor series expansion, we have

$$(\frac{du}{dx})_i \approx \frac{u_{i+1} - u_{i-1}}{2\Delta x}$$ (central difference)

$$(\frac{d^2 u}{dx^2})_i \approx \frac{u_{i+1} - 2u_i + u_{i-1}}{(\Delta x)^2}$$

(b) in 2D

$$a\frac{\partial^2 u}{\partial x^2} + b\frac{\partial^2 u}{\partial x \partial y} + c\frac{\partial^2 u}{\partial y^2} + d\frac{\partial u}{\partial x} + e\frac{\partial u}{\partial y} + fu + g = 0 \quad [94]$$

$$\frac{\partial^2 u}{\partial x \partial y} = \frac{\partial}{\partial x}\left(\frac{\partial u}{\partial y}\right) = \frac{\partial}{\partial y}\left(\frac{\partial u}{\partial x}\right)$$

$$\left(\frac{\partial^2 u}{\partial x \partial y}\right)_{i,j} \approx \frac{\left(\frac{\partial u}{\partial y}\right)_{i+1,j} - \left(\frac{\partial u}{\partial y}\right)_{i-1,j}}{2\Delta x}$$

$$\left(\frac{\partial u}{\partial x}\right)_{i,j} \approx \frac{u_{i+1,j} - u_{i-1,j}}{2\Delta x}$$

$$\left(\frac{\partial u}{\partial y}\right)_{i,j} \approx \frac{u_{i,j+1} - u_{i,j-1}}{2\Delta y}$$

$$\left(\frac{\partial u}{\partial y}\right)_{i+1,j} \approx \frac{u_{i+1,j+1} - u_{i+1,j-1}}{2\Delta y}$$

$$\left(\frac{\partial u}{\partial y}\right)_{i-1,j} \approx \frac{u_{i-1,j+1} - u_{i-1,j-1}}{2\Delta y}$$

$$\left(\frac{\partial^2 u}{\partial x^2}\right)_{i,j} \approx \frac{u_{i+1,j} - 2u_{i,j} + u_{i-1,j}}{(\Delta x)^2}$$

$$\left(\frac{\partial^2 u}{\partial y^2}\right)_{i,j} \approx \frac{u_{i,j+1} - 2u_{i,j} + u_{i,j-1}}{(\Delta y)^2}$$

$$\left(\frac{\partial^2 u}{\partial x \partial y}\right)_{i,j} \approx \frac{u_{i+1,j+1} - u_{i+1,j-1} - u_{i-1,j+1} + u_{i-1,j-1}}{4\Delta x \Delta y}$$
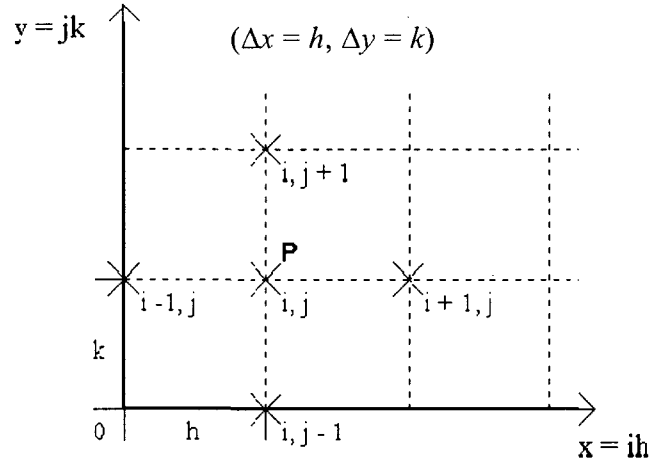
Fig. 3-4 the mesh of FDM

If we cannot or if it is not necessary for us to separate the variables in a time-dependent part and in a spatial-dependent part, such as the equation [96]

$$\frac{\partial u}{\partial t} = \frac{\partial^2 u}{\partial x^2}$$

it may be discretized into:

$$\frac{u(x, t + \Delta t) - u(x, t)}{\Delta t} = \frac{u(x + \Delta x, t) - 2u(x, t) + u(x - \Delta x, t)}{\Delta x^2}$$

$$u(x, t + \Delta t) = u(x, t) + \frac{\Delta t}{\Delta x^2}[u(x + \Delta x, t) - 2u(x, t) + u(x - \Delta x, t)]$$

This discretization is convenient because the "next" value (temporally) may be expressed in terms of "older" values at different positions.

We can introduce i, j, k to represent the spatial position and p to represent time. Then,

$x=i\Delta x$, $y=j\Delta y$, $z=k\Delta z$, $t=p\Delta t$; $u(x,y,z,t)=u_{i,j,k}^{p}$. The above equation can be express as:

$$u_i^{p+1}=u_i^p+\frac{\Delta t}{\Delta x^2}(u_{i+1}^p-2u_i^p+u_{i-1}^p)$$

Plus the boundary condition; we can get the value of every point on the mesh.

3.3. Sample calculation

When the dimension along y-axis is large ($b>>a$), and w is close to b ($w\approx b$), the system reduces to be a 2D problem. In this system, it is good for us to study influence of the electrolyte height h. So,

$$\frac{\partial^2\phi}{\partial x^2}+\frac{\partial^2\phi}{\partial z^2}=0$$
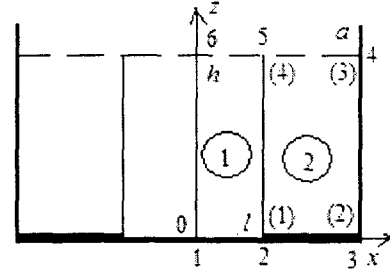
Fig. 3-5 the elements for FEM

Considering the boundary conditions and symmetry, we only need to solve the problem in the domain of $x\geq0$, and divide it into two elements as shown in Fig. 3-5:

Element one, $0\leq x\leq l$;

Element two, $l<x\leq a$.

Because of the rectangular shape of the domain, we choose bilinear polynomial basis (quadrilateral element)

$$<P>=<1\quad \xi\quad \eta\quad \xi\eta>$$

There are four nodes in every element

$<x_i>=<x_1\ z_1;\ x_2\ z_2;\ x_3\ z_3;\ x_4\ z_4>$

In the mapping space, (ξ,η): $(-1,-1)$, $(1,-1)$, $(1,1)$, $(-1,1)$

$$\langle N\rangle=\frac{1}{4}\langle(1-\xi)(1-\eta)\quad(1+\xi)(1-\eta)\quad(1+\xi)(1+\eta)\quad(1-\xi)(1+\eta)\rangle$$

$$\det(J^e)=A_0^e+A_1^e\xi+A_2^e\eta$$

$$A_0^e=[(z_4^e-z_2^e)(x_3^e-x_1^e)-(z_3^e-z_1^e)(x_4^e-x_2^e)]/8$$

$$A_1^e=[(z_3^e-z_4^e)(x_2^e-x_1^e)-(z_2^e-z_1^e)(x_3^e-x_4^e)]/8$$

$$A_2^e=[(z_4^e-z_1^e)(x_3^e-x_2^e)-(z_3^e-z_2^e)(x_4^e-x_1^e)]/8$$

If the element is rectangular, the length is d and the width is h, we get

58

$$x^e = \frac{x_1{}^e + x_2{}^e}{2} + \frac{d}{2}\xi \qquad z^e = \frac{z_1{}^e + z_4{}^e}{2} + \frac{h}{2}\eta$$

$A_0{}^e = dh/4,\ A_1{}^e = 0,\ A_2{}^e = 0$

$\det(J^e) = A_0{}^e = dh/4 \quad dxdz = (dh/4)d\xi d\eta$

$$\frac{\partial N_i}{\partial x} = \frac{\partial N_i}{\partial \xi}\cdot\frac{\partial \xi}{\partial x} + \frac{\partial N_i}{\partial \eta}\cdot\frac{\partial \eta}{\partial x} = \frac{2}{d}\frac{\partial N_i}{\partial \xi},$$

$$\frac{\partial N_i}{\partial z} = \frac{\partial N_i}{\partial \xi}\cdot\frac{\partial \xi}{\partial z} + \frac{\partial N_i}{\partial \eta}\cdot\frac{\partial \eta}{\partial z} = \frac{2}{h}\frac{\partial N_i}{\partial \eta}$$

Element 1: $A_0{}^{(1)} = lh/4$ $\qquad x^{(1)} = \frac{l}{2} + \frac{l}{2}\xi \qquad z^{(1)} = \frac{h}{2} + \frac{h}{2}\eta$

$$\frac{\partial N_i}{\partial x} = \frac{2}{l}\frac{\partial N_i}{\partial \xi}, \qquad \frac{\partial N_i}{\partial z} = \frac{2}{h}\frac{\partial N_i}{\partial \eta}$$

Element 2: $A_0{}^{(2)} = (a-l)h/4$ $\qquad x^{(2)} = \frac{a+l}{2} + \frac{(a-l)}{2}\xi \qquad z^{(2)} = \frac{h}{2} + \frac{h}{2}\eta$

$$\frac{\partial N_i}{\partial x} = \frac{2}{a-l}\frac{\partial N_i}{\partial \xi}, \qquad \frac{\partial N_i}{\partial z} = \frac{2}{h}\frac{\partial N_i}{\partial \eta}$$

Integrate the Laplace equation by parts, we get

$$\int_A (\frac{\partial \phi}{\partial x}\frac{\partial \delta\phi}{\partial x} + \frac{\partial \phi \partial \delta\phi}{\partial z \partial z})dA = \oint_L \frac{\partial \phi}{\partial n}\delta\phi dL$$

$$\int_A [(\sum_{i=1}^{4}\phi_i \frac{\partial N_i}{\partial x})\frac{\partial \delta\phi}{\partial x} + (\sum_{i=1}^{4}\phi_i \frac{\partial N_i}{\partial z})\frac{\partial \delta\phi}{\partial z}]dA = \oint_L \frac{\partial \phi}{\partial n}\delta\phi dL$$

Because $\delta u(x,y)$ is an arbitrary function, we can choose $\delta u = N_1, N_2, N_3$ and N_4. Then

$[K^e]\{\phi^e\} = \{P^e\}$

$$K^e{}_{ij} = \int_A (\frac{\partial N_i}{\partial x}\frac{\partial N_j}{\partial x} + \frac{\partial N_i}{\partial z}\frac{\partial N_j}{\partial z})dA = \int_{-1}^{1}\int_{-1}^{1}(\frac{h}{d}\frac{\partial N_i}{\partial \xi}\frac{\partial N_j}{\partial \xi} + \frac{d}{h}\frac{\partial N_i}{\partial \eta}\frac{\partial N_j}{\partial \eta})d\xi d\eta$$

$P^e{}_i = \oint_L \frac{\partial \phi}{\partial n}N_i dL$ (the direction of the n is the normal outward unit vector to the element)

Please note that the interface between two elements is an interior side, there is no contribution to whole problem in total.

Element 1: please note, only on side one is there $\frac{\partial \phi}{\partial n} \neq 0$. In addition, because of the nature of the shape function, $N_3 = 0$ and $N_4 = 0$ on side one ($\eta = -1$). Thus we get

$$P^{(1)}{}_1 = \frac{1}{\sigma} \int_{side1} [i_D - \kappa_{Mg}(\phi - \phi_{MgCorr})]N_1 dL$$

$$P^{(1)}{}_2 = \frac{1}{\sigma} \int_{side1} [i_D - \kappa_{Mg}(\phi - \phi_{MgCorr})]N_2 dL$$

$$P^{(1)}{}_3 = P^{(1)}{}_4 = 0$$

$$P^{(1)}{}_1 \approx \frac{1}{\sigma} \int_{side1} [i_D - \kappa_{Mg}(\phi - \phi_{MgCorr})]N_1 dx = \frac{1}{\sigma} \int_{-1}^{1} [i_D - \kappa_{Mg}(\phi - \phi_{MgCorr})]\frac{(1-\xi)}{2} \cdot \frac{l}{2} d\xi$$

$$= \frac{i_D l}{2\sigma} - \frac{\kappa_{Mg} l}{\sigma} \int_{-1}^{1} (\phi_1 N_1 + \phi_2 N_2 - \phi_{MgCorr})\frac{(1-\xi)}{4} d\xi$$

$$= \frac{i_D l}{2\sigma} - \frac{\kappa_{Mg} l}{\sigma} \int_{-1}^{1} (\phi_1 \frac{1-\xi}{2} + \phi_2 \frac{1+\xi}{2} - \phi_{MgCorr})\frac{(1-\xi)}{4} d\xi$$

$$= \frac{i_D l}{2\sigma} - \frac{\kappa_{Mg} l}{2\sigma}(\frac{2}{3}\phi_1^{(1)} + \frac{1}{3}\phi_2^{(1)} - \phi_{MgCorr})$$

Similarly, we get

$$P^{(1)}{}_2 = \frac{i_D l}{2\sigma} - \frac{\kappa_{Mg} l}{\sigma} \int_{-1}^{1} (\phi_1 \frac{1-\xi}{2} + \phi_2 \frac{1+\xi}{2} - \phi_{MgCorr})\frac{(1+\xi)}{4} d\xi$$

$$= \frac{i_D l}{2\sigma} - \frac{\kappa_{Mg} l}{2\sigma}(\frac{1}{3}\phi_1^{(1)} + \frac{2}{3}\phi_2^{(1)} - \phi_{MgCorr})$$

Element 2:

$$P^{(2)}{}_1 = -\frac{1}{\sigma} \int_{side1} \kappa_{Zn}(\phi - \phi_{ZnCorr})]N_1 dL = -\frac{\kappa_{Zn}(a-l)}{2\sigma}(\frac{2}{3}\phi_1^{(2)} + \frac{1}{3}\phi_2^{(2)} - \phi_{ZnCorr})$$

$$P^{(2)}{}_2 = -\frac{1}{\sigma} \int_{side1} \kappa_{Zn}(\phi - \phi_{ZnCorr})]N_2 dL = -\frac{\kappa_{Zn}(a-l)}{2\sigma}(\frac{1}{3}\phi_1^{(2)} + \frac{2}{3}\phi_2^{(2)} - \phi_{ZnCorr})$$

$$P^{(2)}{}_3 = P^{(2)}{}_4 = 0$$

$$\frac{1}{6}\begin{bmatrix} \frac{2h}{l}+\frac{2l}{h} & -\frac{2h}{l}+\frac{l}{h} & -\frac{h}{l}-\frac{l}{h} & \frac{h}{l}-\frac{2l}{h} \\ -\frac{2h}{l}+\frac{l}{h} & \frac{2h}{l}+\frac{2l}{h} & \frac{h}{l}-\frac{2l}{h} & -\frac{h}{l}-\frac{l}{h} \\ -\frac{h}{l}-\frac{l}{h} & \frac{h}{l}-\frac{2l}{h} & \frac{2h}{l}+\frac{2l}{h} & -\frac{2h}{l}+\frac{l}{h} \\ \frac{h}{l}-\frac{2l}{h} & -\frac{h}{l}-\frac{l}{h} & -\frac{2h}{l}+\frac{l}{h} & \frac{2h}{l}+\frac{2l}{h} \end{bmatrix} \begin{Bmatrix} \phi_1^{(1)} \\ \phi_2^{(1)} \\ \phi_3^{(1)} \\ \phi_4^{(1)} \end{Bmatrix} = \begin{Bmatrix} \frac{i_D l}{2\sigma} - \frac{\kappa_{Mg} l}{2\sigma}[\frac{2}{3}\phi_1^{(1)} + \frac{1}{3}\phi_2^{(1)} - \phi_{MgCorr}] \\ \frac{i_D l}{2\sigma} - \frac{\kappa_{Mg} l}{2\sigma}[\frac{1}{3}\phi_1^{(1)} + \frac{2}{3}\phi_2^{(1)} - \phi_{MgCorr}] \\ 0 \\ 0 \end{Bmatrix}$$

$$\frac{1}{6}\begin{bmatrix} \dfrac{2h}{l}+\dfrac{2l}{h}+\dfrac{2\kappa_{Mg}l}{\sigma} & -\dfrac{2h}{l}+\dfrac{l}{h}+\dfrac{\kappa_{Mg}l}{\sigma} & -\dfrac{h}{l}-\dfrac{l}{h} & \dfrac{h}{l}-\dfrac{2l}{h} \\[8pt] -\dfrac{2h}{l}+\dfrac{l}{h}+\dfrac{\kappa_{Mg}l}{\sigma} & \dfrac{2h}{l}+\dfrac{2l}{h}+\dfrac{2\kappa_{Mg}l}{\sigma} & \dfrac{h}{l}-\dfrac{2l}{h} & -\dfrac{h}{l}-\dfrac{l}{h} \\[8pt] -\dfrac{h}{l}-\dfrac{l}{h} & \dfrac{h}{l}-\dfrac{2l}{h} & \dfrac{2h}{l}+\dfrac{2l}{h} & -\dfrac{2h}{l}+\dfrac{l}{h} \\[8pt] \dfrac{h}{l}-\dfrac{2l}{h} & -\dfrac{h}{l}-\dfrac{l}{h} & -\dfrac{2h}{l}+\dfrac{l}{h} & \dfrac{2h}{l}+\dfrac{2l}{h} \end{bmatrix} \begin{Bmatrix} \phi_1^{(1)} \\ \phi_2^{(1)} \\ \phi_3^{(1)} \\ \phi_4^{(1)} \end{Bmatrix} = \begin{Bmatrix} \dfrac{i_D l}{2\sigma}+\dfrac{\kappa_{Mg}l}{2\sigma}\phi_{MgCorr} \\[8pt] \dfrac{i_D l}{2\sigma}+\dfrac{\kappa_{Mg}l}{2\sigma}\phi_{MgCorr} \\[8pt] 0 \\[4pt] 0 \end{Bmatrix}$$

Element 2:

$$\frac{1}{6}\begin{bmatrix} \dfrac{2h}{a-l}+\dfrac{2(a-l)}{h} & -\dfrac{2h}{a-l}+\dfrac{a-l}{h} & \dfrac{h}{a-l}-\dfrac{a-l}{h} & \dfrac{h}{a-l}-\dfrac{2(a-l)}{h} \\[8pt] -\dfrac{2h}{a-l}+\dfrac{a-l}{h} & \dfrac{2h}{a-l}+\dfrac{2(a-l)}{h} & \dfrac{h}{a-l}-\dfrac{2(a-l)}{h} & -\dfrac{h}{a-l}-\dfrac{a-l}{h} \\[8pt] \dfrac{h}{a-l}-\dfrac{a-l}{h} & \dfrac{h}{a-l}-\dfrac{2(a-l)}{h} & \dfrac{2h}{a-l}+\dfrac{2(a-l)}{h} & -\dfrac{2h}{a-l}+\dfrac{a-l}{h} \\[8pt] \dfrac{h}{a-l}-\dfrac{2(a-l)}{h} & -\dfrac{h}{a-l}-\dfrac{a-l}{h} & -\dfrac{2h}{a-l}+\dfrac{a-l}{h} & \dfrac{2h}{a-l}+\dfrac{2(a-l)}{h} \end{bmatrix} \begin{Bmatrix} \phi_1^{(2)} \\ \phi_2^{(2)} \\ \phi_3^{(2)} \\ \phi_4^{(2)} \end{Bmatrix} = \begin{Bmatrix} -\dfrac{\kappa_{Zn}(a-l)}{2\sigma}[\dfrac{2}{3}\phi_1^{(2)}+\dfrac{1}{3}\phi_2^{(2)}-\phi_{ZnCorr}] \\[8pt] -\dfrac{\kappa_{Zn}(a-l)}{2\sigma}[\dfrac{1}{3}\phi_1^{(2)}+\dfrac{2}{3}\phi_2^{(2)}-\phi_{ZnCorr}] \\[8pt] 0 \\[4pt] 0 \end{Bmatrix}$$

$$\frac{1}{6}\begin{bmatrix} \dfrac{2h}{a-l}+\dfrac{2(a-l)}{h}+\dfrac{2\kappa_{Zn}(a-l)}{\sigma} & -\dfrac{2h}{a-l}+\dfrac{a-l}{h}+\dfrac{\kappa_{Zn}(a-l)}{\sigma} & \dfrac{h}{a-l}-\dfrac{a-l}{h} & \dfrac{h}{a-l}-\dfrac{2(a-l)}{h} \\[8pt] -\dfrac{2h}{a-l}+\dfrac{a-l}{h}+\dfrac{\kappa_{Zn}(a-l)}{\sigma} & \dfrac{2h}{a-l}+\dfrac{2(a-l)}{h}+\dfrac{2\kappa_{Zn}(a-l)}{\sigma} & \dfrac{h}{a-l}-\dfrac{2(a-l)}{h} & -\dfrac{h}{a-l}-\dfrac{a-l}{h} \\[8pt] \dfrac{h}{a-l}-\dfrac{a-l}{h} & \dfrac{h}{a-l}-\dfrac{2(a-l)}{h} & \dfrac{2h}{a-l}+\dfrac{2(a-l)}{h} & -\dfrac{2h}{a-l}+\dfrac{a-l}{h} \\[8pt] \dfrac{h}{a-l}-\dfrac{2(a-l)}{h} & -\dfrac{h}{a-l}-\dfrac{a-l}{h} & -\dfrac{2h}{a-l}+\dfrac{a-l}{h} & \dfrac{2h}{a-l}+\dfrac{2(a-l)}{h} \end{bmatrix} \begin{Bmatrix} \phi_1^{(2)} \\ \phi_2^{(2)} \\ \phi_3^{(2)} \\ \phi_4^{(2)} \end{Bmatrix} = \begin{Bmatrix} \dfrac{\kappa_{Zn}(a-l)}{2\sigma}\phi_{0Zn} \\[8pt] \dfrac{\kappa_{Zn}(a-l)}{2\sigma}\phi_{0Zn}] \\[8pt] 0 \\[4pt] 0 \end{Bmatrix}$$

Assemble the matrix equations in element 1 and element to global matrix equation:

$$\frac{1}{6}\begin{bmatrix} \dfrac{2h}{l}+\dfrac{2l}{h}+\dfrac{2\kappa_{Mg}l}{\sigma} & -\dfrac{2h}{l}+\dfrac{l}{h}+\dfrac{\kappa_{Mg}l}{\sigma} & 0 & 0 & -\dfrac{h}{l}-\dfrac{l}{h} & \dfrac{h}{l}-\dfrac{2l}{h} \\[8pt] -\dfrac{2h}{l}+\dfrac{l}{h}+\dfrac{\kappa_{Mg}l}{\sigma} & \dfrac{2h}{l}+\dfrac{2h}{a-l}+\dfrac{2a}{h}+\dfrac{2\kappa_{Mg}l}{\sigma}+\dfrac{2\kappa_{Zn}(a-l)}{\sigma} & -\dfrac{2h}{a-l}+\dfrac{a-l}{h}+\dfrac{\kappa_{Zn}(a-l)}{\sigma} & -\dfrac{h}{a-l}-\dfrac{a-l}{h} & \dfrac{h}{l}+\dfrac{h}{a-l}-\dfrac{2a}{h} & \dfrac{h}{l}-\dfrac{l}{h} \\[8pt] 0 & -\dfrac{2h}{a-l}+\dfrac{a-l}{h}+\dfrac{\kappa_{Zn}(a-l)}{\sigma} & \dfrac{2h}{a-l}+\dfrac{2(a-l)}{h}+\dfrac{2\kappa_{Zn}(a-l)}{\sigma} & \dfrac{h}{a-l}-\dfrac{2(a-l)}{h} & -\dfrac{h}{a-l}-\dfrac{a-l}{h} & 0 \\[8pt] 0 & -\dfrac{h}{a-l}-\dfrac{a-l}{h} & \dfrac{h}{a-l}-\dfrac{2(a-l)}{h} & \dfrac{2h}{a-l}+\dfrac{2(a-l)}{h} & -\dfrac{2h}{a-l}+\dfrac{a-l}{h} & 0 \\[8pt] -\dfrac{h}{l}-\dfrac{l}{h} & \dfrac{h}{l}+\dfrac{h}{a-l}-\dfrac{2a}{h} & -\dfrac{h}{a-l}-\dfrac{a-l}{h} & -\dfrac{2h}{a-l}+\dfrac{a-l}{h} & \dfrac{2h}{l}+\dfrac{2h}{a-l}+\dfrac{2a}{h} & -\dfrac{2h}{l}+\dfrac{l}{h} \\[8pt] \dfrac{h}{l}-\dfrac{2l}{h} & -\dfrac{h}{l}-\dfrac{l}{h} & 0 & 0 & -\dfrac{2h}{l}+\dfrac{l}{h} & \dfrac{2h}{l}+\dfrac{2l}{h} \end{bmatrix}$$

61

$$\times \begin{Bmatrix} \phi_1 \\ \phi_2 \\ \phi_3 \\ \phi_4 \\ \phi_5 \\ \phi_6 \end{Bmatrix} = \frac{1}{2} \begin{Bmatrix} \dfrac{i_D l}{\sigma} + \dfrac{\kappa_{Mg} l}{\sigma}\phi_{0Mg} \\ \dfrac{i_D l}{\sigma} + \dfrac{\kappa_{Mg} l}{\sigma}\phi_{0Mg} + \dfrac{\kappa_{Zn}(a-l)}{\sigma}\phi_{0Zn} \\ \dfrac{\kappa_{Zn}(a-l)}{\sigma}\phi_{0Zn} \\ 0 \\ 0 \\ 0 \end{Bmatrix}$$

It is not easy to get an analytic expression of ϕ by a, l and h. Anyway, for a certain problem, the value of a, l and h is fixed. We can put the number in above equation and solve is easily. After we solve out the equation, we can get the value of ϕ_1, ϕ_2, ..., and express the net current density on the exposed surface analytically, namely, on side one ($z = 0$, $\eta = -1$) in element one.

$$i_g \approx -\kappa_{Mg}(\phi - \phi_{MgCorr}) = -\kappa_{Mg}(N_1^{(1)}\phi_1 + N_2^{(1)}\phi_2 - \phi_{MgCorr})$$

$$= -\kappa_{Mg}(\frac{\phi_1 + \phi_2}{2} - \phi_{MgCorr} + \frac{\phi_2 - \phi_1}{2}\xi) = -\kappa_{Mg}[\frac{\phi_1 + \phi_2}{2} - \phi_{MgCorr} + \frac{\phi_2 - \phi_1}{2l}(2x - l)] \qquad (0 \le x \le l)$$

According to symmetric, we can get the solution for all exposed area:

$$i_g = -\kappa_{Mg}(\frac{\phi_1 + \phi_2}{2} - \phi_{MgCorr} + \frac{\phi_2 - \phi_1}{2}\xi) = -\kappa_{Mg}[\frac{\phi_1 + \phi_2}{2} - \phi_{MgCorr} + \frac{\phi_2 - \phi_1}{2l}(2|x| - l)] \qquad (-l \le x \le l)$$

Correspondingly, we know the corrosion rate and the corrosion distribution.

At the point of $x=\pm l$, $i_{tot} = -\kappa_{Mg}(\phi_2 - \phi_{MgCorr})$.

At the point of $x=0$, $i_{tot} = -\kappa_{Mg}(\phi_1 - \phi_{MgCorr})$

Let $a=ml$ ($m>1$), $h=nl$, $p=\kappa/\sigma$,

$$\begin{bmatrix} 2n+\dfrac{2}{n}+2p_{Mg}l & -2n+\dfrac{1}{n}+p_{Mg}l & 0 & 0 & -n-\dfrac{1}{n} & n-\dfrac{2}{n} \\ -2n+\dfrac{1}{n}+p_{Mg}l & 2n+\dfrac{2n}{m-1}+\dfrac{2m}{n}+2p_{Mg}l+2p_{Zn}(m-1)l & -\dfrac{2n}{m-1}+\dfrac{m-1}{n}+p_{Zn}(m-1)l & -\dfrac{n}{m-1}-\dfrac{m-1}{n} & n+\dfrac{n}{m-1}-\dfrac{2m}{n} & -n-\dfrac{1}{n} \\ 0 & -\dfrac{2n}{m-1}+\dfrac{m-1}{n}+p_{Zn}(m-1)l & \dfrac{2n}{m-1}+\dfrac{2(m-1)}{n}+2p_{Zn}(m-1)l & \dfrac{n}{m-1}-\dfrac{2(m-1)}{n} & -\dfrac{n}{m-1}-\dfrac{m-1}{n} & 0 \\ 0 & -\dfrac{n}{m-1}-\dfrac{m-1}{n} & \dfrac{n}{m-1}-\dfrac{2(m-1)}{n} & \dfrac{2n}{m-1}+\dfrac{2(m-1)}{n} & -\dfrac{2n}{m-1}+\dfrac{m-1}{n} & 0 \\ -n-\dfrac{1}{n} & n+\dfrac{n}{m-1}-\dfrac{2m}{n} & -\dfrac{n}{m-1}-\dfrac{m-1}{n} & -\dfrac{2n}{m-1}+\dfrac{m-1}{n} & 2n+\dfrac{2n}{m-1}+\dfrac{2m}{n} & -2n+\dfrac{1}{n} \\ n-\dfrac{2}{n} & -n-\dfrac{1}{n} & 0 & 0 & -2n+\dfrac{1}{n} & 2n+\dfrac{2}{n} \end{bmatrix}$$

$$\times \begin{Bmatrix} \phi_1 \\ \phi_2 \\ \phi_3 \\ \phi_4 \\ \phi_5 \\ \phi_6 \end{Bmatrix} = 3 \begin{Bmatrix} \dfrac{i_D l}{\sigma} + p_{Mg} l \phi_{MgCorr} \\ \dfrac{i_D l}{\sigma} + p_{Mg} l \phi_{MgCorr} + p_{Zn}(m-1) l \phi_{ZnCorr} \\ p_{Zn}(m-1) l \phi_{ZnCorr} \\ 0 \\ 0 \\ 0 \end{Bmatrix}$$

Only ϕ_1 and ϕ_2 contribute to current density on the exposed boundary.

We choose $C_{O_2 sat}=2.5\times10^{-4} M/cm^2$, $D_{O_2}=1.9\times10^{-5} cm^2/s$, $i_{0Mg}=10^{-6} A/cm^2$, $\phi_{MgCorr}=-1.7V$, $i_{0Zn}=10^{-7}A/cm^2$, $\phi_{ZnCorr}=-0.75V$. $\sigma=0.050 S/cm$ (usually, it is 10^{-3}-0.4 S/cm). At 300K, $\kappa_{Mg}=1.5\times10^{-3}A/cm^2V$, $\kappa_{Zn}=1.5\times10^{-4}A/cm^2V$, $p_{Mg}=3.0\times10^{-2}A/cmVS$, $p_{Zn}=3.0\times10^{-3}$ A/cmVS, and $i_D = -\dfrac{9.2\times10^{-4}}{h} A/cm^2$ (the unit of h is cm).

At standard condition and in the linear region, the polarization for anodic reaction on both magnesium and zinc can be expressed as:

$$i_{aMg} = -1.5\times10^{-3}(\phi+1.70),$$

$$i_{aZn} = -1.5\times10^{-4}(\phi+0.76)$$

(1) Let us choose l=1.0mm=0.1cm. The matrix equation becomes:

$$\begin{bmatrix} 2n+\dfrac{2}{n}+0.006 & -2n+\dfrac{1}{n}+0.003 & 0 & 0 & -n-\dfrac{1}{n} & n-\dfrac{2}{n} \\ -2n+\dfrac{1}{n}+0.003 & 2n+\dfrac{2n}{m-1}+\dfrac{2m}{n}+0.006+6(m-1)\times10^{-4} & -\dfrac{2n}{m-1}+\dfrac{m-1}{n}+3(m-1)\times10^{-4} & -\dfrac{n}{m-1}-\dfrac{m-1}{n} & n+\dfrac{n}{m-1}-\dfrac{2m}{n} & -n-\dfrac{1}{n} \\ 0 & -\dfrac{2n}{m-1}+\dfrac{m-1}{n}+3(m-1)\times10^{-4} & \dfrac{2n}{m-1}+\dfrac{2(m-1)}{n}+6(m-1)\times10^{-4} & \dfrac{n}{m-1}-\dfrac{2(m-1)}{n} & -\dfrac{n}{m-1}-\dfrac{m-1}{n} & 0 \\ 0 & -\dfrac{n}{m-1}-\dfrac{m-1}{n} & \dfrac{n}{m-1}-\dfrac{2(m-1)}{n} & \dfrac{2n}{m-1}+\dfrac{2(m-1)}{n} & -\dfrac{2n}{m-1}+\dfrac{m-1}{n} & 0 \\ -n-\dfrac{1}{n} & n+\dfrac{n}{m-1}-\dfrac{2m}{n} & -\dfrac{n}{m-1}-\dfrac{m-1}{n} & -\dfrac{2n}{m-1}+\dfrac{m-1}{n} & 2n+\dfrac{2n}{m-1}+\dfrac{2m}{n} & -2n+\dfrac{1}{n} \\ n-\dfrac{2}{n} & -n-\dfrac{1}{n} & 0 & 0 & -2n+\dfrac{1}{n} & 2n+\dfrac{2}{n} \end{bmatrix}$$

$$\times \begin{Bmatrix} \phi_1 \\ \phi_2 \\ \phi_3 \\ \phi_4 \\ \phi_5 \\ \phi_6 \end{Bmatrix} = 3 \begin{Bmatrix} -\dfrac{1.8\times10^{-3}}{h} - 5.1\times10^{-3} \\ -\dfrac{1.8\times10^{-3}}{h} - 5.1\times10^{-3} - 2.2(m-1)\times10^{-4} \\ -2.2(m-1)\times10^{-4} \\ 0 \\ 0 \\ 0 \end{Bmatrix}$$

Table 3-1 the influence of the electrolyte height for a small film-free area

l=1mm, m=2, a=2l, no diffusion, i_D=0							
n	0.001	0.01	0.1	1	10	100	1000
ϕ_1(V)	-1.700	-0.232	-0.024	-1.6092	-0.0046	-0.2831	-1.2846
ϕ_2(V)	-1.299	-0.001	-0.0016	-1.609	-0.0036	-0.2832	-1.2846
m=2, a=2l, with diffusion							
n	0.001	0.01	0.1	1	10	100	1000
ϕ_1(V)	-5.998×10^3	-81.64	-0.8241	-3.8461	-0.003	-0.2733	-1.2846
ϕ_2(V)	-4.152×10^3	-0.502	-0.0519	-3.845	-0.0024	-0.2734	-1.2846

Table 3-2 the influence from the zinc covered area

l=1mm, n=0.01, no diffusion, i_D=0			With diffusion		
m	5	11	101	5	11	101
ϕ_1(V)	-1.1244	-1.3722	-0.0804	-353.717	-391.3567	-15.849
ϕ_2(V)	-1.0335	-1.3205	-0.3615	-315.0868	-358.6788	-112.8277

$$i_g = -1.5\times10^{-3}(\phi_1 - 1.7 + \frac{\phi_2 - \phi_1}{l}|x|)$$

From the value of ϕ_1 and ϕ_2 in above tables, we know:

(a) Generally, we can schematic the distribution corrosion current as:
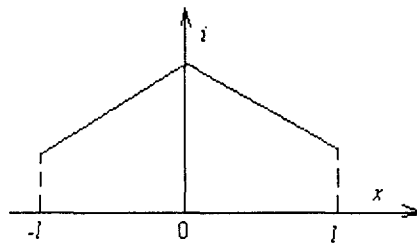
Fig. 3-6 The schematic of corrosion corrent distribution

(b) When the electrolyte depth is thin, the corrosion situation is serious, and the current density distribution on the exposed surface is much difference, especially the corrosion and its distribution from the oxygen diffusion. With the electrolyte depth increasing, the system becomes gradually equipotential body. The corrosion distribution becomes constant.

(c) For a certain film free area in a certain depth electrolyte, the corrosion becomes more serious when the area ratio of protected area and exposed area increases.

(d) From table 3-1, we can see that the value of ϕ_1 and ϕ_2 does not change smoothly. The reason for it may be because the actual distribution of current density is not linear, but we choose a linear approach and only divide the domain into two elements.

(2) Let us choose $l=1.0\text{m}=1.0\times10^2\text{cm}$. Now the matrix equation becomes:

$$
\begin{bmatrix}
2n+\frac{2}{n}+6 & -2n+\frac{1}{n}+3 & 0 & 0 & -n-\frac{1}{n} & n-\frac{2}{n} \\[6pt]
-2n+\frac{1}{n}+3 & 2n+\frac{2n}{m-1}+\frac{2m}{n}+6+0.6(m-1) & -\frac{2n}{m-1}+\frac{m-1}{n}+0.3(m-1) & \frac{n}{m-1}-\frac{m-1}{n} & n+\frac{n}{m-1}-\frac{2m}{n} & -n-\frac{1}{n} \\[6pt]
0 & -\frac{2n}{m-1}+\frac{m-1}{n}+0.3(m-1) & \frac{2n}{m-1}+\frac{2(m-1)}{n}+0.6(m-1) & \frac{n}{m-1}-\frac{2(m-1)}{n} & -\frac{n}{m-1}-\frac{m-1}{n} & 0 \\[6pt]
0 & \frac{n}{m-1}-\frac{m-1}{n} & \frac{n}{m-1}-\frac{2(m-1)}{n} & \frac{2n}{m-1}+\frac{2(m-1)}{n} & -\frac{2n}{m-1}+\frac{m-1}{n} & 0 \\[6pt]
-n-\frac{1}{n} & n+\frac{n}{m-1}-\frac{2m}{n} & -\frac{n}{m-1}-\frac{m-1}{n} & -\frac{2n}{m-1}+\frac{m-1}{n} & 2n+\frac{2n}{m-1}+\frac{2m}{n} & -2n+\frac{1}{n} \\[6pt]
n-\frac{2}{n} & -n-\frac{1}{n} & 0 & 0 & -2n+\frac{1}{n} & 2n+\frac{2}{n}
\end{bmatrix}
$$

$$
\times \begin{Bmatrix} \phi_1 \\ \phi_2 \\ \phi_3 \\ \phi_4 \\ \phi_5 \\ \phi_6 \end{Bmatrix} = 3 \begin{Bmatrix} -\frac{1.8}{h}-3.6 \\[6pt] -\frac{1.8}{h}-3.6-8.4(m-1)\times10^{-2} \\[6pt] -8.4(m-1)\times10^{-2} \\ 0 \\ 0 \\ 0 \end{Bmatrix}
$$

Table 3-3 the influence of the electrolyte height for a large film-free area

	$l=1$m, m=2, $a=2l$, no diffusion, $i_D=0$				m=2, $a=2l$, with diffusion			
n	0.001	0.01	0.1	1	0.001	0.01	0.1	1
ϕ_1(V)	-1.2703	-1.2518	-1.2444	-1.186	-5.1324	-1.191	-1.186	-0.6145
ϕ_2(V)	-1.1648	-1.1164	-1.0498	-1.073	-4.8338	-0.999	-1.073	-0.5700

For a larger film free area, the difference of the current distribution is smaller and the corrosion current density is much smaller.

References

[1] Barbara A. Shaw and Robert G. Kelly, The Electrochemical Society Interface, Spring (2006) p24.

[2] S. M. Sharland, C. P. Jackson and A. J. Diver, Corrosion Science **29** (1989) 1149.

[3] V. Botte, D. Mansutti, and A. Pascarelli, Applied Numerical Mathematics **55** (2005) 253–263.

[4] S. M. Sharland and P. W. Tasker, Corrosion Science **28** (1988) 603-620.

[5] F.R. Pérez, K. E. García, A.L. Morales, Revista Colombiana de Física **38** (2006) 1138.

[6] J. Warkus, M. Raupach and J. Gulikers, Materials and Corrosion **57** (2006) 614.

[7] R.D. Klassen, P.R. Roberge, C.V. Hyatt, Electrochimica Acta **46** (2001) 3705–3713.

[8] Guangling Song, Birgir Johannesson, Sarath Hapugoda, and David StJohn, Corrosion Science **46** (2004) 955–977

[9] John N. Harb and Richard C. Alkire, Corrosion Science **29** (1989) 31-43.

[10] Mark Verbrugge, Corrosion Science **48** (2006) 3489-3512.

[11] Jong-Min Lee, Electrochimica Acta **51** (2006) 3256–3260.

[12] James A. Nesbitt, Oxidation of Metals **44** (1995) 309.

[13] S.M. Sharland, Corrosion Science **29** (1989) 1149.

[14] J.C. Walton, Corrosion Science **30** (1990) 915.

[15] P.O. Gartland, Proceedings of Corrosion/96 Denver (1996) 311.

[16] A. Turnbull and J.G.N. Thomas, J. Electrochem. Soc. **129** (1982) 1412.

[17] B. Vuillemin, R. Oltra, R. Cottis and D. Crusset, Electrochimica Acta **52** (2007) 7570-7576.

[18] G. Engelhardt, M. Urquidi-Macdonald and D. D. Macdonald, Corrosion Science **39** (1997) 419-441.

[19] J. X. Jia, A. Atrens, G. Song and T. H. Muster, Materials and Corrosion **56** (2005) 468.

[20] Jimmy X. Jia, Guangling Song, Andrej Atrens, Corrosion Science **48** (2006) 2133.

[21] K. Jafarzadeh, T. Shahrabi and M. G. Hosseini, J. Mater. Sci. Technol. **24** (2008) 215.

[22] Susanne Bender, Joachim Goellner and Andrej Atrens, Advanced Engineering Materials **10** (2008) 583.

[23] Guangling Song, Andrej Atrens, Xianliang Wu and Bo Zhang, Corrosion Science **39** (1998) 1769-1791.

[24] M.F. Horstemeyer, N. Yang, Ken Gall, D.L. McDowell, J. Fan, and P.M. Gullett, Acta Materialia **52** (2004) 1327–1336.

[25] Andrej Atrens andWolfgang Dietzel, Advanced Engineering Materials **9** (2007) 292.

[26] I. Apachitei, L.E. Fratila-Apachitei and J. Duszczyk, Scripta Materialia **57** (2007) 1012–1015.

[27] Andrey Shkurankov, Sherif Zein El Abedin, and Frank Endres, Aust. J. Chem. **60** (2007) 35–42

[28] Rajan Ambat, Naing Naing Aung, W. Zhou, Corrosion Science **42** (2000) 1433.

[29] Speller, Frank N., Corrosion: Causes and Prevention - An Engineering Problem, 1st edition 1926, 2nd Edition 1935, McGraw-Hill, New York.

[30] Guangling Song and Andrej Atrens, Advanced Engineering Materials **5** (2003) 837.

[31] http://www.cheresources.com/corrosion.shtml

[32] K.H.W. Seah, K.B. Lim, C.H. Chew, S.H. Teoh, Corrosion Science **34** (1993) 1707.

[33] R.J. Grossman, IEEE Trans. Sonics and Ultrasonics SU-31 (1984) 25.

[34] T.W. Retting, M.J. Felsen, Corrosion **32** (1976) 121.

[35] Pierre R. Roberge, Corrosion Basics: An Introduction (2nd edition), 2006 NACE International, Houston.

[36] S. Magaino, A. Kawaguchi, A. Hirata, T. Osaka, J. Electrochem. Soc. **134** (1987) 2993.

[37] A. Arora, Corrosion **40** (1984) 459.

[38] R.H. Jones, M.A. Friesel, Corrosion **48** (1992) 751.

[39] H. Mazille, R. Roth_ea, C. Tronel, Corrosion Science **37** (1995) 1365.

[40] M. Fregonese, H. Idrissi, H. Mazille, L. Renaud, and Y. Cetre, Corrosion Science **43** (2001) 627-641.

[41] C. Gabrielli, S. Joiret, M. Keddam, N. Portail, P. Rousseau, V. Vivier, Electrochimica Acta **53** (2008) 7539–7548.

[42] http:// hyperphysics.phy-astr.gsu.edu/Hbase/chemical/c1

[43] http://members.tripod.com/mg/asm_prop.htm#amchem

[44] http://www.magnesium.com/w3/data-bank/index.php?mgw=166

[45] M. Jönsson, D. Thierry and N. LeBozec, Corrosion Science **48** (2006) 1193.

[46] G. Ben-Hamu, D. Eliezer and K.S. Shin, Materials Science and Engineering, **A 447** (2007) 35.

[47] F. Andreatta, I. Apachitei, A. A. Kodentsov, J. Dzwonczyk, J. Duszczyk, Electrochimica Acta **51** (2006) 3551.

[48] D. Bengtsson Blu¨cher, J.-E. Svensson, L.-G. Johansson,M. Rohwerder, M. Stratmann, J. Electrochem. Soc. **151** (2004) B621.

[49] F. D. A. Aarão Reis, Janusz Stafiej, and J.-P. Badiali, J. Phys. Chem. **B 110** (2006) 17554-17562

[50] D. A. Shifler, et al. Corrosion Science **47** (2005) 2335–2352.

[51] C. P. Gardiner, et al. Corrosion Science **44** (2002) 2459–2478.

[52] S. Hoerle, et al. Corrosion Science **46** (2004), 1401–1429.

[53] R.E. Melchers, et al. Corrosion Science **45** (2003), 923–940

[54] J. S. Newman, Electrochemical Systems, Prentice-Hall, Englewood Cliffs, NJ, 1991.

[55] http://en.wikipedia.org/wiki/

[56] P.W. Atkins, Physical Chemistry, fourth ed., Oxford University Press, Oxford, 1990.

[57] A. Turnbull and M. R. Gardiner, Corrosion Science **22** (1982) 661.

[58] M. Isacsson, H. Rootzen, O. Lunder, Galvanically induced atmospheric corrosion on magnesium alloys: a designed experiment evaluated by extreme value statistics and conventional techniques, SAE, SP-1250, No. 970328, 1997, pp. 43–55.

[59] M. Starostin, A. Smorodin, Y. Cohen, L. Gal-Or, S. Tamir, Galvanic corrosion of magnesium alloys, in: E. Aghion, D. Eliezer (Eds.), Magnesium 2000, Proceedings of the Second Israeli International Conference on Magnesium Science and Technology, Dead Sea, Israel, 2000, pp. 363–370.

[60] G. Gao, G. Cole, M. Richetts, J. Balzer, P. Frantzeskakis, Effects of fastener surface on galvanic corrosion of automotive magnesium components, in: E. Aghion, D. Eliezer (Eds.), Magnesium 2000, Proceedings of the Second Israeli International Conference on Magnesium Science and Technology, Dead Sea, Israel, 2000, pp. 321–338.

[61] D.L. Hawke, Galvanic corrosion of magnesium, SDCE 14th International Die Casting Congress and Exposition, Toronto, Canada, May 1987, Paper No. G-T87-004.

[62] J. Senf, E. Broszeit, M. Gugau, C. Berger, Corrosion and galvanic corrosion of die casted magnesium alloys, in: H.I. Kaplan, J. Hryn, B. Clow (Eds.), Magnesium Technology 2000, TMS, Nashville, 2000, pp. 137–142.

[63] J. I. Skar, Materials and Corrosion **50** (1999) 2.

[64] E. Boese, J. Gollner, A. Heyn, J. Strunz, Materials and Corrosion **52** (2001) 247.

[65] H. O. Teeple, Atmospheric galvanic corrosion of magnesium coupled to other metals, ASTM, STP 175, 1956, pp. 89–115.

[66] G. A. El-Mahdy, A. Nishikata, T. Tsuru, Corrosion Science **42** (2000) 183.

[67] C.J. Slunder, W.K. Boyd, Zinc: Its Corrosion Resistance, 2nd ed., International Lead Zinc Research Organization, Inc., New York, 1986.

[68] Metal Corrosion in the atmosphere, STP 435, ASTM, Philadelphia, PA (1968) 360.

[69] C. A. Nunez-Lopez, H. Habazaki, P. Skeldon, G. E. Thonmpson, H. Karmimzadeh, P. Lyon, and T. E. Wilks, Corrosion Science **38** (1996) 1721.

[70] Y. Bohne, D. Manova, C. Blawert, M. Störmer, W. Dietzel, S. Mandl, Surface Engineering **23** (2007) 339.

[71] Woo-Cheol Kim, Jung-Gu Kim, Ji-Young Lee and Hyun-Kwang Seok, Materials letters **62** (2008) 4146.

[72] C. Scharf, A. Ditze, A. Shkurankov, E. Morales, C. Blawert, W. Dietzel, K. U. Kainer, Advanced Engineering Materials **7** (2006) 1134.

[73] D. L. Albright, F. Bergeron, R. Neelameggham, A. Luo, H. Kaplan and M. O. Pekguleryuz, JOM **54** (2002) 22.

[74] Edward Ghali1, Wolfgang Dietzel and Karl-Ulrich Kainer, Journal of Material Engineering and Performance **13** (2004) 517.

[75] Ming Qian, Da Li and Chang Jin, Sci. Technol. Adv. Mater. **9** (2008) 025002 (7pp)

[76] J. W. Chang, L. M. Peng, X. W. Guo, A. Atrens, P. H. Fu, W. J. Ding, X. S. Wang, Journal of applied electrochemistry 38 (2008) 207.

[77] Ágnes Csanády and Dénes Marton, Journal of Material Science **14** (1979) 2289.

[78] F. Witte, V. Kaese, H. Haferkamp, E. Switzer, A. Meyer-Lindenberg, C.J. Wirth and H. Windhagen, Biomaterials **26** (2005) 3557.

[79] Ming Zhao, Shusen Wu, Ping An, Jirong Luo, Y. Fukuda, H. Nakae, Materials Chemistry and Physics **99** (2006) 54.

[80] S. Bender, J. Goellner, A. Heyn, E. Boese, Materials and Corrosion **58** (2007) 977.

[81] Michiaki Yamasaki, Naoyuki Hayashia, Shogo Izumia and Yoshihito Kawamuraa, Corrosion Science **49** (2007) 255.

[82] Chenglong Liu and Yunchang Xin, J. Vac. Sci. Technol. **A 25** (2007) 334.

[83] Andrej Atrens and Wolfgang Dietzel, Advanced Engineering Materials **9** (2007) 292.

[84] Roy L. Petty, Arthur W. Davidson, and Jacob Kleinberg, J. Am. Chem. Soc. **76** (1954) 363-366.

[85] John O'M. Bockris and Shahed U. M. Khan, Quantum Electrochemistry, 1979 Plenum Press, New York and London, 48.

[86] J. O'M. Bockris, Modern Aspects of Electrochemistry, Vol. 1, 1954 Butterworths, London, 236.

[87] R. A. Marcus, J. Chem. Phys. **43** (1965) 697.

[88] J. O'M. Bockris and D. B. Matthews, Proc. Roy. Soc. **A 292** (1966) 479.

[89] Henry H. Bauer, Journal of Electroanalytical Chemistry **16** (1968) 419.

[90] Jean-Michel Savéant and Didier Tessier, Faraday Discuss. Chem. Soc. **74** (1982) 57.

[91] http://en.wikipedia.org/wiki/Finite_element_method

[92] http://www.eng.buffalo.edu/~abani/fem/node3.html

[93] Gouri Dhatt and Gilbert Touzot (Translated by Gilles Cantin), The Finite Element Method Displayed, John Wiley & Sons.

[94] http://www.puc-rio.br/marco.ind/katia-num.html#finite-differences

[95] http://en.wikibooks.org/wiki/Partial_Differential_Equations/Finite_Difference_Method

[96] Nader G. Zamani, and William J. Altenhof, Introduce to the Finite Element Analysis.

Appendix:

In this section, we give some more details and examples for the application of FEM and FDM. It should be helpful for understanding the FEM and the FDM.

1. FEM

(1) Poisson's equation in 1D

$$\frac{d}{dx}(k\frac{du}{dx}) + f(x) = 0 \qquad x_1 \leq x \leq x_2$$

This can be a thermal conduction problem (k is the thermal conductive coefficient and u is the temperature), a diffusion problem (k is the diffusion coefficient and u is the density of a specific matter) or a loaded spring bar (k is the sect area of the bar by the Young's modulus and u is the displacement of the unit cell at position x) etc. Consider the problem as a loaded spring bar. Let's introduce an arbitrary function $\delta u(x)$, which represents a virtual displacement field. $\delta u(x)$ is also called weighting functions. It possesses the property of $\delta(\delta u)=0$. This method is equivalent to minimizing (or maximizing) a functional in certain cases. In mechanics solids, the functional could be the total potential energy. It meets the Lagrange equation and is minimized. This gives an integral formulation directly from the stationarity property of the functional. Multiplying by the virtual function $\delta u(x)$ and then integrating over

$$\int_{x_1}^{x_2}\frac{d}{dx}(k\frac{du}{dx})\delta u(x)dx + \int_{x_1}^{x_2}f(x)\delta u(x)dx = 0 \qquad \text{Integrating by parts, we get}$$

$$k\frac{d}{dx}\delta u(x)\Big|_{x_1}^{x_2} - \int_{x_1}^{x_2}\frac{d}{dx}(k\frac{du}{dx})\delta u(x)dx + \int_{x_1}^{x_2}f(x)\delta u(x)dx = 0$$

Suppose the boundary conditions are:

$$(k\frac{du}{dx})_{x_2} = P_2^{(e)} \qquad -(k\frac{du}{dx})_{x_1} = P_1^{(e)}, \text{ then}$$

$$\int_{x_1}^{x_2}k\frac{du}{dx}\frac{d[\delta u(x)]}{dx}dx = \int_{x_1}^{x_2}f(x)\delta u(x)dx + P_1^{(e)}\delta u(x_1) + P_2^{(e)}\delta u(x_2)$$

Let's put the approximation $u(x) = u_1 N_1(x) + u_2 N_2(x)$ into above equation, so

$$\int_{x_1}^{x_2}k(u_1\frac{dN_1}{dx} + u_2\frac{dN_2}{dx})\frac{d[\delta u(x)]}{dx}dx = \int_{x_1}^{x_2}f(x)\delta u(x)dx + P_1^{(e)}\delta u(x_1) + P_2^{(e)}\delta u(x_2)$$

The virtual displacement $\delta u(x)$ is now free to be chosen. It is common to let the virtual displacement be $N_1(x)$ or $N_2(x)$. Then

$$\int_{x_1}^{x_2} k(u_1 \frac{dN_1}{dx} + u_2 \frac{dN_2}{dx}) \frac{dN_1(x)}{dx} dx = \int_{x_1}^{x_2} f(x)N_1(x)dx + P_1^{(e)}$$

$$\int_{x_1}^{x_2} k(u_1 \frac{dN_1}{dx} + u_2 \frac{dN_2}{dx}) \frac{dN_2(x)}{dx} dx = \int_{x_1}^{x_2} f(x)N_2(x)dx + P_2^{(e)}$$

$$\begin{bmatrix} \int_{x_1}^{x_2} k \frac{dN_1}{dx} \frac{dN_1}{dx} dx & \int_{x_1}^{x_2} k \frac{dN_2}{dx} \frac{dN_1}{dx} dx \\ \int_{x_1}^{x_2} k \frac{dN_1}{dx} \frac{dN_2}{dx} dx & \int_{x_1}^{x_2} k \frac{dN_2}{dx} \frac{dN_2}{dx} dx \end{bmatrix} \begin{Bmatrix} u_1 \\ u_2 \end{Bmatrix} = \begin{Bmatrix} \int_{x_1}^{x_2} f(x)N_1(x)dx \\ \int_{x_1}^{x_2} f(x)N_2(x)dx \end{Bmatrix} + \begin{Bmatrix} P_1^{(e)} \\ P_2^{(e)} \end{Bmatrix}$$

In the reference space, the above equation becomes

$$\begin{bmatrix} \int_{-1}^{1} k \frac{dN_1}{d\xi} \frac{dN_1}{d\xi} \det[j]d\xi & \int_{-1}^{1} k \frac{dN_2}{d\xi} \frac{dN_1}{d\xi} \det[j]d\xi \\ \int_{-1}^{1} k \frac{dN_1}{d\xi} \frac{dN_2}{d\xi} \det[j]d\xi & \int_{-1}^{1} k \frac{dN_2}{d\xi} \frac{dN_2}{d\xi} \det[j]d\xi \end{bmatrix} \begin{Bmatrix} u_1 \\ u_2 \end{Bmatrix} = \begin{Bmatrix} \int_{-1}^{1} f(x)N_1 \det[J]d\xi \\ \int_{-1}^{1} f(x)N_2 \det[J]d\xi \end{Bmatrix} + \begin{Bmatrix} P_1^{(e)} \\ P_2^{(e)} \end{Bmatrix}$$

$$\frac{2}{x_2 - x_1} \begin{bmatrix} \int_{-1}^{1} k \frac{dN_1}{d\xi} \frac{dN_1}{d\xi} d\xi & \int_{-1}^{1} k \frac{dN_2}{d\xi} \frac{dN_1}{d\xi} d\xi \\ \int_{-1}^{1} k \frac{dN_1}{d\xi} \frac{dN_2}{d\xi} d\xi & \int_{-1}^{1} k \frac{dN_2}{d\xi} \frac{dN_2}{d\xi} d\xi \end{bmatrix} \begin{Bmatrix} u_1 \\ u_2 \end{Bmatrix} = \frac{x_2 - x_1}{2} \begin{Bmatrix} \int_{-1}^{1} f(x)N_1 d\xi \\ \int_{-1}^{1} f(x)N_2 d\xi \end{Bmatrix} + \begin{Bmatrix} P_1^{(e)} \\ P_2^{(e)} \end{Bmatrix}$$

For example: Axial deformation of a bar subjected to a uniform load

$$AE \frac{d^2u}{dx^2} + p_0 = 0 \quad x=[0, L] \text{ with boundary conditions:}$$

$u(0)=0$ and $\left. \frac{du}{dx} \right|_{x=L} = 0$. (The p_0 is an external force)

Where u = axial displacement, E=Young's modulus = 1, A=Cross-sectional area = 1.

We know the exact solution is $u(x) = p_0 Lx - \frac{1}{2} p_0 x^2$

Now, let's use FEM to solve this problem.

(a) Linear approach

① One element

The approximate function is: $u(x) = u_1 N_1(x) + u_2 N_2(x)$

$$N_1 = (1-\xi)/2 \qquad N_2 = (1+\xi)/2 \qquad [J] = \frac{1}{2}\langle -1 \quad 1\rangle \begin{Bmatrix} x_1 \\ x_2 \end{Bmatrix} = \frac{x_2 - x_1}{2} = \frac{L}{2}$$

$$x = \frac{x_1 + x_2}{2} + \frac{x_2 - x_1}{2}\xi = \frac{L}{2} + \frac{L}{2}\xi \rightarrow [J] = \frac{\partial x}{\partial \xi} = \frac{L}{2} \rightarrow [j] = [J]^{-1} = \frac{2}{L}$$

$$\begin{bmatrix} \int_{x_1}^{x_2} dx \frac{dN_1}{dx}\frac{dN_1}{dx} & \int_{x_1}^{x_2} dx \frac{dN_2}{dx}\frac{dN_1}{dx} \\ \int_{x_1}^{x_2} dx \frac{dN_1}{dx}\frac{dN_2}{dx} & \int_{x_1}^{x_2} dx \frac{dN_2}{dx}\frac{dN_2}{dx} \end{bmatrix} \begin{Bmatrix} u_1 \\ u_2 \end{Bmatrix} = \begin{Bmatrix} \int_{x_1}^{x_2} dx p_0 N_1 \\ \int_{x_1}^{x_2} dx p_0 N_2 \end{Bmatrix} + \begin{Bmatrix} P_1 \\ P_2 \end{Bmatrix}$$

$$\begin{bmatrix} \int_{-1}^{1} d\xi \det[j]\frac{dN_1}{d\xi}\frac{dN_1}{d\xi} & \int_{-1}^{1} d\xi \det[j]\frac{dN_2}{d\xi}\frac{dN_1}{d\xi} \\ \int_{-1}^{1} d\xi \det[j]\frac{dN_1}{d\xi}\frac{dN_2}{d\xi} & \int_{-1}^{1} d\xi \det[j]\frac{dN_2}{d\xi}\frac{dN_2}{d\xi} \end{bmatrix} \begin{Bmatrix} u_1 \\ u_2 \end{Bmatrix} = \begin{Bmatrix} \int_{-1}^{1} \det[J]d\xi p_0 N_1 \\ \int_{-1}^{1} \det[J]d\xi p_0 N_2 \end{Bmatrix} + \begin{Bmatrix} P_1 \\ P_2 \end{Bmatrix}$$

$$\begin{bmatrix} \int_{-1}^{1} d\xi \frac{2}{L}\cdot\frac{1}{4} & -\int_{-1}^{1} d\xi \frac{2}{L}\cdot\frac{1}{4} \\ -\int_{-1}^{1} d\xi \frac{2}{L}\cdot\frac{1}{4} & \int_{-1}^{1} d\xi \frac{2}{L}\cdot\frac{1}{4} \end{bmatrix} \begin{Bmatrix} 0 \\ u_2 \end{Bmatrix} = \begin{Bmatrix} \int_{-1}^{1} d\xi \frac{L}{2} p_0 \frac{1-\xi}{2} \\ \int_{-1}^{1} d\xi \frac{L}{2} p_0 \frac{1+\xi}{2} \end{Bmatrix} + \begin{Bmatrix} P_1 \\ 0 \end{Bmatrix}$$

$$\begin{bmatrix} 1/L & -1/L \\ -1/L & 1/L \end{bmatrix} \begin{Bmatrix} 0 \\ u_2 \end{Bmatrix} = \begin{Bmatrix} Lp_0/2 + P_1 \\ Lp_0/2 \end{Bmatrix} \rightarrow \begin{cases} u_1 = 0 \\ u_2 = \dfrac{L^2}{2} p_0 \end{cases} \quad \begin{cases} P_1 = -Lp_0 \\ P_2 = 0 \end{cases}$$

$$\therefore u(\xi) = u_2 N_2(\xi) = \frac{L^2}{2} p_0 \cdot \frac{1+\xi}{2} \qquad\qquad \xi = \frac{2x - L}{L}$$

$$\therefore u(x) = \frac{L^2}{2} p_0 \cdot \frac{1+\xi}{2} = \frac{1}{2} L p_0 x$$

② Two elements

Element 1: $x=[0, L/2]$, $\xi=[-1, 1]$

$$N_1^{(1)} = (1-\xi)/2 \qquad\qquad N_2^{(1)} = (1+\xi)/2$$

$$[J^{(1)}] = \frac{1}{2}\langle -1 \quad 1\rangle \begin{Bmatrix} x_1 \\ x_2 \end{Bmatrix} = \frac{x_2 - x_1}{2} = \frac{L}{4}$$

$$x = \frac{x_1 + x_2}{2} + \frac{x_2 - x_1}{2}\xi = \frac{L}{4} + \frac{L}{4}\xi \rightarrow [J] = \frac{\partial x}{\partial \xi} = \frac{L}{4} \rightarrow [j] = [J]^{-1} = \frac{4}{L}$$

73
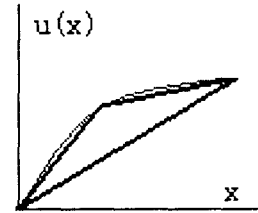
$$\begin{bmatrix} \int_{-1}^{1} d\xi \, \dfrac{4}{L} \cdot \dfrac{1}{4} & -\int_{-1}^{1} d\xi \, \dfrac{4}{L} \cdot \dfrac{1}{4} \\ -\int_{-1}^{1} d\xi \, \dfrac{4}{L} \cdot \dfrac{1}{4} & \int_{-1}^{1} d\xi \, \dfrac{4}{L} \cdot \dfrac{1}{4} \end{bmatrix} \begin{Bmatrix} u_1^{(1)} \\ u_2^{(1)} \end{Bmatrix} = \begin{Bmatrix} \int_{-1}^{1} d\xi \, \dfrac{L}{4} p_0 \dfrac{1-\xi}{2} \\ \int_{-1}^{1} d\xi \, \dfrac{L}{4} p_0 \dfrac{1+\xi}{2} \end{Bmatrix} + \begin{Bmatrix} P_1^{(1)} \\ P_2^{(1)} \end{Bmatrix}$$

$$\begin{bmatrix} 2/L & -2/L \\ -2/L & 2/L \end{bmatrix} \begin{Bmatrix} u_1^{(1)} \\ u_2^{(1)} \end{Bmatrix} = \begin{Bmatrix} Lp_0/4 \\ Lp_0/4 \end{Bmatrix} + \begin{Bmatrix} P_1^{(1)} \\ P_2^{(1)} \end{Bmatrix}$$

Element 2: $x=[L/2, L]$, $\xi=[-1, 1]$

$$N_1^{(2)}=(1-\xi)/2 \qquad N_2^{(2)}=(1+\xi)/2 \qquad [J^{(2)}] = \frac{1}{2}\langle -1 \quad 1 \rangle \begin{Bmatrix} x_1^{(2)} \\ x_2^{(2)} \end{Bmatrix} = \frac{x_2^{(2)} - x_1^{(2)}}{2} = \frac{L}{4}$$

$$x = \frac{x_1^{(2)} + x_2^{(2)}}{2} + \frac{x_2^{(2)} - x_1^{(2)}}{2}\xi = \frac{3L}{4} + \frac{L}{4}\xi \;\rightarrow\; [J] = \frac{\partial x}{\partial \xi} = \frac{L}{4} \;\rightarrow\; [j] = [J]^{-1} = \frac{4}{L}$$

Similarly, we get:

$$\begin{bmatrix} 2/L & -2/L \\ -2/L & 2/L \end{bmatrix} \begin{Bmatrix} u_1^{(2)} \\ u_2^{(2)} \end{Bmatrix} = \begin{Bmatrix} Lp_0/4 \\ Lp_0/4 \end{Bmatrix} + \begin{Bmatrix} P_1^{(2)} \\ P_2^{(2)} \end{Bmatrix}$$

Assembling the global stiffness matrix, we get:

$$\begin{bmatrix} 2/L & -2/L & 0 \\ -2/L & 4/L & -2/L \\ 0 & -2/L & 2/L \end{bmatrix} \begin{Bmatrix} u_1 \\ u_2 \\ u_3 \end{Bmatrix} = \begin{Bmatrix} Lp_0/4 \\ Lp_0/2 \\ Lp_0/4 \end{Bmatrix} + \begin{Bmatrix} P_1^{(1)} \\ P_2^{(1)} + P_1^{(2)} \\ P_2^{(2)} \end{Bmatrix}$$

Consider the boundary conditions:

$$\begin{bmatrix} 2/L & -2/L & 0 \\ -2/L & 4/L & -2/L \\ 0 & -2/L & 2/L \end{bmatrix} \begin{Bmatrix} 0 \\ u_2 \\ u_3 \end{Bmatrix} = \begin{Bmatrix} Lp_0/4 \\ Lp_0/2 \\ Lp_0/4 \end{Bmatrix} + \begin{Bmatrix} P_1^{(1)} \\ 0 \\ 0 \end{Bmatrix}$$

$$u_1 = 0, \; u_2 = \frac{3}{8}L^2 p_0, \; u_3 = \frac{1}{2}L^2 p_0. \qquad P_1^{(1)} = -Lp_0$$

So, $u^{(e)}(\xi) = u_1^{(e)} N_1^{(e)}(\xi) + u_2^{(e)} N_2^{(e)}(\xi)$

$$u^{(1)}(\xi) = \frac{3}{8}L^2 p_0 \cdot \frac{1+\xi}{2} \qquad \text{and} \quad \xi = \frac{4x-L}{L} \qquad x=[0, L/2]$$

$$u^{(1)}(x) = \frac{3}{4}Lp_0 x \qquad x \in [0, \frac{L}{2}]$$

$$u^{(2)}(\xi) = \frac{3}{8}L^2 p_0 N_1(\xi) + \frac{1}{2}L^2 p_0 N_2(\xi) = \frac{3}{8}L^2 p_0 \frac{1-\xi}{2} + \frac{1}{2}L^2 p_0 \frac{1+\xi}{2}$$

$$x = \frac{3L}{4} + \frac{L}{4}\xi \quad \rightarrow \quad \xi = \frac{4x - 3L}{L} \qquad x \in [\frac{L}{2}, L]$$

$$u^{(2)}(x) = \frac{1}{4}Lp_0(x + L)$$

$$u(x) = \begin{cases} \frac{3}{4}Lp_0 x & x \in [0, L/2] \\ \frac{1}{4}Lp_0(x + L) & x \in [L/2, L] \end{cases}$$

By comparing the result of one element situation and two elements situation (please see the above graph), we know that the finite element solution converge with the true solution as the number of elements is increased. Please note that the more the elements, the larger the amount of calculation. We should balance the requirement and the calculation.

(b) Quadratic / parabola approach

$$\frac{d}{dx}(k\frac{du}{dx}) + f(x) = 0 \quad (x_1 \leq x \leq x_3)$$

Similarly, by integrating by parts and combining with

$u(\xi) = N_1(\xi)u_1 + N_2(\xi)u_2 + N_3(\xi)u_3$, we get

$$\int_{x_1}^{x_3} k(u_1\frac{dN_1}{dx} + u_2\frac{dN_2}{dx} + u_3\frac{dN_3}{dx})\frac{d[\delta u(x)]}{dx}dx = \int_{x_1}^{x_3} f(x)\delta u(x)dx + P_1^{(e)}\delta u(x_1) + P_2^{(e)}\delta u(x_2) + P_3^{(e)}\delta(x_3)$$

We can choose the arbitrary virtual function $\delta u(x)$ as $N_1(\xi)$, $N_2(\xi)$ or $N_3(\xi)$ and get

$$k\begin{bmatrix} \int_{x_1}^{x_3}dx\frac{dN_1}{dx}\frac{dN_1}{dx} & \int_{x_1}^{x_3}dx\frac{dN_2}{dx}\frac{dN_1}{dx} & \int_{x_1}^{x_3}dx\frac{dN_3}{dx}\frac{dN_1}{dx} \\ \int_{x_1}^{x_3}dx\frac{dN_1}{dx}\frac{dN_2}{dx} & \int_{x_1}^{x_3}dx\frac{dN_2}{dx}\frac{dN_2}{dx} & \int_{x_1}^{x_3}dx\frac{dN_3}{dx}\frac{dN_2}{dx} \\ \int_{x_1}^{x_3}dx\frac{dN_1}{dx}\frac{dN_3}{dx} & \int_{x_1}^{x_3}dx\frac{dN_2}{dx}\frac{dN_3}{dx} & \int_{x_1}^{x_3}dx\frac{dN_3}{dx}\frac{dN_3}{dx} \end{bmatrix}\begin{Bmatrix} u_1 \\ u_2 \\ u_3 \end{Bmatrix} = \begin{Bmatrix} \int_{x_1}^{x_3}dxf(x)N_1 \\ \int_{x_1}^{x_3}dxf(x)N_2 \\ \int_{x_1}^{x_3}dxf(x)N_3 \end{Bmatrix} + \begin{Bmatrix} P_1 \\ P_2 \\ P_3 \end{Bmatrix}$$

(b) For example: (the same as above)

$$\frac{d^2u}{dx^2} + p_0 = 0 \qquad x=[0, L] \text{ with boundary conditions:}$$

$u(0)=0$ and $\frac{du}{dx}\Big|_{x=L} = 0$

① One element: x=[0,L]

$$\langle N \rangle = \frac{1}{2} \langle -\xi(1-\xi) \quad 2(1-\xi^2) \quad \xi(1+\xi) \rangle$$

$N_1 = -\xi(1-\xi)/2 \qquad N_2 = (1-\xi^2) \qquad N_3 = \xi(1+\xi)/2$

$$x = \frac{1}{2} \langle -\xi(1-\xi) \quad 2(1-\xi^2) \quad \xi(1+\xi) \rangle \left\{ \begin{array}{c} x_1 \\ (x_1+x_3)/2 \\ x_3 \end{array} \right\} = \frac{x_1+x_3}{2} + \frac{x_3-x_1}{2}\xi = \frac{L}{2} + \frac{L}{2}\xi$$

$$[J] = \frac{\partial x}{\partial \xi} = \frac{L}{2} \qquad [j] = [J]^{-1} = \frac{2}{L}$$

$$\begin{bmatrix} \int\limits_{x_1}^{x_3} dx \frac{dN_1}{dx}\frac{dN_1}{dx} & \int\limits_{x_1}^{x_3} dx \frac{dN_2}{dx}\frac{dN_1}{dx} & \int\limits_{x_1}^{x_3} dx \frac{dN_3}{dx}\frac{dN_1}{dx} \\ \int\limits_{x_1}^{x_3} dx \frac{dN_1}{dx}\frac{dN_2}{dx} & \int\limits_{x_1}^{x_3} dx \frac{dN_2}{dx}\frac{dN_2}{dx} & \int\limits_{x_1}^{x_3} dx \frac{dN_3}{dx}\frac{dN_2}{dx} \\ \int\limits_{x_1}^{x_3} dx \frac{dN_1}{dx}\frac{dN_3}{dx} & \int\limits_{x_1}^{x_3} dx \frac{dN_2}{dx}\frac{dN_3}{dx} & \int\limits_{x_1}^{x_3} dx \frac{dN_3}{dx}\frac{dN_3}{dx} \end{bmatrix} \left\{ \begin{array}{c} u_1 \\ u_2 \\ u_3 \end{array} \right\} = \left\{ \begin{array}{c} \int\limits_{x_1}^{x_3} dx\, p_0 N_1 \\ \int\limits_{x_1}^{x_3} dx\, p_0 N_2 \\ \int\limits_{x_1}^{x_3} dx\, p_0 N_3 \end{array} \right\} + \left\{ \begin{array}{c} P_1 \\ P_2 \\ P_3 \end{array} \right\}$$

Boundary conditions are: $u_1=0$, $P_2 = 0$ (fact condition), $P_3=0$

$$\frac{2}{L}\begin{bmatrix} \int\limits_{-1}^{1} d\xi(\xi-\frac{1}{2})^2 & -\int\limits_{-1}^{1} d\xi 2\xi(\xi-\frac{1}{2}) & \int\limits_{-1}^{1} d\xi(\xi^2-\frac{1}{2}) \\ -\int\limits_{-1}^{1} d\xi 2\xi(\xi-\frac{1}{2}) & \int\limits_{-1}^{1} d\xi 4\xi^2 & -\int\limits_{-1}^{1} d\xi 2\xi(\xi+\frac{1}{2}) \\ \int\limits_{-1}^{1} d\xi(\xi^2-\frac{1}{2}) & -\int\limits_{-1}^{1} d\xi 2\xi(\xi+\frac{1}{2}) & \int\limits_{-1}^{1} d\xi(\xi+\frac{1}{2})^2 \end{bmatrix} \left\{ \begin{array}{c} 0 \\ u_2 \\ u_3 \end{array} \right\} = \frac{L}{2}\left\{ \begin{array}{c} -\int\limits_{-1}^{1} d\xi p_0 \xi(1-\xi)/2 \\ \int\limits_{-1}^{1} d\xi p_0(1-\xi^2) \\ \int\limits_{-1}^{1} d\xi p_0 \xi(1+\xi)/2 \end{array} \right\} + \left\{ \begin{array}{c} P_1 \\ 0 \\ 0 \end{array} \right\}$$

$$\frac{2}{L}\begin{bmatrix} 7/6 & -4/3 & 1/6 \\ -4/3 & 8/3 & -4/3 \\ 1/6 & -4/3 & 7/6 \end{bmatrix} \left\{ \begin{array}{c} 0 \\ u_2 \\ u_3 \end{array} \right\} = \frac{Lp_0}{2}\left\{ \begin{array}{c} 1/3 \\ 4/3 \\ 1/3 \end{array} \right\} + \left\{ \begin{array}{c} P_1 \\ 0 \\ 0 \end{array} \right\}$$

$u_1 = 0$, $u_2 = \frac{3}{8}L^2 p_0$, $u_3 = \frac{1}{2}L^2 p_0$. $\quad P_1 = -Lp_0$

(They are exactly the same as the linear two-element situation. The value of the same node should be the same.)

$u(\xi) = N_2(\xi)u_2 + N_3(\xi)u_3 = L^2 p_0 (3+2\xi-\xi^2)/8$, $\quad \xi = (2x-L)/L$

$\therefore u(x) = p_0(2Lx - x^2)/2 = p_0 Lx - \frac{1}{2}p_0 x^2$

It is the exact solution.

② Two elements:

Element 1: x=[0,L/2]

$$\langle N \rangle = \frac{1}{2}\langle -\xi(1-\xi) \quad 2(1-\xi^2) \quad \xi(1+\xi) \rangle$$

$N_1 = -\xi(1-\xi)/2 \qquad N_2 = (1-\xi^2) \qquad N_3 = \xi(1+\xi)/2$

$$x^{(1)} = \frac{x_1^{(1)} + x_3^{(1)}}{2} + \frac{x_3^{(1)} - x_1^{(1)}}{2}\xi = \frac{L}{4} + \frac{L}{4}\xi$$

$$[J] = \frac{\partial x}{\partial \xi} = \frac{L}{4} \qquad [j] = [J]^{-1} = \frac{4}{L}$$

$$\begin{bmatrix} \int_{x_1^{(1)}}^{x_3^{(1)}} dx \frac{dN_1}{dx}\frac{dN_1}{dx} & \int_{x_1^{(1)}}^{x_3^{(1)}} dx \frac{dN_2}{dx}\frac{dN_1}{dx} & \int_{x_1^{(1)}}^{x_3^{(1)}} dx \frac{dN_3}{dx}\frac{dN_1}{dx} \\ \int_{x_1^{(1)}}^{x_3^{(1)}} dx \frac{dN_1}{dx}\frac{dN_2}{dx} & \int_{x_1^{(1)}}^{x_3^{(1)}} dx \frac{dN_2}{dx}\frac{dN_2}{dx} & \int_{x_1^{(1)}}^{x_3^{(1)}} dx \frac{dN_3}{dx}\frac{dN_2}{dx} \\ \int_{x_1^{(1)}}^{x_3^{(1)}} dx \frac{dN_1}{dx}\frac{dN_3}{dx} & \int_{x_1^{(1)}}^{x_3^{(1)}} dx \frac{dN_2}{dx}\frac{dN_3}{dx} & \int_{x_1^{(1)}}^{x_3^{(1)}} dx \frac{dN_3}{dx}\frac{dN_3}{dx} \end{bmatrix} \begin{Bmatrix} u_1^{(1)} \\ u_2^{(1)} \\ u_3^{(1)} \end{Bmatrix} = \begin{Bmatrix} \int_{x_1^{(1)}}^{x_3^{(1)}} dx p_0 N_1 \\ \int_{x_1^{(1)}}^{x_3^{(1)}} dx p_0 N_2 \\ \int_{x_1^{(1)}}^{x_3^{(1)}} dx p_0 N_3 \end{Bmatrix} + \begin{Bmatrix} P_1^{(1)} \\ P_2^{(1)} \\ P_3^{(1)} \end{Bmatrix}$$

$$\frac{4}{L}\begin{bmatrix} \int_{-1}^{1} d\xi (\xi-\tfrac{1}{2})^2 & -\int_{-1}^{1} d\xi 2\xi(\xi-\tfrac{1}{2}) & \int_{-1}^{1} d\xi(\xi^2-\tfrac{1}{2}) \\ -\int_{-1}^{1} d\xi 2\xi(\xi-\tfrac{1}{2}) & \int_{-1}^{1} d\xi 4\xi^2 & -\int_{-1}^{1} d\xi 2\xi(\xi+\tfrac{1}{2}) \\ \int_{-1}^{1} d\xi(\xi^2-\tfrac{1}{2}) & -\int_{-1}^{1} d\xi 2\xi(\xi+\tfrac{1}{2}) & \int_{-1}^{1} d\xi(\xi+\tfrac{1}{2})^2 \end{bmatrix}\begin{Bmatrix} u_1^{(1)} \\ u_2^{(1)} \\ u_3^{(1)} \end{Bmatrix} = \frac{L}{4}\begin{Bmatrix} -\int_{-1}^{1} d\xi p_0 \xi(1-\xi)/2 \\ \int_{-1}^{1} d\xi p_0 (1-\xi^2) \\ \int_{-1}^{1} d\xi p_0 \xi(1+\xi)/2 \end{Bmatrix} + \begin{Bmatrix} P_1^{(1)} \\ P_2^{(1)} \\ P_3^{(1)} \end{Bmatrix}$$

$$\frac{4}{L}\begin{bmatrix} 7/6 & -4/3 & 1/6 \\ -4/3 & 8/3 & -4/3 \\ 1/6 & -4/3 & 7/6 \end{bmatrix}\begin{Bmatrix} u_1^{(1)} \\ u_2^{(1)} \\ u_3^{(1)} \end{Bmatrix} = \frac{Lp_0}{4}\begin{Bmatrix} 1/3 \\ 4/3 \\ 1/3 \end{Bmatrix} + \begin{Bmatrix} P_1^{(1)} \\ P_2^{(1)} \\ P_3^{(1)} \end{Bmatrix}$$

Element 2: x=[L/2,L]

$$\langle N \rangle = \frac{1}{2}\langle -\xi(1-\xi) \quad 2(1-\xi^2) \quad \xi(1+\xi) \rangle$$

$N_1 = -\xi(1-\xi)/2 \qquad N_2 = (1-\xi^2) \qquad N_3 = \xi(1+\xi)/2$

$$x^{(2)} = \frac{x_1^{(2)} + x_3^{(2)}}{2} + \frac{x_3^{(2)} - x_1^{(2)}}{2}\xi = \frac{3L}{4} + \frac{L}{4}\xi$$

$$[J] = \frac{\partial x}{\partial \xi} = \frac{L}{4} \qquad [j] = [J]^{-1} = \frac{4}{L}$$

Similarly, we get:

77

$$\frac{4}{L}\begin{bmatrix} 7/6 & -4/3 & 1/6 \\ -4/3 & 8/3 & -4/3 \\ 1/6 & -4/3 & 7/6 \end{bmatrix}\begin{Bmatrix} u_1^{(2)} \\ u_2^{(2)} \\ u_3^{(2)} \end{Bmatrix} = \frac{Lp_0}{4}\begin{Bmatrix} 1/3 \\ 4/3 \\ 1/3 \end{Bmatrix} + \begin{Bmatrix} P_1^{(2)} \\ P_2^{(2)} \\ P_3^{(2)} \end{Bmatrix}$$

The global stiffness matrix is:

$$\frac{4}{L}\begin{bmatrix} 7/6 & -4/3 & 1/6 & 0 & 0 \\ -4/3 & 8/3 & -4/3 & 0 & 0 \\ 1/6 & -4/3 & 7/3 & -4/3 & 1/6 \\ 0 & 0 & -4/3 & 8/3 & -4/3 \\ 0 & 0 & 1/6 & -4/3 & 7/6 \end{bmatrix}\begin{Bmatrix} 0 \\ u_2 \\ u_3 \\ u_4 \\ u_5 \end{Bmatrix} = \frac{Lp_0}{4}\begin{Bmatrix} 1/3 \\ 4/3 \\ 2/3 \\ 4/3 \\ 1/3 \end{Bmatrix} + \begin{Bmatrix} P_1 \\ 0 \\ 0 \\ 0 \\ 0 \end{Bmatrix}$$

The solution is

$$u_1 = 0, \ u_2 = \frac{7}{32}L^2 p_0, \ u_3 = \frac{3}{8}L^2 p_0, \ u_4 = \frac{15}{32}L^2 p_0, \ u_5 = \frac{1}{2}L^2 p_0. \ P_1 = -Lp_0$$

$$u(\xi) = \begin{cases} u_1 N_1(\xi) + u_2 N_2(\xi) + u_3 N_3(\xi) = \frac{1}{32}L^2 p_0(7 + 6\xi - \xi^2) & x \in [0, L/2] \\ u_3 N_1(\xi) + u_4 N_2(\xi) + u_5 N_3(\xi) = \frac{1}{32}L^2 p_0(15 + 2\xi - \xi^2) & x \in [L/2, L] \end{cases}$$

$$\xi = \begin{cases} (4x - L)/L & x \in [0, L/2] \\ (4x - 3L)/L & x \in [L/2, L] \end{cases}$$

$$\therefore u(x) = \begin{cases} Lp_0 x - \frac{1}{2}p_0 x^2 & x \in [0, L/2] \\ Lp_0 x - \frac{1}{2}p_0 x^2 & x \in [L/2, L] \end{cases}$$

$$\therefore u(x) = p_0 Lx - \frac{1}{2}p_0 x^2 \quad x = [0, L]$$

From the results we know that if the order of the interpolation (shape) function set is same as the order of the equation, we only need one element but still get the exact solution (this comment is only for 1D).

To verify this comment, let's see one more example. The equation is the same, but we change the boundary conditions to: $u(0) = u(L) = 0$. Namely,

$$\frac{d^2 u}{dx^2} + p_0 = 0 \quad x = [0, L] \text{ with boundary conditions:}$$

$u(0) = 0$ and $u(L) = 0$.

The exact solution of this problem is: $u(x) = \frac{1}{2}p_0 Lx - \frac{1}{2}p_0 x^2$.

Obviously, when we use FEM to solve this problem and we choose the linear approach, then divide the region into one element, the solution is $u(x)=0$. If we choose the linear approach and divide the region into two elements, the solution is easy to get by analyzing (please see the figure):

$$\therefore u(x) = \begin{cases} \frac{1}{4}p_0 Lx & x \in [0, L/2] \\ \frac{1}{4}p_0 L^2 - \frac{1}{4}p_0 Lx & x \in [L/2, L] \end{cases}$$
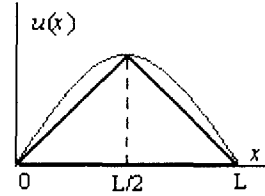
Now, let us try to solve this problem by using quadratic approach and in one element.

$$N_1 = -\xi(1-\xi)/2 \qquad N_2 = (1-\xi^2) \qquad N_3 = \xi(1+\xi)/2$$

$$\frac{2}{L}\begin{bmatrix} 7/6 & -4/3 & 1/6 \\ -4/3 & 8/3 & -4/3 \\ 1/6 & -4/3 & 7/6 \end{bmatrix}\begin{Bmatrix} 0 \\ u_2 \\ 0 \end{Bmatrix} = \frac{Lp_0}{2}\begin{Bmatrix} 1/3 \\ 4/3 \\ 1/3 \end{Bmatrix} + \begin{Bmatrix} P_1 \\ 0 \\ P_3 \end{Bmatrix}$$

$u_1 = 0$, $u_2 = \frac{1}{8}L^2 p_0$, $u_3 = 0$. $u(\xi) = u_2 N_2 = \frac{1}{8}L^2 p_0 (1-\xi^2)$, $\xi = (2x-L)/L$

$$\therefore u(x) = u_2 N_2 = \frac{1}{2}p_0 Lx - \frac{1}{2}p_0 x^2)$$

It is the same as the exact solution.

(c) Cubic approach (the same example as above)

$$\frac{d^2 u}{dx^2} + p_0 = 0 \qquad x=[0, L] \text{ with boundary conditions:}$$

$$u(0)=0 \quad \text{and} \quad \frac{du}{dx}\Big|_{x=L} = 0$$

Similarly, we can easily get

$x_1 \le x \le x_4 \rightarrow -1 \le \xi \le 1$

$$\langle N \rangle = \frac{1}{16}\langle -(1-\xi)(1-9\xi^2) \quad 9(1-\xi^2)(1-3\xi) \quad 9(1-\xi^2)(1+3\xi) \quad -(1+\xi)(1-9\xi^2) \rangle$$

$$x = \frac{x_1 + x_4}{2} + \frac{x_4 - x_1}{2}\xi = \frac{L}{2} + \frac{L}{2}\xi \rightarrow \qquad [J] = \frac{\partial x}{\partial \xi} = \frac{L}{2}$$

For one element, it is easy to get:

$$\frac{2}{L}\begin{bmatrix} \dfrac{16}{105} & -\dfrac{3}{70} & \dfrac{33}{280} & \dfrac{19}{840} \\ -\dfrac{3}{70} & \dfrac{27}{35} & -\dfrac{27}{280} & -\dfrac{3}{70} \\ \dfrac{33}{280} & -\dfrac{27}{280} & \dfrac{27}{35} & \dfrac{33}{280} \\ \dfrac{19}{840} & -\dfrac{3}{70} & \dfrac{33}{280} & \dfrac{16}{105} \end{bmatrix}\begin{Bmatrix} 0 \\ u_2 \\ u_3 \\ u_4 \end{Bmatrix} = \frac{L}{2}p_0\begin{Bmatrix} 1/4 \\ 3/4 \\ 3/4 \\ 1/4 \end{Bmatrix} + \begin{Bmatrix} P_1 \\ 0 \\ 0 \\ 0 \end{Bmatrix}$$

And we can expect to get:

$$u(x) = p_0 Lx - \tfrac{1}{2}p_0 x^2 \quad x=[0,L]$$

When we use cubic (three orders) interpolation function set to solve the same problem, even though the amount of calculation is much larger than quadratic approximation, the result is the same. Usually, the order of the shape functions is less than or equal to the order of the equation.

(2) Poisson's equation in 2D

$$L(u) + f_A = (\frac{\partial^2}{\partial x^2} + \frac{\partial^2}{\partial y^2})u + f_A = 0 \qquad \text{(If } f_A = 0 \text{, it becomes Laplace equation)}$$

with the boundary condition $\varepsilon(u) = f_S$ on boundary S.

Similar to 1D, the weighted residual method gives the integral form:

$$W = \int_A \delta u(x,y)[(\frac{\partial^2}{\partial x^2} + \frac{\partial^2}{\partial y^2})u + f_A]dxdy = 0$$

where approximation $u(x,y) = \sum_{i=1}^{n} u_i N_i(x,y)$,

After integration by parts, we get

$$\int_A (\frac{\partial u}{\partial x}\frac{\partial \delta u}{\partial x} + \frac{\partial u \partial \delta u}{\partial y \partial y})dA = \int_A f_A \delta u dA + \oint_l \frac{\partial u}{\partial n}\delta u dl$$

$$\int_A [(\sum_{i=1}^{n} u_i \frac{\partial N_i}{\partial x})\frac{\partial \delta u}{\partial x} + (\sum_{i=1}^{n} u_i \frac{\partial N_i}{\partial y})\frac{\partial \delta u}{\partial y}]dA = \int_A f_A \delta u dA + \oint_l \frac{\partial u}{\partial n}\delta u dl$$

Because $\delta u(x,y)$ is an arbitrary function, we can choose $\delta u = N_1, N_2, \dots N_i, \dots N_n$. Then

$$[K^e]\{u^e\} = \{F^e\} + \{P^e\}$$

$$K^e_{ij} = \int_A (\frac{\partial N_i}{\partial x}\frac{\partial N_j}{\partial x} + \frac{\partial N_i}{\partial y}\frac{\partial N_j}{\partial y})dA$$

$$F^e_i = \int_A (f_A N_i)dA$$

$$P^e_i = \oint_l \frac{\partial u}{\partial n}N_i dl \quad \text{(the direction of the } n \text{ is the normal outward unit vector to the element)}$$

(a) Linear approach

The same Poisson's equation $(\frac{\partial^2}{\partial x^2} + \frac{\partial^2}{\partial y^2})u(x,y) + f_A = 0$ ($|x|<1$, $|y|<1$)

with boundary condition u(x, y) = 0 on the boundary $x = \pm1$ $y = \pm1$.

If the local node numbers for all elements follow a counterclockwise order with the second node being the right angle, the associated stiffness matrices are the same for the equal triangles.

① If we divide the domain into two elements like the figure below

Element 1: (x, y): 1(-1, -1), 2(1,-1), 3(1, 1)

Element 2: (x, y): 1(1, 1), 2(-1, 1), 3(-1,-1)

Because of the boundary condition,

$u_1^{(e)}=0$, $u_2^{(e)}=0$, $u_3^{(e)}=0$. It causes $u = \sum_i u_i N_i = 0$.
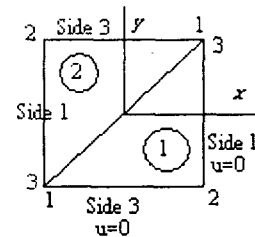
In this way, we cannot get a proper solution.

But, if we change the boundary condition to:

$u(-1, y)=u(x, -1)=0$ and $\left.\frac{\partial u(x,1)}{\partial x}\right|_{x=1} = \left.\frac{\partial u(1,y)}{\partial y}\right|_{y=1} = 0$, then

we can divide the domain into two elements.

② Let's divide the domain into eight elements (see figure on the right). Because of the symmetry, we only need to consider the half of the square.
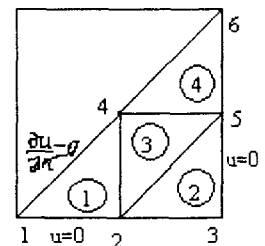
	Element nodes (order 1, 2, 3)		
Element 1	1(-1,-1)	2(0, -1)	4(0, 0)
Element 2	2(0, -1)	3(1, -1)	5(1, 0)
Element 3	5(1, 0)	4(0, 0)	2(0,-1)
Element 4	4(0, 0)	5(1, 0)	6(1, 1)

Element 1:

$$\langle x \quad y \rangle = \langle 1 - \xi - \eta \quad \xi \quad \eta \rangle \begin{bmatrix} -1 & -1 \\ 0 & -1 \\ 0 & 0 \end{bmatrix} = \langle \xi + \eta - 1 \quad \eta - 1 \rangle$$

$x = \xi + \eta - 1 \qquad y = \eta - 1$

$N_1^{(1)} = 1 - \xi - \eta = -x \quad N_2^{(1)} = \xi = x - y \quad N_3^{(1)} = \eta = y + 1$

$u^{(1)}(x,y) = u_1^{(1)} N_1^{(1)} + u_2^{(1)} N_2^{(1)} + u_3^{(1)} N_3^{(1)}$. Because we know this is in element 1, we will not use (1) to indicate for convenience.

$$\int_A [(\sum_{i=1}^{3} u_i \frac{\partial N_i}{\partial x}) \frac{\partial \delta u}{\partial x} + (\sum_{i=1}^{3} u_i \frac{\partial N_i}{\partial y}) \frac{\partial \delta u}{\partial y}] dA = \int_A f_A \delta u dA + \oint_l \frac{\partial u}{\partial n} \delta u dl$$

$$\iint dxdy (u_1 \frac{\partial N_1}{\partial x} + u_2 \frac{\partial N_2}{\partial x} + u_3 \frac{\partial N_3}{\partial x}) \frac{\partial N_1}{\partial x} + (u_1 \frac{\partial N_1}{\partial y} + u_2 \frac{\partial N_2}{\partial y} + u_3 \frac{\partial N_3}{\partial y}) \frac{\partial N_1}{\partial y}] = \iint dxdy f_A N_1 + \oint_l \frac{\partial u}{\partial n} N_1 dl$$

$$\iint dxdy (u_1 \frac{\partial N_1}{\partial x} + u_2 \frac{\partial N_2}{\partial x} + u_3 \frac{\partial N_3}{\partial x}) \frac{\partial N_2}{\partial x} + (u_1 \frac{\partial N_1}{\partial y} + u_2 \frac{\partial N_2}{\partial y} + u_3 \frac{\partial N_3}{\partial y}) \frac{\partial N_2}{\partial y}] = \iint dxdy f_A N_2 + \oint_l \frac{\partial u}{\partial n} N_2 dl$$

$$\iint dxdy (u_1 \frac{\partial N_1}{\partial x} + u_2 \frac{\partial N_2}{\partial x} + u_3 \frac{\partial N_3}{\partial x}) \frac{\partial N_3}{\partial x} + (u_1 \frac{\partial N_1}{\partial y} + u_2 \frac{\partial N_2}{\partial y} + u_3 \frac{\partial N_3}{\partial y}) \frac{\partial N_3}{\partial y}] = \iint dxdy f_A N_3 + \oint_l \frac{\partial u}{\partial n} N_3 dl$$

$$\oint_l \frac{\partial u}{\partial n} N_1 dl = \int_{Side\,1} \frac{\partial u}{\partial n} N_1 dl + \int_{Side\,2} \frac{\partial u}{\partial n} N_1 dl + \int_{Side\,3} \frac{\partial u}{\partial n} N_1 dl$$

$$\oint_l \frac{\partial u}{\partial n} N_2 dl = \int_{Side\,1} \frac{\partial u}{\partial n} N_2 dl + \int_{Side\,2} \frac{\partial u}{\partial n} N_2 dl + \int_{Side\,3} \frac{\partial u}{\partial n} N_2 dl$$

$$\oint_l \frac{\partial u}{\partial n} N_3 dl = \int_{Side\,1} \frac{\partial u}{\partial n} N_3 dl + \int_{Side\,2} \frac{\partial u}{\partial n} N_3 dl + \int_{Side\,3} \frac{\partial u}{\partial n} N_3 dl$$

Because of the nature of the shape functions,

$$\int_{Side\,1} \frac{\partial u}{\partial n} N_1 dl = \int_{Side\,2} \frac{\partial u}{\partial n} N_2 dl = \int_{Side\,3} \frac{\partial u}{\partial n} N_3 dl = 0$$

Note that the direction of the normal outward unit vector depends on the particular element and therefore the normal derivatives differ by a minus sign. Using this fact together with the observation that the linear shape functions from different elements coincides when restricted to common edges, allows us to ignore the contribution of $\{P^e\}$ on interior edges. Therefore, one should consider P_i^e only when an edge of the element lies on the global boundary.

$$\frac{\partial u}{\partial n} = u_1 \frac{\partial N_1}{\partial n} + u_2 \frac{\partial N_2}{\partial n} + u_3 \frac{\partial N_3}{\partial n}$$

Side 1: interior edge, $N_1=0$

Side 2: $\dfrac{\partial u}{\partial n} = 0$, $N_2=0$

Side 3: $\dfrac{\partial u}{\partial n}$ is unknown, $u=0$ and $N_3=0$.

$$\therefore P^{(1)}_1 = \oint_l \frac{\partial u}{\partial n} N_1^{(1)} dl = \int_{Side\,3} \frac{\partial u}{\partial n} N_1^{(1)} dl$$

$$P^{(1)}_2 = \oint_l \frac{\partial u}{\partial n} N_2^{(1)} dl = \int_{Side\,3} \frac{\partial u}{\partial n} N_2^{(1)} dl$$

$$P^{(1)}_3 = \oint_l \frac{\partial u}{\partial n} N_3^{(1)} dl = 0$$

$$K^{(1)} = \begin{bmatrix} 1/2 & -1/2 & 0 \\ -1/2 & 1 & -1/2 \\ 0 & -1/2 & 1/2 \end{bmatrix}$$

$$F^{(1)} = f_A \left\{ \begin{array}{c} -\int\limits_{-1}^{0} dx \int\limits_{-1}^{x} dy\, x \\[6pt] \int\limits_{-1}^{0} dx \int\limits_{-1}^{x} dy(x-y) \\[6pt] \int\limits_{-1}^{0} dx \int\limits_{-1}^{x} dy(y+1) \end{array} \right\} = f_A \left\{ \begin{array}{c} 1/6 \\ 1/6 \\ 1/6 \end{array} \right\}$$

$$\begin{bmatrix} 1/2 & -1/2 & 0 \\ -1/2 & 1 & -1/2 \\ 0 & -1/2 & 1/2 \end{bmatrix} \left\{ \begin{array}{c} u_1^{(1)} \\ u_2^{(1)} \\ u_3^{(1)} \end{array} \right\} = f_A \left\{ \begin{array}{c} 1/6 \\ 1/6 \\ 1/6 \end{array} \right\} + \left\{ \begin{array}{c} P_1^{(1)} \\ P_2^{(1)} \\ 0 \end{array} \right\}$$

Element 2:

$$\langle x \quad y \rangle = \langle 1-\xi-\eta \quad \xi \quad \eta \rangle \begin{bmatrix} 0 & -1 \\ 1 & -1 \\ 1 & 0 \end{bmatrix} = \langle \xi+\eta \quad \eta-1 \rangle$$

$x = \xi + \eta \qquad y = \eta - 1$

$N_1^{(2)} = 1 - \xi - \eta = 1 - x \quad N_2^{(2)} = \xi = x - y - 1 \quad N_3^{(2)} = \eta = y + 1$

Similarly, we get

$$K^{(2)} = \begin{bmatrix} 1/2 & -1/2 & 0 \\ -1/2 & 1 & -1/2 \\ 0 & -1/2 & 1/2 \end{bmatrix} \qquad F^{(2)} = f_A \begin{Bmatrix} 1/6 \\ 1/6 \\ 1/6 \end{Bmatrix}$$

Side 1: $\dfrac{\partial u}{\partial n}$ is unknown, $u=0$ and $N_1=0$

Side 2: interior edge, $N_2=0$

Side 3: $\dfrac{\partial u}{\partial n}$ is unknown, $u=0$ and $N_3=0$.

$$P^{(2)}_1 = \oint_l \frac{\partial u}{\partial n} N_1{}^{(2)} dl = \int_{Side\,3} \frac{\partial u}{\partial n} N_1{}^{(2)} dl$$

$$P^{(2)}_2 = \oint_l \frac{\partial u}{\partial n} N_2{}^{(2)} dl = \int_{Side\,1} \frac{\partial u}{\partial n} N_2{}^{(2)} dl + \int_{Side\,3} \frac{\partial u}{\partial n} N_2{}^{(2)} dl$$

$$P^{(2)}_3 = \oint_l \frac{\partial u}{\partial n} N_3{}^{(2)} dl = \int_{Side\,1} \frac{\partial u}{\partial n} N_3{}^{(2)} dl$$

$$\begin{bmatrix} 1/2 & -1/2 & 0 \\ -1/2 & 1 & -1/2 \\ 0 & -1/2 & 1/2 \end{bmatrix} \begin{Bmatrix} u_1{}^{(2)} \\ u_2{}^{(2)} \\ u_3{}^{(2)} \end{Bmatrix} = f_A \begin{Bmatrix} 1/6 \\ 1/6 \\ 1/6 \end{Bmatrix} + \begin{Bmatrix} P_1{}^{(2)} \\ P_2{}^{(2)} \\ P_3{}^{(2)} \end{Bmatrix}$$

Element 3: three sides are interior edges.

$$\langle x \quad y \rangle = \langle 1-\xi-\eta \quad \xi \quad \eta \rangle \begin{bmatrix} 1 & 0 \\ 0 & 0 \\ 0 & -1 \end{bmatrix} = \langle 1-\xi-\eta \quad -\eta \rangle$$

$$x = 1-\xi-\eta \qquad y = -\eta$$

$$N_1{}^{(3)} = 1-\xi-\eta = x \quad N_2{}^{(3)} = \xi = x-y-1 \quad N_3{}^{(3)} = \eta = -y$$

$$\begin{bmatrix} 1/2 & -1/2 & 0 \\ -1/2 & 1 & -1/2 \\ 0 & -1/2 & 1/2 \end{bmatrix} \begin{Bmatrix} u_1{}^{(3)} \\ u_2{}^{(3)} \\ u_3{}^{(3)} \end{Bmatrix} = f_A \begin{Bmatrix} 1/6 \\ 1/6 \\ 1/6 \end{Bmatrix}$$

Element 4:

$$\langle x \quad y \rangle = \langle 1-\xi-\eta \quad \xi \quad \eta \rangle \begin{bmatrix} 0 & 0 \\ 1 & 0 \\ 1 & 1 \end{bmatrix} = \langle \xi+\eta \quad \eta \rangle$$

$$x = \xi + \eta \qquad y = \eta$$

$$N_1^{(4)} = 1 - \xi - \eta = 1 - x \quad N_2^{(4)} = \xi = x - y \quad N_3^{(4)} = \eta = y$$

Side 1: $\dfrac{\partial u}{\partial n}$ is unknown, $u = 0$ and $N_1 = 0$

Side 2: $\dfrac{\partial u}{\partial n} = 0$ and $N_2 = 0$

Side 3: interior edge, $N_3 = 0$

$$P^{(4)}_1 = \oint_l \frac{\partial u}{\partial n} N_1^{(4)} dl = 0$$

$$P^{(4)}_2 = \oint_l \frac{\partial u}{\partial n} N_2^{(4)} dl = \int_{Side1} \frac{\partial u}{\partial n} N_2^{(4)} dl$$

$$P^{(4)}_3 = \oint_l \frac{\partial u}{\partial n} N_3^{(4)} dl = \int_{Side1} \frac{\partial u}{\partial n} N_3^{(4)} dl$$

$$\begin{bmatrix} 1/2 & -1/2 & 0 \\ -1/2 & 1 & -1/2 \\ 0 & -1/2 & 1/2 \end{bmatrix} \begin{Bmatrix} u_1^{(4)} \\ u_2^{(4)} \\ u_3^{(4)} \end{Bmatrix} = f_A \begin{Bmatrix} 1/6 \\ 1/6 \\ 1/6 \end{Bmatrix} + \begin{Bmatrix} 0 \\ P_2^{(4)} \\ P_3^{(4)} \end{Bmatrix}$$

Now, let's assembly the four element matrices into a global matrix

$$\begin{bmatrix} 1/2 & -1/2 & 0 & 0 & 0 & 0 \\ -1/2 & 1+1/2+1/2 & -1/2 & -1/2-1/2 & 0 & 0 \\ 0 & -1/2 & 1 & 0 & -1/2 & 0 \\ 0 & -1/2-1/2 & 0 & 1/2+1+1/2 & -1/2-1/2 & 0 \\ 0 & 0 & -1/2 & -1/2 & 1/2+1/2+1 & -1/2 \\ 0 & 0 & 0 & 0 & -1/2 & 1/2 \end{bmatrix} \begin{Bmatrix} u_1=0 \\ u_2=0 \\ u_3=0 \\ u_4 \\ u_5=0 \\ u_6=0 \end{Bmatrix} = f_A \begin{Bmatrix} 1/6 \\ 1/6+1/6+1/6 \\ 1/6 \\ 1/6+1/6+1/6 \\ 1/6+1/6+1/6 \\ 1/6 \end{Bmatrix} + \begin{Bmatrix} P_1^{(1)} \\ P_2^{(1)}+P_1^{(2)} \\ P_2^{(2)} \\ 0 \\ P_3^{(2)}+P_2^{(4)} \\ P_3^{(4)} \end{Bmatrix}$$

$$\therefore u_4 = 1/4 f_A$$

$$\therefore u(x, y) = \begin{cases} \frac{1}{4} f_A(y+1) & element - 1 \\ 0 & element - 2 \\ \frac{1}{4} f_A(x - y + 1) & element - 3 \\ \frac{1}{4} f_A(1 - x) & element - 4 \end{cases}$$
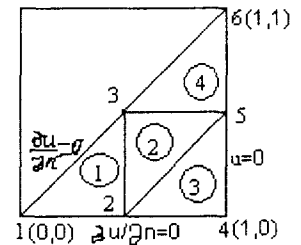
According to the symmetry (symmetric axis is $y = x$), we can get the solution of another half domain.

85

Because of the symmetry of the 2x2 square, we can also solve the problem in the area which is composed by three points (0, 0), (1, 0) and (1, 1). We divide the one-eighth area into four elements. Because of the symmetry, we can get solutions of the other seven "1/8" domains.

Element	Node 1	Node 2	Node 3
1	1(0, 0)	2(0.5, 0)	3(0.5, 0.5)
2	5(1, 0.5)	3(0.5, 0.5)	2(0.5, 0)
3	2(0.5, 0)	4(1, 0)	5(1,0.5)
4	3(0.5, 0.5)	5(1, 0.5)	6(1, 1)

Element1: $\langle x \quad y \rangle = \langle 1-\xi-\eta \quad \xi \quad \eta \rangle \begin{bmatrix} 0 & 0 \\ .5 & 0 \\ .5 & .5 \end{bmatrix} = \langle 0.5(\xi+\eta) \quad .5\eta \rangle$

$N_1^{(1)}=1-\xi-\eta=1-2x \quad N_2^{(1)}=\xi=2(x-y) \quad N_3^{(1)}=\eta=2y$

Element2: $\langle x \quad y \rangle = \langle 1-\xi-\eta \quad \xi \quad \eta \rangle \begin{bmatrix} 1 & 0.5 \\ 0.5 & 0.5 \\ 0.5 & 0 \end{bmatrix} = \langle 1-0.5(\xi+\eta) \quad .5(1-\eta) \rangle$

$N_1^{(2)}=1-\xi-\eta=2x-1 \quad N_2^{(2)}=\xi=1-2(x-y) \quad N_3^{(2)}=\eta=1-2y$

Element 3: $\langle x \quad y \rangle = \langle 1-\xi-\eta \quad \xi \quad \eta \rangle \begin{bmatrix} .5 & 0 \\ 1 & 0 \\ 1 & .5 \end{bmatrix} = \langle 0.5(1+\xi+\eta) \quad .5\eta \rangle$

$N_1^{(3)}=1-\xi-\eta=2-2x \quad N_2^{(3)}=\xi=2(x-y)-1 \quad N_3^{(3)}=\eta=2y$

Element 4: $\langle x \quad y \rangle = \langle 1-\xi-\eta \quad \xi \quad \eta \rangle \begin{bmatrix} 0.5 & 0.5 \\ 1 & 0.5 \\ 1 & 1 \end{bmatrix} = \langle 0.5+0.5(\xi+\eta) \quad .5(1+\eta) \rangle$

$N_1^{(4)}=1-\xi-\eta=2-2x \quad N_2^{(4)}=\xi=2(x-y) \quad N_3^{(4)}=\eta=2y-1$

Similarly, we get

$$\begin{bmatrix} 1/2 & -1/2 & 0 & 0 & 0 & 0 \\ -1/2 & 2 & -1 & -1/2 & 0 & 0 \\ 0 & -1 & 2 & 0 & -1 & 0 \\ 0 & -1/2 & 0 & 1 & -1/2 & 0 \\ 0 & 0 & -1 & -1/2 & 2 & -1/2 \\ 0 & 0 & 0 & 0 & -1/2 & 1/2 \end{bmatrix} \begin{Bmatrix} u_1 \\ u_2 \\ u_3 \\ u_4=0 \\ u_5=0 \\ u_6=0 \end{Bmatrix} = f_A \begin{Bmatrix} 1/24 \\ 3/24 \\ 3/24 \\ 1/24 \\ 3/24 \\ 1/24 \end{Bmatrix} + \begin{Bmatrix} 0 \\ 0 \\ 0 \\ P_2^{(3)} \\ P_3^{(3)}+P_2^{(4)} \\ P_3^{(4)} \end{Bmatrix} \longrightarrow$$

$$\begin{bmatrix} 1/2 & -1/2 & 0 \\ -1/2 & 2 & -1 \\ 0 & -1 & 2 \end{bmatrix} \begin{Bmatrix} u_1 \\ u_2 \\ u_3 \end{Bmatrix} = f_A \begin{Bmatrix} 1/24 \\ 3/24 \\ 3/24 \end{Bmatrix}$$

$u_1 = 0.3125 f_A$, $u_2 = 0.22917 f_A$, $u_3 = 0.17708 f_A$

$$\therefore u(x,y) = \begin{cases} u_1 N_1^{(1)} + u_2 N_2^{(1)} + u_3 N_3^{(1)} = f_A(.3125 - .167x - .104y) & element - 1 \\ u_3 N_2^{(2)} + u_2 N_3^{(2)} = f_A(.40625 - .35416x - .10418y) & element - 2 \\ u_2 N_1^{(3)} = 0.45834 f_A(1-x) & element - 3 \\ u_3 N_1^{(4)} = 0.35416 f_A(1-x) & element - 4 \end{cases}$$

According to the symmetry, we can get the approximate function of u in other domains.

(b) Bilinear Element (quadrilateral, four nodes)

For example 1: Rainfall estimation in a certain area

Suppose we got m dispersed sample value of the amount of rainfall from m stations. We can divide the area A into n elements (depend on the number of dispersed sample value). In every element, there are 4 nodes, which can be labeled i, j, k and l.

$$Q = \sum_{e=1}^{n} Q^e$$

$$Q^e = \int_{A^e} u(x,y)dA = \int_{-1}^{1}\int_{-1}^{1} u(\xi,\eta) \det(J) d\xi d\eta$$

$$= \int_{-1}^{1}\int_{-1}^{1} \langle P \rangle [P_n]^{-1} \{u_n\} \det(J) d\xi d\eta \qquad [\det(J) = A_0 + A_1\xi + A_2\eta]$$

$$= \int_{-1}^{1}\int_{-1}^{1} (A_0 + A_1\xi + A_2\eta) \langle 1 \quad \xi \quad \eta \quad \xi\eta \rangle d\xi d\eta [P_n]^{-1} \{u_n\}$$

$$= \left\langle A_0 \quad \frac{A_1}{3} \quad \frac{A_2}{3} \right\rangle \begin{Bmatrix} u_i + u_j + u_k + u_l \\ -u_i + u_j + u_k - u_l \\ -u_i - u_j + u_k + u_l \end{Bmatrix}$$

For example 2: the same Poisson's equation $(\frac{\partial^2}{\partial x^2} + \frac{\partial^2}{\partial y^2})u(x,y) + f_A = 0$ ($|x|<1$, $|y|<1$)

with boundary condition u(x, y)= 0 on the boundary $x = \pm1$ $y = \pm1$

$$\int_A [(\sum_{i=1}^n u_i \frac{\partial N_i}{\partial x})\frac{\partial \delta u}{\partial x} + (\sum_{i=1}^n u_i \frac{\partial N_i}{\partial y})\frac{\partial \delta u}{\partial y}]dA = \int_A f_A \delta u dA + \oint_l \frac{\partial u}{\partial n}\delta u dl$$

$$[K^e]\{u^e\} = \{F^e\} + \{P^e\}$$

Because $a=b=2$,

$$K^e_{ij} = \int_A (\frac{\partial N_i}{\partial x}\frac{\partial N_j}{\partial x} + \frac{\partial N_i}{\partial y}\frac{\partial N_j}{\partial y})dA = \int_{-1}^1\int_{-1}^1 (\frac{\partial N_i}{\partial \xi}\frac{\partial N_j}{\partial \xi} + \frac{\partial N_i}{\partial \eta}\frac{\partial N_j}{\partial \eta})\det[J]d\xi d\eta$$

$$F^e_i = \int_A (f_A N_i)dA = f_A \int_{-1}^1\int_{-1}^1 N_i \det[J]d\xi d\eta$$

$$P^e_i = \oint_l \frac{\partial u}{\partial n}N_i dl \quad \text{(The direction of the } \boldsymbol{n} \text{ is the normal outward unit vector to the}$$

element)

$$u^{(e)}(x,y) = u_1^{(e)}N_1^{(e)} + u_2^{(e)}N_2^{(e)} + u_3^{(c)}N_3^{(e)} + u_4 N_4^{(e)}.$$

$$[K^e] = \frac{1}{6}\begin{bmatrix} 4 & -1 & -2 & -1 \\ -1 & 4 & -1 & -2 \\ -2 & -1 & 4 & -1 \\ -1 & -2 & -1 & 4 \end{bmatrix}$$

$$\{F^e\} = \frac{1}{4}a^2 f_A \begin{Bmatrix} 1 \\ 1 \\ 1 \\ 1 \end{Bmatrix},$$
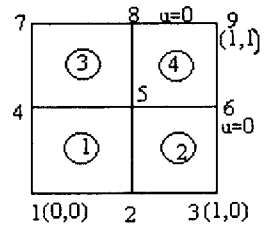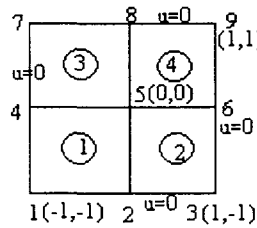
Where a is the length of the four sides of each element (it is square in this problem)

If we divide the 2x2 square into one element, then it should be $u_1 = u_2 = u_3 = u_4 = 0$ since the four nodes are on the boundary. It makes $u(x,y)=0$. If we divide the total domain into four elements, then $a=1$ and $u_1 = u_2 = u_3 = u_4 = u_6 = u_7 = u_8 = u_9 = 0$, but $u_5 \neq 0$. According to the rules of symmetry, we only have to consider one of the 4 domains.

$$\frac{1}{6}\begin{bmatrix} 4 & -1 & & -1 & -2 & & & & \\ -1 & 8 & -1 & 2 & 1 & -1 & & & \\ & -1 & 4 & & 2 & -1 & & & \\ -1 & -2 & & 8 & -2 & & -1 & -2 & \\ -2 & -2 & -2 & -2 & 16 & -2 & 2 & -2 & -2 \\ & -2 & -1 & & -2 & 8 & & 2 & -1 \\ & & & -1 & -2 & & 4 & -1 & \\ & & & -2 & -2 & -2 & -1 & 8 & -1 \\ & & & & -2 & -1 & & -1 & 4 \end{bmatrix}\begin{Bmatrix} u_1=0 \\ u_2=0 \\ u_3=0 \\ u_4=0 \\ u_5 \\ u_6=0 \\ u_7=0 \\ u_8=0 \\ u_9=0 \end{Bmatrix} = \frac{f_A}{4}\begin{Bmatrix} 1 \\ 2 \\ 1 \\ 2 \\ 4 \\ 2 \\ 1 \\ 2 \\ 1 \end{Bmatrix} + \begin{Bmatrix} P_1 \\ P_2 \\ P_3 \\ P_4 \\ 0 \\ P_6 \\ P_7 \\ P_8 \\ P_9 \end{Bmatrix}$$

We can easily get $u_5=(3/8)f_A$. If we divide the 1/4 domain into 4 elements, then $a=1/2$ and $u_3=u_6=u_7=u_8=u_9=0$. However, $u_1 \neq 0$, $u_2 \neq 0$, $u_4 \neq 0$ and $u_5 \neq 0$.

$$\frac{1}{6}\begin{bmatrix} 4 & -1 & 0 & -1 & -2 & 0 & 0 & 0 & 0 \\ & 8 & -1 & -2 & -2 & -2 & 0 & 0 & 0 \\ & & 4 & 0 & -2 & -1 & 0 & 0 & 0 \\ & & & 8 & -2 & 0 & -1 & -2 & 0 \\ & & & & 16 & -2 & -2 & -2 & -2 \\ & & & & & 8 & 0 & -2 & -1 \\ & & & & & & 4 & -1 & 0 \\ & & & & & & & 8 & -1 \\ & & & & & & & & 4 \end{bmatrix}\begin{Bmatrix} u_1 \\ u_2 \\ u_3=0 \\ u_4 \\ u_5 \\ u_6=0 \\ u_7=0 \\ u_8=0 \\ u_9=0 \end{Bmatrix} = \frac{f_A}{16}\begin{Bmatrix} 1 \\ 2 \\ 1 \\ 2 \\ 4 \\ 2 \\ 1 \\ 2 \\ 1 \end{Bmatrix} + \begin{Bmatrix} 0 \\ 0 \\ P_2^{(2)} \\ 0 \\ 0 \\ P_2^{(3)}+P_2^{(4)} \\ P_4^{(4)} \\ P_3^{(3)}+P_4^{(4)} \\ P_3^{(4)} \end{Bmatrix} \rightarrow$$

$$\frac{1}{6}\begin{bmatrix} 4 & -1 & -1 & -2 \\ -1 & 8 & -2 & -2 \\ -1 & -2 & 8 & -2 \\ -2 & -2 & -2 & 16 \end{bmatrix}\begin{Bmatrix} u_1 \\ u_2 \\ u_4 \\ u_5 \end{Bmatrix} = \frac{f_A}{16}\begin{Bmatrix} 1 \\ 2 \\ 2 \\ 4 \end{Bmatrix} \rightarrow \begin{Bmatrix} u_1 \\ u_2 \\ u_4 \\ u_5 \end{Bmatrix} = f_A\begin{Bmatrix} .31071 \\ .24107 \\ .24107 \\ .19286 \end{Bmatrix}$$

(3) Matrix Formulation of the FEM

Let us start from Galerkin integral forms and choose weighting function $\psi \equiv \delta u$:

$$W = \int_V \delta u [L(u) + f_V]dV = 0$$

$$W = \sum_{e=1}^{n} W^e = \sum_{e=1}^{n} \int_V \delta u [L(u) + f_V]dV = 0 \qquad W^e = \int_V \delta u^e [L(u^e) + f_V]dV = 0$$

In the element domain V^e: $u^e = \langle N \rangle \{u_n\}$ $\qquad \delta u^e = \langle N \rangle \{\delta u_n\}$

$$W^e = \left\langle \delta u_n \right\rangle [\ \int_{V^e} \{N\} L(\left\langle N \right\rangle) dV \{u_n\} + \int_{V^e} \{N\} f_V dV\ ]$$

E.g. $W = \sum_e W^e = \sum_e \int_{V^e} \delta u (\dfrac{\partial^2 u}{\partial x^2} + \dfrac{\partial^2 u}{\partial y^2} + f_V) dV = 0$

After integral by parts:

$$W = \sum_e W^e = \sum_e (\int_{V^e} [\left\langle \delta(\dfrac{\partial u}{\partial x}) \quad \delta(\dfrac{\partial u}{\partial y}) \right\rangle [D] \begin{Bmatrix} \partial u / \partial x \\ \partial u / \partial y \end{Bmatrix} - \delta u f_V] dV - \int_{S_f^e} \delta u (f_S - \alpha u) dS = 0$$

$$[D] = \begin{bmatrix} 1 & 0 \\ 0 & 1 \end{bmatrix} = I$$

$$W^e = \left\langle \delta u_n \right\rangle ([k]\{u_n\} - \{f\})$$

$$W = \sum_e W^e = \sum_e \left\langle \delta u_n \right\rangle ([k]\{u_n\} - \{f\}) = 0$$

$$W = \left\langle \delta U_n \right\rangle ([K]\{U_n\} - \{F\}) = 0$$

$[K]$ is the global system matrix. $\{F\}$ is the global right-handed side load vector. $\{U_n\}$ is the global vector of all nodal values of the unknown function u. $\{\delta U_n\}$ is an arbitrary variation

$$[K]\{U_n\} - \{F\} = 0 \qquad \text{or} \qquad [K]\{U_n\} = \{F\}$$

For unsteady problems, terms like $\partial u / \partial t$ and $\partial^2 u / \partial t^2$ may appear and introduce additional corresponding expressions in the element integral form:

$$W^e = \int_{V^e} \delta u^e \dfrac{\partial u^e}{\partial t} dV + \cdots \qquad \text{and} \qquad W^e = \int_{V^e} \delta u^e \dfrac{\partial^2 u^e}{\partial t^2} dV + \cdots$$

After discretization with $u^e = \left\langle N \right\rangle \{u_n\}$ $\quad \delta u^e = \left\langle N \right\rangle \{\delta u_n\}$, these supplementary terms become:

$$W^e = \left\langle \delta u^e \right\rangle [c] \left\{ \dfrac{du^e}{dt} \right\} + \cdots \qquad \text{and} \qquad W^e = \left\langle \delta u^e \right\rangle [m] \left\{ \dfrac{d^2 u^e}{dt^2} \right\} + \cdots$$

Because $u = \left\langle N \right\rangle \{u_n\}$, $\quad \dfrac{\partial u}{\partial x} = \left\langle \dfrac{\partial N}{\partial x} \right\rangle \{u_n\}$, $\quad \dfrac{\partial u}{\partial y} = \left\langle \dfrac{\partial N}{\partial y} \right\rangle \{u_n\}, \dots$

$$\delta u = \left\langle N \right\rangle \{\delta u_n\}, \quad \delta(\dfrac{\partial u}{\partial x}) = \left\langle \dfrac{\partial N}{\partial x} \right\rangle \{\delta u_n\}, \quad \delta(\dfrac{\partial u}{\partial y}) = \left\langle \dfrac{\partial N}{\partial y} \right\rangle \{\delta u_n\}, \dots$$

Then: $\{\partial u\} = \left\{ \begin{array}{c} u \\ \partial u / x \\ \vdots \end{array} \right\} = \left[\begin{array}{c} \langle N \rangle \\ \langle \partial N / \partial x \rangle \\ \cdots \end{array} \right] \{u_n\} = [B]\{u_n\}$

$\{\delta(\partial u)\} = \left\{ \begin{array}{c} \delta u \\ \delta(\partial u / x) \\ \vdots \end{array} \right\} = \left[\begin{array}{c} \langle N \rangle \\ \langle \partial N / \partial x \rangle \\ \cdots \end{array} \right] \{\delta u_n\} = [B_\delta]\{\delta u_n\}$

For self-adjoint operators L: $\{\delta(\partial u)\} \equiv \delta(\{\partial u\})$, $[B_\delta] \equiv [B]$

$W^e = \langle \delta u_n \rangle (\int_{V^e} [B_\delta]^T [D][B] dV \{u_n\} - \int_{V^e} \{N\} f_V dV - \int_{S_f^e} \{N\} f_S dS)$

$[k] = \int_{V^e} [B_\delta]^T [D][B] dV \qquad \{f\} = \int_{V^e} \{N\} f_V dV + \int_{S_f^e} \{N\} f_S dS)$

For the 2D Poisson's equation

$\{\partial u\} = \left\{ \begin{array}{c} \partial u / \partial x \\ \partial u / \partial y \end{array} \right\} = \left[\begin{array}{c} \langle \partial N / \partial x \rangle \\ \langle \partial N / \partial y \rangle \end{array} \right] \{u_n\} = [B]\{u_n\} \qquad [B] = \left[\begin{array}{c} \langle \partial N / \partial x \rangle \\ \langle \partial N / \partial y \rangle \end{array} \right]$

$\{\delta(\partial u)\} = \left\{ \begin{array}{c} \delta(\partial u / \partial x) \\ \delta(\partial u / \partial y) \end{array} \right\} = \left[\begin{array}{c} \langle \partial N / \partial x \rangle \\ \langle \partial N / \partial y \rangle \end{array} \right] \{\delta u_n\} = [B]\{\delta u_n\}$

$[K] = \int_{V^e} [B]^T [D][B] dV + \int_{S_f^e} \alpha \{N\} \langle N \rangle dS \qquad \{f\} = \int_{V^e} \{N\} f_V dV + \int_{S_f^e} \{N\} f_S dS$

For a concentrated force f_i at point $x=x_i$, f_S becomes: $f_S(x_i)=f_i\delta(x_i)$

Corresponding vector $\{f\}$ is: $\{f\}=\{N(x_i)\}f_i$

(4) Transformation in the space of the element of reference

All derivatives and integrations in space **x** must be transformed in the space ξ

$u = \langle N \rangle \{u_n\}, \quad \dfrac{du}{dx} = \dfrac{d\xi}{dx} \left\langle \dfrac{dN(\xi)}{d\xi} \right\rangle \{u_n\}$

$[B_x]=[Q][B_\xi]$. For 2D Poisson's equation

$[B_x] = \left[\begin{array}{c} \langle \partial N / \partial x \rangle \\ \langle \partial N / \partial y \rangle \end{array} \right] = \left[\begin{array}{cc} \partial \xi / \partial x & \partial \eta / \partial x \\ \partial \xi / \partial y & \partial \eta / \partial y \end{array} \right] \left[\begin{array}{c} \langle \partial N / \partial \xi \rangle \\ \langle \partial N / \partial \eta \rangle \end{array} \right] = [Q][B_\xi]$

$[Q]=[j]=[J]^{-1}$

$$[k] = \int_{V^e} [B_\xi]^T [Q]^T [D][Q][B_\xi] dV$$

$$\int_{V^e} \cdots dV = \int_{V_r^e} \cdots \det(J) d\xi d\eta d\zeta$$

1D: $\displaystyle\int_{-1}^{1} \cdots \det(J) d\xi$

2D: Triangle $\displaystyle\int_{\xi=0}^{\xi=1} d\xi \int_{\eta=0}^{\eta=1-\xi} \cdots \det(J) d\eta$ Quadrilateral $\displaystyle\int_{-1}^{1}\int_{-1}^{1} \cdots \det(J) d\xi d\eta$

3D: Tetrahedron $\displaystyle\int_{\xi=0}^{\xi=1} d\xi \int_{\eta=0}^{\eta=1-\xi} d\eta \int_{\zeta=0}^{\zeta=1-\xi-\eta} \cdots \det(J) d\zeta$

Hexahedron $\displaystyle\int_{-1}^{1}\int_{-1}^{1}\int_{-1}^{1} \cdots \det(J) d\xi d\eta d\zeta$ Prism $\displaystyle\int_{\xi=0}^{\xi=1} d\xi \int_{\eta=0}^{\eta=1-\xi} d\eta \int_{\zeta=-1}^{\zeta=1} \cdots \det(J) d\zeta$

$$l = \int_S \cdots dS = \int_{S_1}^{S_2} \cdots J_S dS_r$$

$$x = \langle N(s) \rangle \{x_n\} \text{ etc.} \qquad J_S = \sqrt{{x_{,S}}^2 + {y_{,S}}^2 + {z_{,S}}^2}$$

E.g. For a four-node element, the side $\xi=1$ of a quadrilateral element $s \equiv \eta$, $ds \equiv d\eta$

$$\langle P \rangle = \langle 1 \quad \xi \quad \eta \quad \xi\eta \rangle \qquad \langle N \rangle = \tfrac{1}{4}\langle (1-\xi)(1-\eta) \quad (1+\xi)(1-\eta) \quad (1+\xi)(1+\eta) \quad (1-\xi)(1+\eta) \rangle$$

$$\langle N(s) \rangle = \langle N(\xi=1,\eta) \rangle = \left\langle 0 \quad \frac{1-\eta}{2} \quad \frac{1+\eta}{2} \quad 0 \right\rangle$$

$$x_{,\eta} = \langle N_{,\eta}(\xi=1,\eta) \rangle \{x_n\} = \left\langle 0 \quad -\frac{1}{2} \quad \frac{1}{2} \quad 0 \right\rangle \begin{Bmatrix} x_1 \\ x_2 \\ x_3 \\ x_4 \end{Bmatrix} = \frac{1}{2}(x_3 - x_2) \quad x_{,\eta} = \partial x / \partial\eta$$

$$y_{,\eta} = \langle N_{,\eta}(\xi=1,\eta) \rangle \{y_n\} = (y_3 - y_2)/2$$

$$J_S = \sqrt{{x_{,\eta}}^2 + {y_{,\eta}}^2} = \tfrac{1}{2}\sqrt{(x_3-x_2)^2 + (y_3-y_2)^2} \qquad l = \int_S \cdots dS = \int_{-1}^{1} \cdots J_S d\eta$$

Surface integration in three dimensions: integral $\int_S \cdots dS$ is written in terms of surface

coordinates s_1 and s_2 that are generally (ξ, η) or (η, ζ) or (ξ, ζ)

$$\int_S \cdots dS \rightarrow \int_S \cdots J_S ds_1 ds_2 \qquad x = \langle N(s_1, s_2) \rangle \{x_n\}$$

$$J_S = \sqrt{(x_{,s_1} y_{,s_2} - y_{,s_1} x_{,s_2})^2 + (y_{,s_1} z_{,s_2} - z_{,s_1} y_{,s_2})^2 + (z_{,s_1} x_{,s_2} - x_{,s_1} z_{,s_2})^2}$$

E.g. Surface integration for an eight-node element (on face $\zeta=1$)

$s_1 \equiv \xi \quad s_2 \equiv \eta, \quad ds_1 \equiv d\xi \quad ds_2 \equiv d\eta \quad P = <1 \quad \xi \quad \eta \quad \zeta \quad \xi\eta \quad \eta\zeta \quad \zeta\xi \quad \xi\eta\zeta >$

$<N> = (1/8) < a_2 b_2 c_2 \quad a_1 b_2 c_2 \quad a_1 b_1 c_2 \quad a_2 b_1 c_2 \quad a_2 b_2 c_1 \quad a_1 b_2 c_1 \quad a_1 b_1 c_1 \quad a_2 b_1 c_1 >$

$a_1 = 1+\xi \quad a_2 = 1-\xi \quad b_1 = 1+\eta \quad b_2 = 1-\eta \quad c_1 = 1+\zeta \quad c_2 = 1-\zeta$

$<N(s1, s2) = <N(\xi, \eta, \zeta = 1)>$

$= (1/4) <0 \quad 0 \quad 0 \quad 0 \quad (1-\xi)(1-\eta) \quad (1+\xi)(1-\eta) \quad (1+\xi)(1+\eta) \quad (1-\xi)(1+\eta)>$

$<N_{,\xi}(\xi, \eta, \zeta = 1)> = (1/4) <0 \quad 0 \quad 0 \quad 0 \quad -(1-\eta) \quad (1-\eta) \quad (1+\eta) \quad -(1+\eta)>$

$<N_{,\eta}(\xi, \eta, \zeta = 1)> = (1/4) <0 \quad 0 \quad 0 \quad 0 \quad -(1-\xi) \quad -(1+\xi) \quad (1+\xi) \quad (1-\xi)>$

$<x_{,\xi} \quad y_{,\xi} \quad z_{,\xi}> = <N_{,\xi}>[\{x_n\} \quad \{y_n\} \quad \{z_n\}] \qquad <x_{,\eta} \quad y_{,\eta} \quad z_{,\eta}> = <N_{,\eta}>[\{x_n\} \quad \{y_n\} \quad \{z_n\}]$

$$l = \int_{-1}^{1}\int_{-1}^{1} \cdots J_s(\xi, \eta) d\xi d\eta$$

$$[k] = \int_{V_r^e} [B_{\delta\xi}]^T [Q_{\delta}]^T [D][Q][B_{\xi}] \det(J) d\xi d\eta d\zeta$$

$$\{f\} = \int_{V_r^e} \{N\} f_V \det(J) d\xi d\eta d\zeta + \int_{S_r^e} \{N\} f_S J_s ds_1 ds_2$$

Classical forms of W^e.

Terms	$[B_\delta]^T$	$[D]$	$[B]$	Property of $[k]$	
Symmetrical quadratic $\int_{V^e} \delta u \cdot u \, dV$	$\{N\}$	1	$<N>$	constant	Symmetrical
$\int_{V^e} \delta(\frac{\partial u}{\partial x}) \cdot \frac{\partial u}{\partial x} dV$	$\left\{\frac{\partial N}{\partial x}\right\}$	1	$\left\langle\frac{\partial N}{\partial x}\right\rangle$	constant	Symmetrical
$\int_{V^e} \delta(\frac{\partial^2 u}{\partial x^2}) \cdot \frac{\partial^2 u}{\partial x^2} dV$	$\left\{\frac{\partial^2 N}{\partial x^2}\right\}$	1	$\left\langle\frac{\partial^2 N}{\partial x^2}\right\rangle$	constant	Symmetrical
$\int_{V^e} \delta(\frac{\partial^m u}{\partial x^m}) \cdot \frac{\partial^m u}{\partial x^m} dV$	$\left\{\frac{\partial^m N}{\partial x^m}\right\}$	1	$\left\langle\frac{\partial^m N}{\partial x^m}\right\rangle$	constant	Symmetrical
Non-symmetric quadratic $\int_{V^e} \delta u \cdot \frac{\partial u}{\partial x} dV$	$\{N\}$	1	$\left\langle\frac{\partial N}{\partial x}\right\rangle$	constant	Non-symmetrical

Integral term	Test	Middle	Right	Coefficient	Symmetry
$\int_{V^e} \delta(\frac{\partial^m u}{\partial x^m})\cdot\frac{\partial^n u}{\partial x^n}dV$	$\{\frac{\partial^m N}{\partial x^m}\}$	1	$\langle\frac{\partial^n N}{\partial x^n}\rangle$	constant	Non-symmetrical If $m\neq n$
Non-Linear $\int_{V^e} \delta u\cdot u\cdot\frac{\partial u}{\partial x}dV$	$\{N\}$ $\{N\}$	$\langle\frac{\partial N}{\partial x}\rangle\{u_n\}$ $<N>\{u_n\}$	$<N>$ $\langle\frac{\partial N}{\partial x}\rangle$	Function of $\{u_n\}$	Symmetrical Non-symmetrical
$\int_{V^e} \delta(\frac{\partial u}{\partial x})\cdot\frac{\partial u}{\partial x}\cdot\frac{\partial u}{\partial x}dV$	$\{\frac{\partial N}{\partial x}\}$	$\langle\frac{\partial N}{\partial x}\rangle\{u_n\}$	$\langle\frac{\partial N}{\partial x}\rangle$	Function of $\{u_n\}$	Symmetrical
$\int_{V^e} \delta(\frac{\partial^m u}{\partial x^m})\cdot D(u,\frac{\partial u}{\partial x},\cdots)\cdot\frac{\partial^n u}{\partial x^n}dV$	$\{\frac{\partial^m N}{\partial x^m}\}$	$D(\{u_n\})$	$\langle\frac{\partial^n N}{\partial x^n}\rangle$	Function of $\{u_n\}$	Non-symmetrical If $m\neq n$
Quadratic contour integral terms $\int_{S^e} \delta u\cdot u\,dS$	$\{N\}$	1	$<N>$	constant	Symmetrical
Linear volume integral terms $\int_{V^e} \delta u\cdot f_V\,dV$	$\{N\}$	1	f_V	$W^e=<\delta u_n>\{f\}$ $\{f\}=\int_{V^e}\{N\}f_V\,dV$	
Linear Surface integral terms $\int_{S_f^e} \delta u\cdot f_S\,dS$	$\{N\}$	1	f_S	$W^e=<\delta u_n>\{f\}$ $\{f\}=\int_{S_f^e}\{N\}f_S\,dS$	
Non-stationary terms $\int_{V^e} \delta u\cdot\frac{\partial u}{\partial t}dV$	$\{N\}$	1	$<N>$	$W^e=<\delta u_n>[c]\{du_n/dt\}$ $[c]=\int_{V^e}\{N\}\langle N\rangle dV$	
$\int_{V^e} \delta u\cdot\frac{\partial^2 u}{\partial t^2}dV$	$\{N\}$	1	$<N>$	$W^e=<\delta u_n>[m]\{d^2u_n/dt^2\}$ $[m]=\int_{V^e}\{N\}\langle N\rangle dV$	

E.g. For 2D Poisson's Equation with a triangular element

$<P>=<1\ \ \xi\ \ \eta>$

$$\langle N\rangle=\langle P\rangle[P_n]^{-1}=\langle 1\ \ \xi\ \ \eta\rangle\begin{bmatrix}1 & 0 & 0\\ -1 & 1 & 0\\ -1 & 0 & 1\end{bmatrix}=\langle 1-\xi-\eta\ \ \xi\ \ \eta\rangle$$

$$[J]=\begin{bmatrix}-1 & 1 & 0\\ -1 & 0 & 1\end{bmatrix}\begin{pmatrix}x_1 & y_1\\ x_2 & y_2\\ x_3 & y_3\end{pmatrix}=\begin{bmatrix}x_2-x_1 & y_2-y_1\\ x_3-x_1 & y_3-y_1\end{bmatrix}$$

$\det(J)=2A=(x_2-x_1)(y_3-y_1)-(x_3-x_1)(y_2-y_1)$

$$[j]=[J]^{-1}=\frac{1}{2A}\begin{bmatrix}y_3-y_1 & -(y_2-y_1)\\ -(x_3-x_1) & x_2-x_1\end{bmatrix}$$

$$[B_\xi] = \begin{bmatrix} \langle \partial N / \partial \xi \rangle \\ \langle \partial N / \partial \eta \rangle \end{bmatrix} = \begin{bmatrix} -1 & 1 & 0 \\ -1 & 0 & 1 \end{bmatrix}$$

$$[B] = [Q][B_\xi] = [j][B_\xi] = \frac{1}{2A} \begin{bmatrix} y_2 - y_3 & y_3 - y_1 & y_1 - y_2 \\ x_3 - x_2 & x_1 - x_3 & x_2 - x_1 \end{bmatrix}$$

$$[D] = d \begin{bmatrix} 1 & 0 \\ 0 & 1 \end{bmatrix}$$

Where d is the isotropic conductivity coefficient (for Laplace equation, $d=1$).

$$[k] = \int_0^1 \int_0^{1-\xi} d[B]^T[B]\det(J)d\xi d\eta = A \cdot d[B]^T[B] \quad \text{([B] is constant)}$$

For the case where: $x_1=y_1=0$; $x_2=a, y_2=0$; $x_3=0, y_3=a$

$$[k] = \frac{d}{2} \begin{bmatrix} 2 & -1 & -1 \\ -1 & 1 & 0 \\ -1 & 0 & 1 \end{bmatrix} \qquad [m] = \int_0^1 \int_0^{1-\xi} \{N\} < N > \det(J)d\xi d\eta$$

$$[m] = \frac{A}{12} \begin{bmatrix} 2 & 1 & 1 \\ 1 & 2 & 1 \\ 1 & 1 & 2 \end{bmatrix}$$

For the case f_V is constant and f_S is zero:

$$\{f\} = \int_0^1 d\xi \int_0^{1-\xi} \{N\} f_V \det(J)d\eta = 2Af_V \int_0^1 d\xi \int_0^{1-\xi} d\eta \begin{Bmatrix} 1-\xi-\eta \\ \xi \\ \eta \end{Bmatrix} = \frac{Af_V}{3} \begin{Bmatrix} 1 \\ 1 \\ 1 \end{Bmatrix}$$

(5) Gaussian quadrature[96]

Suppose we have transformed a integration from **x** space to ξ space and got

(1) $I = \int_{-1}^1 f(\xi)d\xi$ (1D)

Gaussian quadrature of order one

$I = \int_{-1}^1 f(\xi)d\xi \approx w_1 f(\xi_1) = 2f(0)$ w is the Gaussian weight

For linear polynomials, it integrates exactly. $I = \int_{-1}^1 f(\xi)d\xi = 2f(0)$

Gaussian quadrature of order two

$$I = \int_{-1}^{1} f(\xi)d\xi \approx w_1 f(\xi_1) + w_2 f(\xi_2) = f(-\frac{1}{\sqrt{3}}) + f(\frac{1}{\sqrt{3}})$$

For cubic polynomials, it integrates exactly.

The three point Gaussian quadrature has the following form

$$I = \int_{-1}^{1} f(\xi)d\xi \approx w_1 f(\xi_1) + w_2 f(\xi_2) + w_3 f(\xi_3) = \frac{5}{9} f(-\sqrt{0.6}) + \frac{8}{9} f(0) + \frac{5}{9} f(\sqrt{0.6})$$

For "2n-1", it integrates exactly.

(2) $I = \int_{-1}^{1}\int_{-1}^{1} f(\xi,\eta)d\xi d\eta$ (2D)

$$I = \int_{-1}^{1}\int_{-1}^{1} f(\xi,\eta)d\xi d\eta = \int_{-1}^{1}\left[\int_{-1}^{1} f(\xi,\eta)d\xi\right]d\eta = \int_{-1}^{1}\left[\sum_{j=1}^{n} w_j f(\xi_j,\eta)\right]d\eta = \sum_{i=1}^{n} w_i\left[\sum_{j=1}^{n} w_j f(\xi_j,\eta_i)\right]$$

$$= \sum_{i=1}^{n}\sum_{j=1}^{n} w_i w_j f(\xi_j,\eta_i)$$

For 1x1 Gaussian: $I = \int_{-1}^{1}\int_{-1}^{1} f(\xi,\eta)d\xi d\eta \approx 2f(0,0)$

For 2x2 Gaussian:

$$I = \int_{-1}^{1}\int_{-1}^{1} f(\xi,\eta)d\xi d\eta \approx f(-\frac{1}{\sqrt{3}},-\frac{1}{\sqrt{3}}) + f(\frac{1}{\sqrt{3}},-\frac{1}{\sqrt{3}}) + f(\frac{1}{\sqrt{3}},\frac{1}{\sqrt{3}}) + f(-\frac{1}{\sqrt{3}},\frac{1}{\sqrt{3}})$$

For 3x3 Gaussian:

$$I = \int_{-1}^{1}\int_{-1}^{1} f(\xi,\eta)d\xi d\eta$$

$$\approx (\frac{8}{9})^2 f(0,0) + (\frac{5}{9})^2 f(-\sqrt{.6},-\sqrt{.6}) + \frac{8}{9}\cdot\frac{5}{9} f(0,-\sqrt{.6}) + (\frac{5}{9})^2 f(\sqrt{.6},-\sqrt{.6}) + \frac{5}{9}\cdot\frac{8}{9} f(\sqrt{.6},0)$$

$$+ (\frac{5}{9})^2 f(\sqrt{.6},\sqrt{.6}) + \frac{8}{9}\cdot\frac{5}{9} f(0,\sqrt{.6}) + (\frac{5}{9})^2 f(-\sqrt{.6},\sqrt{.6}) + \frac{5}{9}\cdot\frac{8}{9} f(-\sqrt{.6},0)$$

2. FDM

(1) 1D

96

The theory of FDM is simple and direct. Let's take the same Poisson equation as an example.

$$\frac{d^2u}{dx^2} + p_0 = 0 \quad x=[0, L] \text{ with boundary conditions:}$$

$u(0)=0$ and $\left.\frac{du}{dx}\right|_{x=L} = 0$.

Let's divide the domain into n sub-domains. There are $n+1$ nodes, $i=1$ corresponds to $x=0$, $i=n+1$ corresponds to $x=L$. $\Delta x = L/n$. Then, we get

$u_1=0$, $\left(\frac{du}{dx}\right)_{n+1} \approx \frac{u_{n+2} - u_n}{2L/n} = 0$.

$\left(\frac{d^2u}{dx^2}\right)_i = -p_0$

$\left(\frac{du}{dx}\right)_i = u_i' \approx \frac{u_{i+1} - u_{i-1}}{2L/n}$ (Central difference)

$\left(\frac{d^2u}{dx^2}\right)_i \approx \frac{u_{i+1} - 2u_i + u_{i-1}}{(L/n)^2}$

so, $u_{i+1} - 2u_i + u_{i-1} + p_0(L/n)^2 = 0$. Let's $i=1, 2, \ldots n+1$, we get

$u_2 - u_0 = 2Lu_1'/n$

$u_2 - 2u_1 + u_0 + p_0(L/n)^2 = 0$, eliminate u_0, we get

$2u_2 - 2u_1 + p_0(L/n)^2 = 2Lu_1'/n$

The fact is that $u_2' = u_3' = \cdots = u_n' = 0$

$u_1 = 0$ and $u_{n+1}' = 0$ are boundary conditions

Then, we get a group of equations

$2u_2 - 2u_1 + p_0(L/n)^2 = 2Lu_1'/n$

$u_3 - 2u_2 + u_1 + p_0(L/n)^2 = 0$

$u_4 - 2u_3 + u_2 + p_0(L/n)^2 = 0$

. . . .

$u_{n+1} - 2u_n + u_{n-1} + p_0(L/n)^2 = 0$

$$\begin{cases} u_{n+2} - 2u_{n+1} + u_n + p_0(L/n)^2 = 0 \\ u_{n+2} - u_n = 0 \end{cases} \rightarrow -2u_{n+1} + 2u_n + p_0(L/n)^2 = 0$$

We can write it as the form of matrix and get

$$\begin{bmatrix} -2 & 2 & 0 & \cdots & 0 & 0 & 0 \\ 1 & -2 & 1 & \cdots & 0 & 0 & 0 \\ 0 & 1 & -2 & \cdots & 0 & 0 & 0 \\ \vdots & \vdots & \vdots & \vdots & \vdots & \vdots & \vdots \\ 0 & 0 & 0 & \cdots & -2 & 1 & 0 \\ 0 & 0 & 0 & \cdots & 1 & -2 & 1 \\ 0 & 0 & 0 & \cdots & 0 & 2 & -2 \end{bmatrix} \begin{Bmatrix} u_1 = 0 \\ u_2 \\ u_3 \\ \vdots \\ u_{n-1} \\ u_n \\ u_{n+1} \end{Bmatrix} = -\frac{L^2 p_0}{n^2} \begin{Bmatrix} 1 \\ 1 \\ 1 \\ \vdots \\ 1 \\ 1 \\ 1 \end{Bmatrix} + \frac{2L}{n} \begin{Bmatrix} u_1' \\ u_2' = 0 \\ u_3' = 0 \\ \vdots \\ u_{n-1}' = 0 \\ u_n' = 0 \\ 0 \end{Bmatrix}$$

When $n=1$, we get: $u_1 = 0$, $u_2 = \frac{1}{2}p_0 L^2$

When $n=2$, we get: $u_1 = 0$, $u_2 = \frac{3}{8}L^2 p_0$, $u_3 = \frac{1}{2}L^2 p_0$

The value is exactly the same as the one we got by FEM.

Example 2: $\dfrac{d^2u}{dx^2} + p_0 = 0$ $x=[0, L]$ with boundary conditions:

$u(0)=0$ and $u(L) = 0$.

We still divide the domain into n sub-domains. From the boundary condition, we get

$u_1 = 0$ and $u_{n+1} = 0$

$u_i' \approx \dfrac{u_{i+1} - u_{i-1}}{2L/n}$ (Central difference)

$u_i'' = p_0 \approx \dfrac{u_{i+1} - 2u_i + u_{i-1}}{(L/n)^2}$

$u_{i+1} - u_{i-1} = 2Lu_i'/n$.

$u_{i+1} - 2u_i + u_{i-1} + p_0(L/n)^2 = 0$

$$\begin{cases} u_2 - u_0 = 2Lu_1'/n \\ u_2 - 2u_1 + u_0 + p_0(L/n)^2 = 0 \end{cases} \rightarrow 2u_2 - 2u_1 + p_0(L/n)^2 = 2Lu_1'/n$$

$u_3 - 2u_2 + u_1 + p_0(L/n)^2 = 0$

$u_4 - 2u_3 + u_2 + p_0(L/n)^2 = 0$

. . . .

$$\begin{cases} u_{n+2} - 2u_{n+1} + u_n + p_0(L/n)^2 = 0 \\ u_{n+2} - u_n = 2Lu'_{n+1}/n \end{cases} \rightarrow -2u_{n+1} + 2u_n + p_0(L/n)^2 = -2Lu'_{n+1}/n$$

$$\begin{bmatrix} -2 & 2 & 0 & \cdots & 0 & 0 & 0 \\ 1 & -2 & 1 & \cdots & 0 & 0 & 0 \\ 0 & 1 & -2 & \cdots & 0 & 0 & 0 \\ \vdots & \vdots & \vdots & \vdots & \vdots & \vdots & \vdots \\ 0 & 0 & 0 & \cdots & -2 & 1 & 0 \\ 0 & 0 & 0 & \cdots & 1 & -2 & 1 \\ 0 & 0 & 0 & \cdots & 0 & 2 & -2 \end{bmatrix} \begin{Bmatrix} u_1 = 0 \\ u_2 \\ u_3 \\ \vdots \\ u_{n-1} \\ u_n \\ u_{n+1} = 0 \end{Bmatrix} = -\frac{L^2 p_0}{n^2} \begin{Bmatrix} 1 \\ 1 \\ 1 \\ \vdots \\ 1 \\ 1 \\ 1 \end{Bmatrix} + \frac{2L}{n} \begin{Bmatrix} u'_1 \\ u'_2 = 0 \\ u'_3 = 0 \\ \vdots \\ u'_{n-1} = 0 \\ u'_n = 0 \\ -u'_{n+1} \end{Bmatrix}$$

When $n=1$, we get: $u_1 = 0$, $u_2 = 0$.

When $n=2$, we get: $u_1 = 0$, $u_2 = \frac{1}{8}L^2 p_0$, $u_3 = 0$

The results are the same as the one we got by FEM.

(2) 2D

For Example: the same Poisson's equation $(\frac{\partial^2}{\partial x^2} + \frac{\partial^2}{\partial y^2})u(x,y) + f_A = 0$ ($|x|<1$, $|y|<1$)

with boundary condition $u(x, y)= 0$ on the boundary $x = \pm 1$ $y = \pm 1$.

Because of the symmetry of the problem, we only need to consider the ¼ area in the first quadrant. The solutions for other domains can be gotten by symmetry. Now the boundary conditions become: $u(x, y)= 0$ on the boundary $x = 1$ and $y = 1$; $\partial u/\partial x = 0$ on the boundary $x=0$ and $\partial u/\partial y = 0$ on the boundary $y = 0$.

According to the symmetry, we can divide the area into $n \times n$ sub-domains and choose $\Delta x = \Delta y = h = 1/n$. There are $n+1$ nodes along x axis and $n+1$ nodes along y axis. And there are $(n+1)(n+1)$ values of u. They are $u_{i,j}$, $i,j= 1, 2, \ldots, n+1$.

$$\left. \begin{array}{l} \left(\frac{\partial^2 u}{\partial x^2}\right)_{i,j} \approx \frac{u_{i+1,j} - 2u_{i,j} + u_{i-1,j}}{(1/n)^2} \\ \left(\frac{\partial^2 u}{\partial y^2}\right)_{i,j} \approx \frac{u_{i,j+1} - 2u_{i,j} + u_{i,j-1}}{(1/n)^2} \end{array} \right\} \rightarrow u_{i+1,j} + u_{i-1,j} + u_{i,j+1} + u_{i,j-1} - 4u_{i,j} + \frac{1}{n^2}f_A = 0$$

Boundary conditions:

$u_{n+1,j} = u_{i,n+1} = 0$, and

$$\left(\frac{\partial u}{\partial x}\right)_{1,j} = u'_{1,j} \approx \frac{u_{2,j} - u_{0,j}}{2(1/n)} = 0, \qquad \left(\frac{\partial u}{\partial y}\right)_{i,1} = u'_{i,1} \approx \frac{u_{i,2} - u_{i,0}}{2(1/n)} = 0$$

$$\therefore u_{0,j} = u_{2,j} \quad \text{and} \quad u_{i,0} = u_{i,2}$$

When $n=1$, we get: $u_{2,1} = u_{1,2} = u_{22} = 0$

$$u_{0,1} = u_{2,1} = 0, \quad u_{0,2} = u_{2,0} = u_{2,2} = 0, \quad u_{1,0} = u_{1,2} = 0$$

$$u_{2,1} + u_{0,1} + u_{1,2} + u_{1,0} - 4u_{1,1} + \frac{1}{n^2} f_A = 0$$

$$u_{1,1} = \frac{1}{4} f_A.$$

When $n=2$, $u_{3,1} = u_{3,2} = u_{3,3} = u_{1,3} = u_{2,3} = 0$,

$$u_{0,1} = u_{2,1}, \quad u_{0,2} = u_{2,2}, \quad u_{0,3} = u_{2,3}, \quad u_{1,0} = u_{1,2}, \quad u_{2,0} = u_{2,2}, \quad u_{3,0} = u_{3,2}, \quad u_{2,0} = u_{0,2}$$

$$u_{2,1} + u_{0,1} + u_{1,2} + u_{1,0} - 4u_{1,1} + \frac{1}{n^2} f_A = 0 \rightarrow 2u_{2,1} + 2u_{1,2} - 4u_{1,1} + \frac{1}{n^2} f_A = 0$$

$$u_{3,1} + u_{1,1} + u_{2,2} + u_{2,0} - 4u_{2,1} + \frac{1}{n^2} f_A = 0 \rightarrow u_{3,1} + u_{1,1} + 2u_{2,2} - 4u_{2,1} + \frac{1}{n^2} f_A = 0$$

$$u_{2,2} + u_{0,2} + u_{1,3} + u_{1,1} - 4u_{1,2} + \frac{1}{n^2} f_A = 0 \rightarrow 2u_{2,2} + u_{1,3} + u_{1,1} - 4u_{1,2} + \frac{1}{n^2} f_A = 0$$

$$u_{3,2} + u_{1,2} + u_{2,3} + u_{2,1} - 4u_{2,2} + \frac{1}{n^2} f_A = 0$$

Then we get a group of equations:

$$\begin{cases} 2u_{2,1} + 2u_{1,2} - 4u_{1,1} + f_A/4 = 0 \\ u_{1,1} + 2u_{2,2} - 4u_{2,1} + f_A/4 = 0 \\ 2u_{2,2} + u_{1,1} - 4u_{1,2} + f_A/4 = 0 \\ u_{1,2} + u_{2,1} - 4u_{2,2} + f_A/4 = 0 \end{cases} \qquad \begin{cases} u_{1,1} = 9f_A/32 \\ u_{1,2} = 7f_A/32 \\ u_{2,1} = 7f_A/32 \\ u_{2,2} = 11f_A/64 \end{cases}$$

From the examples we know that, in 2D situation, the result is different from the one we got by FEM. Just as we pointed out at the beginning, the finite element method is an approximation to its solution. It makes sure that the value at the node is exactly the same as the real value. The finite difference method is an approximation to the differential equation. This cannot make sure the value at the node is exactly the same as the real value. In fact, the Taylor expansion always neglects the small higher order of non-linear terms.

More generally,

$$u_{2,1} + u_{0,1} + u_{1,2} + u_{1,0} - 4u_{1,1} + \frac{1}{n^2} f_A = 0 \rightarrow 2u_{2,1} + 2u_{1,2} - 4u_{1,1} + \frac{1}{n^2} f_A = 0$$

$$u_{3,1} + u_{1,1} + u_{2,2} + u_{2,0} - 4u_{2,1} + \frac{1}{n^2} f_A = 0 \rightarrow u_{3,1} + u_{1,1} + 2u_{2,2} - 4u_{2,1} + \frac{1}{n^2} f_A = 0$$

$$u_{4,1} + u_{2,1} + u_{3,2} + u_{3,0} - 4u_{3,1} + \frac{1}{n^2} f_A = 0 \rightarrow u_{4,1} + u_{2,1} + 2u_{3,2} - 4u_{3,1} + \frac{1}{n^2} f_A = 0$$

$$\cdots\cdots\cdots$$

$$u_{n+1,1} + u_{n-1,1} + u_{n,2} + u_{n,0} - 4u_{n,1} + \frac{1}{n^2} f_A = 0 \rightarrow u_{n+1,1} + u_{n-1,1} + 2u_{n,2} - 4u_{n,1} + \frac{1}{n^2} f_A = 0$$

$$u_{2,2} + u_{0,2} + u_{1,3} + u_{1,1} - 4u_{1,2} + \frac{1}{n^2} f_A = 0 \rightarrow 2u_{2,2} + u_{1,3} + u_{1,1} - 4u_{1,2} + \frac{1}{n^2} f_A = 0$$

$$u_{3,2} + u_{1,2} + u_{2,3} + u_{2,1} - 4u_{2,2} + \frac{1}{n^2} f_A = 0$$

$$u_{4,2} + u_{2,2} + u_{3,3} + u_{3,1} - 4u_{3,2} + \frac{1}{n^2} f_A = 0$$

$$\cdots\cdots\cdots$$

$$u_{n+1,2} + u_{n-1,2} + u_{n,3} + u_{n,1} - 4u_{n,2} + \frac{1}{n^2} f_A = 0$$

$$u_{2,3} + u_{0,3} + u_{1,4} + u_{1,2} - 4u_{1,3} + \frac{1}{n^2} f_A = 0 \rightarrow 2u_{2,3} + u_{1,4} + u_{1,2} - 4u_{1,3} + \frac{1}{n^2} f_A = 0$$

$$u_{3,3} + u_{1,3} + u_{2,4} + u_{2,2} - 4u_{2,3} + \frac{1}{n^2} f_A = 0$$

$$u_{4,3} + u_{2,3} + u_{3,4} + u_{3,2} - 4u_{3,3} + \frac{1}{n^2} f_A = 0$$

$$\cdots\cdots\cdots$$

$$u_{n+1,3} + u_{n-1,3} + u_{n,4} + u_{n,2} - 4u_{n,3} + \frac{1}{n^2} f_A = 0$$

$$\cdots\cdots\cdots$$

$$u_{2,n} + u_{0,n} + u_{1,n+1} + u_{1,n-1} - 4u_{1,n} + \frac{1}{n^2} f_A = 0 \rightarrow 2u_{2,n} + u_{1,n+1} + u_{1,n-1} - 4u_{1,n} + \frac{1}{n^2} f_A = 0$$

$$u_{3,n} + u_{1,n} + u_{2,n+1} + u_{2,n-1} - 4u_{2,n} + \frac{1}{n^2} f_A = 0$$

$$u_{4,n} + u_{2,n} + u_{3,n+1} + u_{3,n-1} - 4u_{3,n} + \frac{1}{n^2} f_A = 0$$

$$\cdots\cdots\cdots$$

$$u_{n+1,n} + u_{n-1,n} + u_{n,n+1} + u_{n,n-1} - 4u_{n,n} + \frac{1}{n^2} f_A = 0$$

Vita Auctoris

NAME: Long Jian Liu

BORN: Sichuan, China, 1963

EDUCATION: Lanzhou University, Lanzhou, China

1982-1986 B. Sc. Theoretical Physics

Fudan University, Shanghai, China

1990-1993 M. Sc. Electrons, Ions and Vacuum Physics.

University of Windsor, Windsor, Ontario, Canada

2007-2008 M. Sc.